Department of Neurology
Helsinki University Central Hospital
Helsinki, Finland

# Brain Diffusion and Perfusion Magnetic Resonance Imaging in Healthy Subjects and in Patients with Ischemic Stroke, Carotid Stenosis, and Leukoaraiosis

**Johanna Helenius**

ACADEMIC DISSERTATION

To be publicly discussed with the permission of the Medical Faculty of the University of Helsinki in Auditorium 1, Meilahti Hospital, on the 19th of March, 2004, at 12 noon.

Helsinki, 2004

ISBN 952-91-6804-7 (paperback)
ISBN 952-10-1616-7 (pdf)

Yliopistopaino 2004

**Cover:** Sami Heinomo

**Supervisors:**

Turgut Tatlisumak, MD, PhD
Docent of Neurology
Department of Neurology
Helsinki University Central Hospital
Helsinki, Finland

Markku Kaste, MD, PhD, FAHA
Professor of Neurology
Department of Neurology
Helsinki University Central Hospital
University of Helsinki
Helsinki, Finland

**Reviewers:**

Joachim Röther, MD, PhD
Professor of Neurology
Vice-Director
Head of the Stroke Unit and Neurological Intensive Care Unit
University Hospital Hamburg Eppendorf, Germany

Steven Warach, MD, PhD
Chief, Section on Stroke Diagnostics and Therapeutics
NIH/NINDS
Bethesda, Maryland, USA

**Opponent:**

Ritva Vanninen, MD, PhD
Docent of Radiology
Department of Clinical Radiology
University of Kuopio
Kuopio, Finland

# CONTENTS

# ABSTRACT

Diffusion-weighted and dynamic susceptibility contrast magnetic resonance imaging (DWI and DSC MRI, respectively) are used worldwide to evaluate abnormal water diffusion and cerebral blood circulation in clinical settings, especially in the imaging of acute stroke. However, diffusion and perfusion parameters of healthy populations have not been extensively studied to date. These parameters are essential for the more quantitative comparison of disease states with healthy brains. In addition, the feasibility of DWI and DSC MRI to detect changes induced by high-grade carotid stenosis (CS), carotid endarterectomy (CEA), and leukoaraiosis (LA), has received little attention. Accordingly, the purpose of this thesis was to determine the normal absolute values of diffusion and perfusion parameters, and their dependence on age, gender, and brain hemisphere, to assess the influence of CS, CEA, and LA on these parameters, and to identify differences between asymptomatic and symptomatic CS patients (ACS and SCS, respectively).

Eighty healthy subjects (40 male, 40 female) aged 22 to 85 years, 10 patients with acute ischemic stroke, 46 patients with unilateral high-grade CS, and 85 subjects with LA were imaged with DWI and/or DSC MRI, and with conventional images at 1.5 Tesla. Healthy subjects and patients with LA were imaged in one imaging session each. CS patients were imaged three times: preoperatively, and 3 and 100 days after CEA, and ischemic stroke patients five times: less than 6 hours, 24 hours, one week, one month, and 3 months after the insult. Maps of the average apparent diffusion coefficient ($ADC_{av}$), cerebral blood volume (CBV), cerebral blood flow (CBF), and mean transit time (MTT) were created. Several regions of the brain and the lesions of ischemic stroke and LA were selected for the analyses.

Generally, the diffusion and perfusion parameters in the selected regions of the healthy brain did not differ with age, gender, or brain hemisphere. By contrast, the $ADC_{av}$ values, CBF, and MTT of CS patients were different between hemispheres before CEA. However, postoperatively and in the chronic phase, no such differences were detected in these patients. The perfusion parameters of ACS and SCS patients showed slightly different patterns before and after CEA, but no differences in the $ADC_{av}$ values between these two groups were found. The $ADC_{av}$ values of the leukoaraiotic regions or the normal-appearing white matter (WM) and the severity of LA correlated significantly; the more severe the LA, the higher the $ADC_{av}$ values. The leukoaraiotic regions, the normal-appearing WM, and ischemic stroke in its various phases could be distinguished

from each other based solely on analysis of $ADC_{av}$ values. An exception was ischemic stroke at one month, when the $ADC_{av}$ values overlapped with those of LA.

In conclusion, measurements of brain diffusion and perfusion with DWI and DSC MRI can detect and distinguish several diseases at various stages. Normal $ADC_{av}$ values and perfusion parameters lie within a narrow range in healthy individuals, regardless of age and gender. In CS patients, the term 'preleukoaraiosis' was introduced to define the ipsilateral normal-appearing WM with high $ADC_{av}$ values, which were partly reversible by CEA. Cerebral perfusion measurements with DSC MRI disclosed typical patterns in ACS and SCS patients, but the $ADC_{av}$ values appeared not to be useful in differentiating these patient groups. The regions of LA and the normal-appearing WM of the subjects with LA showed characteristic changes in the $ADC_{av}$ values, and DWI could be used to differentiate acute and chronic ischemic stroke lesions from LA. DWI and DSC MRI have become widely used MRI sequences in clinical settings since they are fairly easy to use and they provide additional information to the conventional MRI. However, the quantitative analysis of the $ADC_{av}$ values or perfusion parameters requires expertise and accuracy.

## LIST OF ORIGINAL PUBLICATIONS

This thesis is based on the following original articles referred to in the text by their Roman numerals (I-V). The original articles are reprinted with written permissions of the copyright holders.

I **Helenius J,** Soinne L, Perkiö J, Salonen O, Kangasmäki A, Kaste M, Carano RAD, Aronen HJ, Tatlisumak T. Diffusion-Weighted MR Imaging in Normal Human Brains in Various Age Groups. *AJNR Am J Neuroradiol* 2002;23:194-199.

II **Helenius J**, Perkiö J, Soinne L, Østergaard L, Carano RAD, Salonen O, Savolainen S, Kaste M, Aronen HJ, Tatlisumak T. Cerebral Hemodynamics in a Healthy Population Measured by Dynamic Susceptibility Contrast Magnetic Resonance Imaging. *Acta Radiol* 2003;44:538-546.

III Soinne L, **Helenius J**, Saimanen E, Salonen O, Lindsberg PJ, Kaste M, Tatlisumak T. Brain Diffusion Changes in Carotid Occlusive Disease Treated with Endarterectomy. *Neurology* 2003;61:1061-1065.

IV Soinne L, **Helenius J**, Tatlisumak T, Saimanen E, Salonen O, Lindsberg PJ, Kaste M. Cerebral Hemodynamics in Asymptomatic and Symptomatic Patients with High-Grade Carotid Stenosis Undergoing Carotid Endarterectomy. *Stroke* 2003;34:1655-1661.

V **Helenius J**, Soinne L, Salonen O, Kaste M, Tatlisumak T. Leukoaraiosis, Ischemic Stroke, and Normal White Matter on Diffusion-Weighted MRI. *Stroke* 2002;33:45-50.

# ABBREVIATIONS

| | |
|---|---|
| ACS | asymptomatic carotid stenosis |
| AD | Alzheimer's disease |
| ADC | apparent diffusion coefficient |
| $ADC_{av}$ | average apparent diffusion coefficient |
| AIF | arterial input function |
| CBF | cerebral blood flow |
| CBV | cerebral blood volume |
| CEA | carotid endarterectomy |
| CNS | central nervous system |
| CS | carotid stenosis |
| CSF | cerebrospinal fluid |
| CT | computed tomography |
| DSC MRI | dynamic susceptibility contrast magnetic resonance imaging |
| DWI | diffusion-weighted magnetic resonance imaging |
| ECA | external carotid artery |
| EPI | echo-planar imaging |
| FOV | field of view |
| Gd-DTPA | gadolinium diethylenetriaminepenta-acetic acid |
| GE | gradient-echo |
| GM | gray matter |
| HI | hyperintensity |
| ICA | internal carotid artery |
| LA | leukoaraiosis |
| MCA | middle cerebral artery |
| MRI | magnetic resonance imaging |
| MS | multiple sclerosis |
| MTT | mean transit time, the CBV:CBF ratio |
| PET | positron emission tomography |
| PI | perfusion magnetic resonance imaging |
| PVH | periventricular hyperintensity |
| RF | radiofrequency |
| ROI | region of interest |
| rtPA | recombinant tissue plasminogen activator |
| SCS | symptomatic carotid stenosis |
| SD | standard deviation |
| SE | spin-echo |
| SPECT | single photon emission computed tomography |
| SVD | singular value decomposition |
| T | Tesla |
| TE | echo time |
| TIA | transient ischemic attack |
| TR | repetition time |
| WM | white matter |
| WsR | watershed regions |

# INTRODUCTION

Ischemic stroke is the third leading cause of death, with 4.5 million deaths a year, and the leading cause of disability worldwide. Its economic burden is tremendous, among the highest of all diseases, and the human burden to patients and their relatives is immeasurable. Every year, 12,000 people in Finland (Fogelholm et al., 1997) and 500,000 in USA suffer strokes (Bonita, 1992). Despite developments in prevention, diagnosis, therapy, rehabilitation, awareness, and services, ischemic stroke continues to be a major public health problem. Therefore, management in the hyperacute phase, before the brain tissue-at-risk evolves into infarction, is imperative. Acute and rehabilitation care of stroke patients in specialized stroke units and secondary prevention including revascularizing therapies are also important, both in improving prognosis and in reducing economic burden.

One of the major risk factors for ischemic stroke, and thus an important factor in the prevention of recurrent strokes, is tight carotid stenosis (CS), as it may lead to misery perfusion (Baron et al., 1981; Klijn et al., 1997), artery-to-artery embolism in the brain, and brain infarction. Carotid endarterectomy (CEA) improves the long-term survival and outcome of patients with symptomatic CS (SCS) (North American Symptomatic Carotid Endarterectomy Trial, 1991), but is less beneficial in asymptomatic CS (ASC) (Chambers et al., 2002).

Leukoaraiosis (LA), another risk factor for ischemic stroke (Inzitari et al., 1997), may lead to cognitive decline and other disabling neurological symptoms. The term LA refers to bilateral and either patchy or diffuse areas of hypodensity in the cerebral white matter (WM) on computed tomography (CT) or hyperintensity on T2-weighted magnetic resonance imaging (MRI) (Hachinski et al., 1987). Its main causes are thought to be chronic cerebral ischemia and hypoperfusion, but the general pathogenesis and its clinical significance are still incompletely understood (Pantoni and Garcia, 1995; 1997).

Diffusion-weighted magnetic resonance imaging (DWI) reveals ischemic regions in the brain immediately upon an acute stroke patient being submitted for imaging studies (Baird and Warach, 1998; Gonzalez et al., 1999). It has become an essential part of the imaging of hyperacute stroke patients, and its utility has also been investigated in several other brain diseases (Schaefer et al., 2000). It is thought to provide neuropathological information on the mechanisms of LA in vivo (Okada et al., 1999) and to detect minor and silent infarctions after CEA (Müller et al., 2000; Feiwell et al., 2001; Jaeger et al., 2002). DWI is based on the random translational movement of water molecules in

biological media (diffusion). The net diffusion in biological media is referred to as the apparent diffusion coefficient (ADC) (Le Bihan et al., 1986).

Perfusion imaging (PI) with dynamic susceptibility contrast magnetic resonance imaging (DSC MRI) has also shown promise in assessing various aspects of cerebral hemodynamics in ischemic stroke (Barber et al., 1998) and in other brain diseases (Cha et al., 2002). It is performed by combining the simultaneous use of a paramagnetic contrast medium and rapid collection of the MR signal during the passage of the contrast medium bolus through the brain (Villringer et al., 1988). The acquired data sets contain information about cerebral perfusion in the form of cerebral blood volume (CBV) (Belliveau et al., 1990; Rosen et al., 1991), cerebral blood flow (CBF) (Østergaard et al., 1996a; Østergaard et al., 1996b), and the contrast medium mean transit time (MTT), the CBV:CBF ratio (Meier and Zierler, 1954; Stewart, 1984).

Since DWI and DSC MRI are increasingly used to determine abnormal and pathologic water diffusion and cerebral blood circulation, respectively, a comprehensive study assessing diffusion and perfusion parameters in a representative healthy population is essential for the more quantitative comparison of disease states with healthy brains. In addition, the feasibility of DWI and DSC MRI to detect changes in diffusion and brain perfusion induced by CS, CEA, and LA has previously received too little attention.

# REVIEW OF THE LITERATURE

## HEALTHY BRAIN

The central nervous system (CNS) consists of the cerebrum, cerebellum, brain stem, and spinal cord. The cerebrum is divided into four lobes in both hemispheres, the frontal, temporal, parietal, and occipital lobes, each of which consist of a cerebral cortex with neurons (gray matter, GM) and WM with axons (Netter, 1991). The WM forms fibers and tracts from the cerebrum to the brain stem and spinal cord (Fitzek et al., 2001). The cerebral cortex has a higher water content and a substantially higher blood flow than the WM (de Groot and Chusid, 1991). Inside the brain is the ventricular system, which contains cerebrospinal fluid (CSF) that is formed in the choroid plexuses of the ventricles and drains through the arachnoid granules into the venous system (Netter, 1991).

The brain receives its blood supply from four main arteries, two common carotid arteries and two vertebral arteries. Carotid arteries are divided into internal (ICA) and external carotid arteries (ECA), the former of which is mainly responsible for circulation in the anterior parts of the brain. The main branches of ICA are the anterior (ACA) and middle cerebral arteries (MCA), supplying the frontal lobes and parts of the parietal and temporal lobes of the brain. The basal ganglia and thalamus are also partly supplied by these arteries and their branches. Vertebral arteries unite to form the basilar artery, which sends two posterior cerebral arteries (PCA) supplying the posterior parts of the brain, brain stem, and cerebellum. Branches of the PCA also supply the occipital lobes and the posterior parts of the temporal lobes (Tatu et al., 1996; 1998). The blood drainage occurs via the cerebral venous system. This unites the small venules to the large venous sinuses of the subarachnoidal space; the largest of these are the superior sagittal sinus, cavernous sinus, straight sinus, sigmoid sinus, transverse sinus, and the confluence of the sinuses. Finally, the sinuses drain into two internal jugular veins, which drain into the subclavian vein (Netter, 1991).

Fortunately, additional branches of collateral arteries supply the territories of the main arteries discussed above. The collateral arteries are important in the survival of brain tissue when blood supply is diminished in the region of a main artery either acutely due to thromboembolism of the artery or chronicly due to tight CS. As the GM receives leptomeningeal collateral supply, it survives better than the WM in chronic ischemic disturbances such as CS. The thalamus receives lenticulostriate branches from the MCA, anterior choroidal branches from the ICA, and posterior choroidal branches from the PCA. Generally, the collateral supply is highly variable between humans, explaining the

different sizes of brain infarcts sustained after occlusion of the feeding artery, which can jeopardize the patient's life (Netter, 1991; Tatu et al, 1996; 1998).

CBF is approximated to be 45-55 mL/100 g/min (Lassen, 1985). In the GM, it is about 80 mL/100 g/min, and in the WM 20 mL/100 g/min. In other parts of the brain, the blood flow depends of the amount of GM and WM and their distribution.

## AGING

With age, neuronal cell loss occurs in many regions of the brain, but this change is not a universal phenomenon. The pattern of cell loss in healthy people is also different from that observed in such diseases as Alzheimer's disease (AD). As neuroplasticity can be detected in the normal aging brain, it may, at least partly, compensate the age-related neuronal loss. The average neuron and water content of the brain, i.e. the average brain weight, declines with age, resulting in sulcal widening and ventricular enlargement. However, a wide variation exists among subjects. The intracellular pigments lipofuscin and neuromelanin accumulate in several regions of the brain, and even the typical AD-change, the appearance of extracellular amyloid deposits, may occur in the normal aging brain. In neurotransmitter systems, the effect of age is not fully understood. Cholinergic, adrenergic, serotonergic, and dopaminergic neurotransmitters seem to decrease with age, but the effect of diseases on the levels of these neurotransmitters may have interfered with the results for healthy people in previous studies. Atherosclerotic changes, an increase in connective tissue, and the thickening of intima cause the blood vessels to become more rigid, elongated, and tortuous with age. Expansion of perivascular spaces (Virchow Robin space), the formation of lacunae, and changes in the WM (LA) are also frequent findings in elderly people (Mrak et al., 1997; Hamill and Pilgrim, 2000).

In addition to autopsy studies, various imaging methods have been used to examine age-related changes in the human brain. The findings have been variable, from a clear correlation between age and changes in cerebral anatomy and physiology to no correlation at all. Generally, though, the WM lesions, LA, and amount of CSF have been found to increase, the cortical and deep GM to remain fairly constant, and the brain surface area and amount of WM to decline with age (Agartz et al., 1992; Chang et al., 1996; Salonen et al., 1997; Silver et al., 1997; Guttmann et al., 1998). All of these changes may alter the results of imaging studies (Agartz et al., 1991; Breger et al., 1991; Bakshi et al., 2000), supporting the need for using age-matched controls in studies of brain diseases.

### GENDER

The search for gender-related differences in cerebral anatomy and physiology has been extensive, with negligible or highly variable results. The findings of some studies of small differences in the amounts of GM, WM, and CSF, and women having more GM and less WM and CSF (Gur et al., 1999) or higher fractional anisotropy in WM (Szeszko et al., 2003) than men, have not received support from other reports (Agartz et al, 1992; Silver et al, 1997). Nevertheless, the use of gender-matched controls in addition to age-matched ones is recommended for more reliable comparison of disease states and normal brains.

## ISCHEMIC STROKE

### EPIDEMIOLOGY

Each year about 12,000 people suffer a stroke in Finland, and about 5,000 of them die either acutely or during the first year after the insult (Fogelholm et al, 1997). Stroke is the third leading cause of death in Finland and in most other industrialized countries and is the leading cause of disability. The economic burden to society due to hospitalization and long-term disability is tremendous. Furthermore, one-third of strokes occur in working-aged people, being a more common cause of early retirement in Finland than ischemic heart disease. Stroke is defined as an abrupt focal or global neurological syndrome caused by ischemia or hemorrhage. By definition, these symptoms must continue for more than 24 hours or result in death to qualify for the diagnosis of stroke. More than 80% of all strokes are ischemic, and the remainder is either intracerebral or subarachnoid hemorrhages. In the following paragraphs, the term stroke refers solely to ischemic stroke; the risk factors, pathophysiology, clinical aspects, and management of intracerebral and subarachnoid hemorrhages will not be discussed.

Risk factors for ischemic stroke are well-defined and overlap those of ischemic heart disease. While many of these factors are modifiable, others, like age and gender, are not. Hypertension is the most important modifiable risk factor, followed by smoking and hyperlipidemia. Patients with heart disease (chronic atrial fibrillation, myocardial infarction, valvular heart disease, or congestive heart failure) (Takahashi et al., 2002), CS, transient ischemic attacks (TIA), silent brain infarcts (Jørgensen et al., 1994), diabetes, obesity, physical inactivity, recent infection, excessive alcohol intake, disturbances in hemocoagulation, elevation of plasma fibrinogen, antiphospholipid antibodies, and anticardiolipin antibodies are known to have an increased risk for stroke. The postpartum phase of pregnancy, vasculitis, collagenoses, CADASIL (cerebral autosomal dominant

arteriopathy with subcortical infarcts and leukoencephalography), and homocysteinuria also increase the risk. The roles of elevated plasma homocysteine, oral contraceptives, and hormone-replacement therapy after menopause remain obscure. Most modifiable risk factors express themselves by accelerating atherosclerosis. Non-modifiable risk factors, such as older age, male sex, family history, and genetics, do not themselves cause atherosclerosis, but increase risk all the same (Biller and Love, 2000; Bogousslavsky et al., 2000).

## PATHOPHYSIOLOGY

Acute focal or diffuse cerebral ischemia initiates a cascade of complex biochemical events. Cerebral ischemia is caused by the interruption of CBF to the microcirculation, after which glucose and oxygen transport diminishes. Impairment of brain energy metabolism follows, leading to loss of aerobic glycolysis, and further, to intracellular accumulation of sodium and calcium ions, release of excitotoxic neurotransmitters, elevation of lactate levels with local acidosis, free radical production, cell swelling, overactivation of lipases and proteases, and finally, to cell death. Many affected neurons undergo apoptosis after brain ischemia, and ischemic brain injury is exacerbated by leukocyte infiltration and development of brain edema (Dirnagl et al., 1999).

Interruption of CBF causes suppression of electrical activity within seconds and inhibition of synaptic excitability within minutes, followed by inhibition of electrical excitability and then cell death. When CBF is focally decreased below 18 mL/100 g/min, the brain tissue reaches a threshold of electrical failure, and when flow is decreased below 8 mL/100 g/min, the threshold of membrane failure is approached and cell death may occur. The region between these two thresholds marks the upper and lower limits of the ischemic penumbra, the area of poor perfusion, in which the neurons are functionally silent but structurally intact and potentially salvageable with hyperacute management (see thrombolysis below) (Astrup et al., 1981). The region below the lower threshold is called the ischemic core, with the occurrence of irreversible cell death, i.e. brain infarct (Hossmann, 1994).

In autopsy studies, the changes induced by ischemic stroke can be seen clearly six hours after the insult. Initially, the neurons swell, then they shrink and become hyperchromatic and pyknotic. Chromatolysis appears, the nuclei become eccentric, and the surrounding astrocytes swell and fragmentate. In focal blood vessels, the endothelial cells swell and the neutrophils begin to infiltrate the ischemic lesion. Within 48 hours, the microglia proliferate, ingest the products of the neuronal and astrocyte breakdown, and form macrophages. The process of neovascularity with the proliferation of capillaries

begins. The ischemic core is gradually reabsorbed, and a cavity of glial and fibrovascular elements forms. In large ischemic lesions, the cavity finally consists of three different zones: an inner area of coagulative necrosis, a medial zone of vacuolated neutrophils, leukocytic infiltrates, swollen axons, and thickened capillaries, and an outer zone of hyperplastic astrocytes and variable changes in nuclear staining (Biller and Love, 2000).

## CLINICAL ASPECTS

Stroke manifests clinically with a wide variety of symptoms, depending on the size and location of the lesion. A lesion in the carotid territory (anterior circulation) presents with contralateral hemiparesis, hemianesthesia, dysphasia or hemineglect depending on the side of the lesion, conjugate eye deviation to the side of the ischemic lesion in large infarcts, and/or homonymous hemianopia. Stroke in the vertebrobasilar territory (posterior circulation) is associated with hemianopia, cortical blindness, vertigo, nausea, ataxia, nystagmus, gaze palsies, dysarthria, and a variety of other symptoms caused by lesions in the nuclei of cranial nerves. In addition to symptomatic lesions, asymptomatic lesions are fairly common, especially among older subjects.

The classification of etiology of the ischemic stroke has been done in several ways in the literature. One of the most useful and reliable is the TOAST (the Trial of Org 10172 in Acute Stroke Treatment) criterion (Adams et al., 1993; Gordon et al., 1993), which includes five different categories of likely etiology. These are stroke due to 1) large-artery atherosclerosis, 2) cardioembolism, or 3) small-vessel occlusion, 4) stroke of other determined etiology, such as carotid dissections, and 5) stroke of undetermined etiology. The classification and search for the etiology underlying ischemic stroke are important, as the etiology affects outcome, management, and secondary prevention of stroke.

CT has been used for the diagnosis of stroke for almost three decades and is still the method of choice in most centers. It is widely available and inexpensive and has a good sensitivity in detecting fresh blood, thus differentiating ischemic lesions from hemorrhagic ones. However, increasingly available worldwide, MRI offers an even more accurate method for the diagnosis of acute stroke. The more accurate diagnosis allows for better management, making MRI a very attractive alternative (Shuaib et al., 1992). Additionally, the newer MRI techniques, DWI and PI, have created a whole new perspective to the diagnosis of hyperacute stroke (discussed below).

## MANAGEMENT

Since acute stroke is a medical emergency, management should be initiated before hospital admission by paramedics (Kaste et al., 2000). Unfortunately, one of the leading causes of failure in proper management is the late arrival of the patient to the hospital. Therefore, such informative procedures as campaigns directed at the public about symptoms and signs of stroke are important alongside the continuing education of paramedics (Kaste et al, 2000). General management of acute stroke includes monitoring and supporting the cardiorespiratory functions, maintaining glucose, fluid, and electrolyte balance, treatment of fever, and prevention and treatment of infections and seizures. While blood pressure is frequently elevated, it should not be treated too aggressively, since low blood pressure may worsen the cerebral perfusion, leading to worse outcome. Prophylaxis of deep venous thrombosis is recommended. Depression and other related medical problems should be treated where appropriate. Rehabilitation begins at the acute stroke unit and continues after discharge (Hacke et al., 2000; Kaste et al, 2000).

### THROMBOLYSIS

Despite the numerous compounds studied for neuroprotective therapy of acute stroke over the past two decades, none has thus far proven effective. The only effective treatment for clinical use is thrombolytic therapy with recombinant tissue plasminogen activator (rtPA). It accelerates fibrinolysis of the thrombus within the occluded artery, and, by recanalization of the occluded artery, helps restore blood flow to the ischemic region. Thrombolytic treatment leads to a favorable outcome when given to a patient fulfilling the criteria. These criteria include an ischemic stroke with the onset of symptoms occurring less than three hours earlier, a CT lesion not exceeding one-third of the MCA region, and therapy being initiated within three hours of stroke onset. The exclusion criteria include rapidly improving neurological signs, seizure, intracranial hemorrhage, hypoglycemia, hyperglycemia, any recent severe bleeding, recent myocardial infarction, recent head injury, earlier intracerebral or subarachnoidal hemorrhage, use of anticoagulants, any bleeding disorders, major surgery within the past two weeks, and high blood pressure (Hacke et al, 2000). The time window for thrombolytic treatment is generally accepted to be three hours after the onset of symptoms. However, a pooled analysis of ATLANTIS (Clark et al., 1999), ECASS (Hacke et al., 1995), and NINDS rtPA (The National Institute of Neurological Disorders and Stroke rt-PA, 1995) trials suggests that the time window may be longer (Kaste, 2003). In some centers, thrombolytic treatment has been successfully administered to patients with diffusion-perfusion mismatch even four hours after insult (Röther et al., 2002; Schellinger et al.,

2003) (see below). In such cases, it is essential that a clear demarcation of the irreversibly damaged ischemic core and the ischemic but still viable and thus salvageable tissue-at-risk-of-infarction is seen on DWI combined with PI and MRA or alternatively on CT combined with CT angiography and CT source image analysis (Schellinger et al, 2003).

### PREVENTION OF RECURRENCE OF STROKE

After an initial stroke, the preventive methods for recurrent strokes become even more important. Prevention can be divided into three categories, all of which are equally important, but with their relative importance differing between individual patients. These categories are antithrombotic therapy, risk factor management, and surgical management (CEA or carotid stenting). Antithrombotic agents lay the foundation for stroke prevention. The use of low-dose aspirin for stroke prevention is recommended (Barnett et al., 1996). This may be combined with dipyridamole for a possible additive effect, and multicenter studies for combining aspirin with clopidogrel are underway. Warfarin is indicated in stroke patients with atrial fibrillation and in some other specific subgroups of stroke patients, but may be replaced in the future by new drugs. The management of risk factors is the key to successful stroke prevention and must be planned carefully according to current medical knowledge (Bogousslavsky et al, 2000). Hypertension, hyperlipidemia, diabetes, various heart diseases, and possible hematologic diseases should be treated aggressively after the acute phase. The patient should be motivated to give up smoking and excessive consumption of alcohol, salt, and fat, and to increase physical activity and lose weight. Surgical management includes CEA, carotid stenting, and some experimental interventions. In the following paragraphs, the background and the basic concepts underpinning CEA are discussed.

## CAROTID STENOSIS AND ENDARTERECTOMY

### EPIDEMIOLOGY

One of the most common causes of ischemic stroke is artery-to-artery embolism, from tight CS to brain arteries. Approximately 15% of all strokes is caused by SCS. In addition to SCS, ACS is prevalent in the general population, especially in the elderly. However, when compared with SCS, ACS is associated with a relatively low risk for stroke.

Risk factors for CS overlap those of general atheroclerosis. Hypertension, hyperlipidemia, diabetes, infections, age, obesity, smoking, excessive alcohol intake, and physical inactivity all increase the risk for atherosclerotic changes in carotid arteries. Risk

factors should be treated rigorously for decreasing the risk for stroke. However, treatment of hypertension in very tight CS or occlusion should not be too aggressive due to increased risk for cerebral ischemia induction (Biller and Love, 2000).

## PATHOPHYSIOLOGICAL AND CLINICAL ASPECTS

Tight CS and occlusion may compromise cerebral hemodynamics. While the failure in hemodynamics has traditionally been associated with the symptomatic status of CS, its role is still controversial (Klijn et al, 1997) and far less important than embolic seeding from CS. The degree of CS correlates poorly with the perfusion pressure of the brain, and many studies have been unable to detect any significant hemodynamic abnormality in the majority of patients with high-grade CS (Powers et al., 1987; Powers, 1991; Nighoghossian et al., 1994). However, several other reports have indicated the importance of cerebral hemodynamics in association with the risk of ischemic stroke in patients with CS or occlusion (Silvestrini et al., 1996; Yamauchi et al., 1996; Markus and Cullinane, 2001; Vernieri et al., 2001).

## MANAGEMENT

In patients with SCS, the benefit of CEA on final outcome has been established in large randomized trials (North American Symptomatic Carotid Endarterectomy Trial, 1991; European Carotid Surgery Trialists', 1998). Because of reduced risk for artery-to-artery embolism, CEA may also ameliorate the hemodynamic state, as suggested by postoperative improvement in cerebrovascular reactivity and CBF (Vanninen et al., 1995; Kluytmans et al., 1998a; Wiart et al., 2000; Markus and Cullinane, 2001; Rutgers et al., 2001). Several studies including both ACS and SCS patients have detected hemodynamic melioration after CEA (Hartl et al., 1994; Kluytmans et al, 1998a; Wiart et al, 2000; Rutgers et al, 2001), but some findings suggest differences in hemodynamics between these patient populations (Silvestrini et al, 1996; Derdeyn et al., 1999). CEA is beneficial in patients with a surgically accessible SCS of over 70%, who are otherwise healthy, and have had hemispheric TIAs or minor hemispheric infarcts (Barnett et al., 2002). In carefully selected patients, an early CEA (<four weeks after stroke) was found to be beneficial in preventing carotid occlusions and recurrent strokes and reducing costs of medical care (Kahn et al., 1999).

In ACS patients, the advantage of CEA is less clear (Chambers et al, 2002). In this subgroup, because CEA appears to offer only a marginal benefit, surgeons must have an

exceptionally low complication rate. Therefore, the current preferred treatment for this patient group is medical. However, a subgroup of ASC patients may benefit more strongly from CEA, but the characteristics of such a group have not yet been determined (Barnett et al, 2002). In patients with total or subtotal carotid occlusion, the choice of treatment is even more challenging (Klijn et al, 1997).

Despite information about the utility of CEA in different subgroups, the counseling of individual patients is difficult because of the wide spectrum of individual comorbidities and possible outcomes (Bogousslavsky et al, 2000; Bamford, 2001). The future management of CS may change based on results of ongoing and forthcoming studies with functional imaging techniques (PI, positron emission tomography (PET), single photon emission computed tomography (SPECT), and CT perfusion imaging) since all previous multicenter studies have been founded on the anatomy of the carotid artery imaged with traditional angiography, and not the functional state of the brain.

## LEUKOARAIOSIS (LA)

### EPIDEMIOLOGY

The term LA or Binswangers disease (Babikian and Ropper, 1987) refers to radiological findings of bilateral and either patchy or diffuse areas of hypodensity of the WM on CT or hyperintensity on T2-weighted MRI (Hachinski et al, 1987). LA is a common finding, and its frequency in older patient groups has ranged between 21% and 100% depending on the imaging method used and the study population (Pantoni and Garcia, 1995); its exact frequency is still under debate since no agreement between the various LA rating scales exists between centers (Mäntylä et al., 1997; Scheltens et al., 1998; Pantoni et al., 2002), and CT and different sequences of MRI detect LA differently (Mäntylä et al., 1999a). Thus, classification of leukoaraiotic lesions remains problematic.

Risk factors for LA in part overlap those for ischemic stroke (Pantoni and Garcia, 1995). Risk increases with age, especially beyond the age of 65 years, even in neurologically and neuropsychologically healthy subjects (Pantoni and Garcia, 1995; Mrak et al, 1997; Shintani et al., 1998; van Gijn, 1998; Hamill and Pilgrim, 2000; Longstreth et al., 2001). Failure of blood supply in the small arteries of the brain (Oishi and Mochizuki, 1998), chronic brain ischemia due to various reasons, diabetes (Pantoni and Garcia, 1995; Mäntylä et al., 1999b), brain blood pressure dysregulation, and especially high systemic pressure (Matsubayashi et al., 1997; Shintani et al, 1998; Wiszniewska et al., 2000) are associated with LA. Disturbed flow of CSF (Pantoni and Garcia, 1997) increases periventricular WM changes, and LA is found in AD, in vascular dementia (Barber et al.,

1999), and in several hereditary diseases including CADASIL (cerebral autosomal dominant arteriopathy with subcortical infarcts and leukoencephalography) (Pantoni and Garcia, 1995).

## PATHOPHYSIOLOGICAL AND CLINICAL ASPECTS

Chronic cerebral ischemia and hypoperfusion due to various reasons are thought to be the main etiologies for LA. However, the pathogenesis and clinical significance of LA are incompletely understood, and because the term LA overall is controversial in the literature, no universal conclusions can be drawn (Pantoni and Garcia, 1997). Some individuals, regardless of the severity of LA, remain neurologically and neuropsychologically asymptomatic for prolonged periods (Rao et al., 1989), while others develop cognitive impairment (Ylikoski et al., 1993; Breteler et al., 1994; Yamauchi et al., 2000), mood and psychiatric disorders, gait disturbance, urinary dysfunctions (Sakakibara et al., 1999), disability, and even dementia (Babikian and Ropper, 1987; Tarvonen-Schröder et al., 1996; Barber et al, 1999). In general, LA does seem to increase morbidity and mortality (Briley et al., 2000), and to enhance the risk for ischemic stroke (Pantoni and Garcia, 1995; Steifler et al., 2002; Inzitari, 2003).

In autopsy studies, leukoaraiotic regions have been found to consist of periventricular venous collagenosis (Moody et al., 1995; Brown et al., 2002), perivascular degeneration, arteriolar tortuosity (Brown et al, 2002), lacunar infarcts, incomplete infarctions, apoptosis (Brown et al., 2000; Brown et al, 2002), gliosis, axonal loss, and proliferation of glial cells (Pantoni and Garcia, 1997; Murdoch, 2000). Axonal loss leads to an increase in water content of affected brain tissue. The findings suggest that an inflammatory reaction, changes in myelin, and compromised axonal transport, all of which are affected in chronic ischemia, may play important roles in the pathophysiology of LA (Akiguchi et al., 1997; Kurumatani et al., 1998; Brown et al, 2002). Further support for the role of chronic ischemia comes from the markers of chronic endothelial dysfunction and prothrombic changes in LA patients (Hassan et al., 2003).

### MANAGEMENT

Although the prognosis of an individual LA patient is unpredictable, the prognosis of leukoaraiotic patients in general, especially in the most severe groups, is worse than for those without this condition (Briley et al, 2000). Therefore, the need for primary and secondary preventive measures is clear (Inzitari et al, 1997). As the etiology and pathogenesis of LA seem to be manifold, a single best course of treatment does not exist, but some basic guidelines can be followed. Since chronic brain ischemia is the most important etiology, preventive and management methods should be targeted against it (Pantoni and Garcia, 1995; Inzitari et al, 1997). Antithrombotic agents, such as aspirin with or without dipyridamole and clopidogrel, may represent an important component in prevention, especially in subjects with risk factors for vascular diseases. Equally important is aggressive treatment of risk factors for vascular diseases, hypertension, diabetes, dyslipidemia, and heart diseases, at the latest after the finding of severe LA lesions, and all subjects should be motivated to give up smoking and excessive consumption of alcohol. Therapies that help to stabilize the endothelium, such as statins and angiotensin converting enzyme inhibitors, may also have a role in treating patients with LA (Hassan et al, 2003).

## IMAGING METHODS

### PRINCIPLES OF MAGNETIC RESONANCE IMAGING (MRI)

MRI is based on measuring relaxation behavior of hydrogen atoms when these are placed in an external magnetic field and transiently perturbed with radiowaves at a suitable frequency. Hydrogen atoms with positively charged spinning nuclei are surrounded by dipolar magnetic fields. When placed into an external magnetic field, the nuclei align themselves with the magnetic field. Slightly over half of the nuclei align parallell and the rest antiparallell to the magnetic field. The net effect is a weak magnetic vector aligned in the direction of the external magnetic field – a phenomenon known as longitudinal magnetization.

The nuclei precess along the external magnetic field lines at a certain precession frequency. This frequency is dependent on the external magnetic field, which is usually 0.1-3 Tesla (T) in the MRI equipment used in human studies. The stronger the magnetic

field of the MRI equipment, the higher the precession frequency of the nuclei. This frequency can be calculated by using the Larmor equation as follows:

$$\omega_0=\gamma B_0$$

in which $\omega_0$ is the precession frequency, $B_0$ is the strength of the external magnetic field, and $\gamma$ is the gyro-magnetic ratio.

In MRI, a radiofrequency (RF) pulse at the same frequency as the precession frequency (calculated by the Larmor equation) is applied through the transmitter coil, and the nuclei that were aligned with the external magnetic field absorb the energy and reverse their direction. The longitudinal magnetization decreases, and as the nuclei begin to precess synchronically, a transversal magnetization is established. This produces a voltage (the magnetic resonance signal) in the receiver coil. The RF pulse is then switched off, allowing the nuclei to relax back to their original alignment.

The relaxation time, in which 63% of the magnitude of the original longitudinal vector is returned to its original alignment, is called T1 (spin-lattice) relaxation time (=longitudinal relaxation). Spin-lattice refers to the excited proton (spin) energy transfer to its surroundings (lattice) rather than to another spin. When the RF emission is switched off, the synchronic precession begins to disappear. The relaxation time at which 37% of the synchronic precession disappears is called T2 (spin-spin) relaxation time (=transversal relaxation). Spin-spin refers to the energy transfer from one excited proton to another. In biological tissues, T1 is about 300 to 2000 ms, and T2 about 30 to 150 ms; water having a substantially longer T1 and T2 than lipid-containing tissues.

In MRI, the object measured is a proton and its relaxation behavior. The proton measured in conventional MRI is the proton of a hydrogen atom since it is present abundantly in all tissues. Therefore, MR images are basically gathered from water and lipids in various tissues. An MR image represents a display of spatially localized signal intensities. These signal intensities are represented on the final image as points of relative brightness (hyperintensity) or darkness (hypointensity), depending on the strength of the magnetic field, imaging technique (pulse sequence), tissue characteristics (T1 and T2 relaxation times, the density of mobile protons), and other factors, such as magnetic susceptibility, chemical shift, diffusion, and blood flow. Images are T1-weighted, T2-weighted, or proton density-weighted depending on the pulse sequence characteristics, repetition time (TR), and echo time (TE) chosen. T1-weighting is produced by the choice of a short TE to minimize the effect of T2, along with a short TR. T2-weighting is accomplished when a long TR is combined with a long TE. A long TR with a short TE eliminates both T1 and T2 effects, and results in a proton density-weighted image.

Dephasing, produced by molecular interactions and spatial variation of the external magnetic field, shortens the measured T2, and is termed T2* (T2 star).

In MRI studies, many sequences are either spin-echo (SE) or gradient-echo (GE) based. In a SE sequence, a 90° RF pulse is followed by one or more 180° RF pulses to rephase the dephasing protons, thus resulting in one or more SEes. With this sequence, T1-weighted, T2-weighted, or proton density-weighted images can be achieved. In a GE sequence, a flip angle smaller than 90° is added, and instead of a 180° RF pulse, a gradient field, is added to the existing magnetic field. Whereas SE are more sensitive to microvasculature than GE, GE-based sequences exhibit better signal-to-noise ratios.

Being a paramagnetic substance, gadolinium diethylenetriaminepenta-acetic acid (Gd-DTPA) is used as a MR contrast medium. The contrast medium changes the signal intensity by shortening T1 and T2 in their surroundings. This results in a signal increase in T1-weighted images and a signal decrease in T2-weighted images. T1-weighted images are therefore preferred after contrast medium injection in conventional MRI (Stark and Bradley, 1992; Horowitz, 1995; Haacke et al., 1999).

MRI is contraindicated in subjects with ferromagnetic implants, material, or devices because of risks associated with possible movement or dislodgement of the object and potential hazards, including induction of an electric current, excessive heating, and misinterpretation of an artifact produced by the presence of the object as an abnormality. Factors that can influence the risk are strength of the static and gradient magnetic fields, degree of ferromagnetism of the object, mass and geometry of the object, location and orientation of the object in situ, and length of time that the object has been in its place. All of these factors should be carefully considered before a subject with a ferromagnetic object undergoes MRI (Shellock et al., 1993).

## DIFFUSION-WEIGHTED MAGNETIC RESONANCE IMAGING (DWI)

### METHODOLOGY

DWI provides an image contrast that is dependent on the molecular motion of water (diffusion), which is called Brownian movement. After Stejskal and Tanner (1965) described a DW SE T2-weighted pulse sequence with two extra gradient pulses equal in magnitude and opposite in direction, it took several decades for that sequence to become clinically feasible (Le Bihan et al, 1986) due to limitations of MR equipment.

In DWI, the water molecules in the magnetic field are labelled with rapidly changing magnetic gradients. Short but strong diffusion gradients are applied symmetrically before and after a 180° RF pulse in conventional SE T2-weighted sequence. According to Fick's law, true diffusion is the net movement of molecules due

to a concentration gradient. With MRI, however, molecular motion due to concentration gradients cannot be differentiated from molecular motion due to pressure gradients, thermal gradients, ionic interactions, or perfusion. Therefore, when measuring the molecular motion (diffusion) with DWI, only the ADC can be calculated. The ADC maps can demonstrate diffusion differences (or differences in signal intensities) in tissues without interference of these other matters. The signal intensity (SI) of a DW image is best expressed as

$$SI=SI_0 \times \exp(-b \times ADC)$$

where $SI_0$ is the signal intensity on a T2-weighted (b=0) image, and

$$b=\gamma^2 G^2 \delta^2 (\Delta - \delta/3)$$

where b is the diffusion sensitivity factor, $\gamma$ is the gyromagnetic ratio, G is the magnitude of gradient pulses, $\delta$ is the gradient duration, and $\Delta$ is the time between two balanced gradient pulses.

With the development of high-performance gradients, DWI has become clinically feasible. It can be performed with a SE echo-planar imaging (EPI) sequence, a sequence that markedly decreases imaging time and motion artifacts, and increases sensitivity to signal changes due to molecular motion. Most clinically used MR equipment are capable of EPI. However, EPI may be associated with distortions (Haselgrove and Moore, 1996), N/2 ghost images, susceptibility/chemical shift artifacts, and eddy current artifacts (Edelman et al., 1994; Jezzard et al., 1998), especially if the systems are unstable or unoptimized. Other methods performing DWI with and without echo-planar gradients have also been developed (Brockstedt et al., 1998; Bammer et al., 1999).

Diffusion is not isotropic (same in all directions) in biological tissues since water diffuses more easily along the direction of myelinated tracts rather than across them (diffusion anisotropy) (Harada et al., 1991; Sakuma et al., 1991). Because cellular structures are distributed anisotropically, the measurement of diffusion is also direction-dependent (Sakuma et al, 1991), emphasizing the need for measuring diffusion in several directions. Thus, to obtain a rotationally invariant estimate of isotropic diffusion, DW images must be acquired in at least three orthogonal directions (Ulug et al., 1997). The postprocessing of these images begins with the calculation of the natural logarithms of the images, which should be averaged to form a rotationally invariant resultant image. Using a linear least-squares regression on a pixel-by-pixel basis, the resultant image and the natural logarithm of the reference T2-weighted image are fitted to the b values (see below). The negative slope of the fitted line is the average ADC ($ADC_{av}$).

Diffusion-weighting is expressed by a b value, which is dependent on the sequence characteristics. The b value increases with increasing diffusion-weighting. Sufficient diffusion-weighting is usually achieved with b values of 800-2000 s/mm$^2$, 1000 being the most common clinically used b value. However, in some studies, the optimal b value for contrast in, for example, acute ischemic lesions has been found to be 1662, so a b value of 1500 may be better than the standard b value of 1000 (Pereira et al., 2002). Quantitative measurements of ADC (and $ADC_{av}$) depend on b values (Yoshiura et al., 2001; Wilson et al., 2002). $ADC_{av}$ estimates with two b values (usually b=0 and b=1000) have been found to be adequate for measuring diffusion in the human brain, as they provide good agreement with $ADC_{av}$ estimates with six b values (Xing et al., 1997; Burdette et al., 1998) and shorten the imaging time substantially.

## IMAGING OF THE HEALTHY BRAIN

The $ADC_{av}$ values in the healthy human brain have been found to range between 0.8 and 1.4 x10$^{-3}$ mm$^2$/s in the cortical GM, 0.6 and 0.9 x10$^{-3}$ mm$^2$/s in the WM, 0.7 and 1.1 x10$^{-3}$ mm$^2$/s in the basal ganglia and thalamus, and 2.2 and 3.3 x10$^{-3}$ mm$^2$/s in the CSF (Chien et al., 1990; Le Bihan et al., 1992; Gideon et al., 1994; Falconer and Narayana, 1997; Engelter et al., 2000b; Tanner et al., 2000) (Table 1). With age, these values appear to remain fairly constant in the cortical GM and to increase in the CSF, whereas in the WM, basal ganglia, and thalamus, the findings have varied considerably, and no firm conclusions can be drawn (Gideon et al, 1994; Engelter et al, 2000b; Chen et al., 2001; Nusbaum et al., 2001; Rovaris et al., 2003). In neonates with incomplete myelination of the brain, $ADC_{av}$ values are clearly higher than in adults, especially in the WM (Toft et al., 1996; Neil et al., 1998; Tanner et al, 2000; Zhai et al., 2003). During maturation of the brain $ADC_{av}$ values decrease to the level of those in the adult brain. No studies have reported differences between the genders based on $ADC_{av}$ values.

Quantitative measurements of $ADC_{av}$ values for normal and pathologic structures are important when either focal or diffuse abnormalities are suspected because minor changes may be difficult to detect visually. However, the normal and absolute $ADC_{av}$ values may differ between centers, as several factors affect these values. The variability in measurement protocols, imaging characteristics, and sequence characteristics (b value, diffusion time, gradient strength, TE, TR, cardiac gating) may influence $ADC_{av}$ values considerably (Yoshiura et al, 2001; Wilson et al, 2002) and must be considered when comparing values between centers and studies.

| Reference | N M/F | Age Years | GM | WH | BG/THA | CSF |
|---|---|---|---|---|---|---|
| Chien et al., 1990 | 13 / 5 | 20-35 | 1.0±0.2 | 0.7±0.1 | na | 2.2±0.2 |
| Engelter et al., 2000 | 16 /16 | 24-80 | na | 0.7±0.0 | 0.7±0.0 | na |
| Falconer et al., 1997 | 6 / 0 | na | 0.9±0.1 | 0.9±0.0 | 1.0±0.2 | na |
| Gideon et al., 1994 | 11 / 6 | 22-76 | 1.4±0.2 | 0.6±0.2 | 1.1±0.3 | 3.1±0.2 |
| Le Bihan et al., 1992 | review | na | 0.8±0.0 | 0.9±0.1 | na | 2.9±0.1 |
| Tanner et al., 2000 | 5 / 0 | 20-30 | 0.9±0.2 | 0.8±0.1 | na | 3.3±0.5 |

**Table 1.** $ADC_{av}$ values ($x10^{-3}$ $mm^2/s$) ± SDs of the healthy human brain. GM=gray matter, WM=white matter, BG=basal ganglia, THA=thalamus, BG/THA=BG and/or THA, CSF=cerebrospinal fluid, M=males, F=females, na=data not available.

### IMAGING OF ISCHEMIC STROKE

DWI reveals acute ischemic regions in the brain as bright areas within 2-3 minutes of focal ischemia induction in experimental stroke models (Moseley et al., 1990; Röther et al., 1996; Li et al., 1999; Hoehn et al., 2001), and as soon as an acute stroke patient is available for imaging studies (Baird and Warach, 1998; Gonzalez et al, 1999). In hyperacute stage (<6 hours), it is superior to CT and conventional MRI for diagnosing stroke (Warach et al., 1992; Lutsep et al., 1997; van Everdingen et al., 1998; Gonzalez et al, 1999; Fiebach et al., 2002; Mullins et al., 2002; Saur et al., 2003), and is especially useful in differentiating acute ischemic lesions from chronic ones (Marks et al., 1996; Singer et al., 1998; Lindgren et al., 2000; Oliveira-Filho et al., 2000). It even detects small (4 mm) and neurologically silent lesions, which often remain undiagnosed by CT or conventional MRI (Warach et al., 1995; Britt et al., 2000; Fiebach et al, 2002).

A rapid decrease in $ADC_{av}$ values occurs in acute brain ischemia (Warach et al, 1992; Burdette et al., 1999; Weber et al., 2000; Hoehn et al, 2001; Ahlhelm et al., 2002). Thus, hyperacute and acute ischemic lesions of the brain appear hypointense on the $ADC_{av}$ maps. The $ADC_{av}$ values of the ischemic lesion begin to increase over 5 to 10

| Reference | N | Time after Stroke Onset | | | | |
|---|---|---|---|---|---|---|
| | | **<6 H** | **6-48 H** | **2-14 D** | **15-60 D** | **>60 D** |
| Ahlhelm et al., 2002 | 52 | 0.3±0.6 | 0.2±0.7 | 0.3±0.2 | na | 2.0±na |
| Latour et al., 2002 | 31 | 0.6±0.1 | na | na | na | na |
| Lutsep et al., 1997 | 26 | 0.3±0.3 | 0.6±0.1 | 0.5±0.2 | 1.6±0.9 | 2.6±0.4 |
| Marks et al., 1996 | 29 | na | 0.4±0.1 | 0.4±0.1 | 1.6±0.8 | na |
| Schlaug et al., 1997 | 101 | 0.5±0.2 | 0.5±0.1 | 0.6±0.1 | 1.5±0.2 | na |
| van Everdingen et al., 1998 | 42 | na | na | 0.7±0.1 | na | na |
| Warach et al., 1995 | 40 | 0.5±0.2 | 0.4±0.2 | 0.5±0.2 | 1.9±0.6 | na |

**Table 2.** $ADC_{av}$ values ($x10^{-3}$ $mm^2/s$) ± SDs of ischemic strokes of various ages. N=number of included patients, na=data not available, H=hours, D=days.

days, approaching normal brain $ADC_{av}$ values, a phenomenon called pseudonormalization (Warach et al, 1995; Burdette et al, 1999; Ahlhelm et al, 2002). At this stage, the ischemic lesion disappears on DW images. In chronic brain infarcts, the $ADC_{av}$ values are substantially higher than those of normal brain tissue (Warach et al, 1992; Weber et al, 2000; Ahlhelm et al, 2002), as diffusion in necrotic regions approaches that of free water due to cavitation and replacement of brain tissue with water. The typical increase of $ADC_{av}$ values over time after acute ischemic stroke occurs, however, slower in small lacunar lesions (Geijer et al., 2001).

The $ADC_{av}$ values of ischemic stroke in hyperacute phase (<6 hours) have been found to range between 0.29 and 0.64 $x10^{-3}$ $mm^2/s$, in acute phase (<48 hours) between 0.15 and 0.63 $x10^{-3}$ $mm^2/s$, in subacute phase (<2 weeks) between 0.34 and 0.73 $x10^{-3}$ $mm^2/s$, in recent chronic phase (<2 months) between 1.5 and 1.9 $x10^{-3}$ $mm^2/s$, and in later chronic phase (>2 months) >2.0 $x10^{-3}$ $mm^2/s$ (Warach et al, 1995; Marks et al, 1996; Lutsep et al, 1997; Schlaug et al., 1997; van Everdingen et al, 1998; Ahlhelm et al, 2002; Latour and Warach, 2002) (Table 2).

DWI has become an essential part of the clinical imaging of patients with hyperacute stroke, as it is a reliable tool in weighing the possibilities for active intervention with thrombolytic therapy. The lesion seen on the hyperacute DW images generally predicts the lesion core, the region of irreversible damage. However, reversal of the DW image lesion back to normal without intervention has also been seen (Grant et al., 2001; Fiehler et al., 2002a; Fiehler et al., 2002b), although this does not confirm that the ischemic lesion tissue has fully recovered (Li et al, 1999). DWI lesion volumes have been said correlate with the final outcome of acute stroke (van Everdingen et al, 1998; Wardlaw et al., 2002). However, this depends on the time point of the DWI study: obviously, the correlation is better at later time points than in the hyperacute stages (Schellinger et al., 2001). The combination of DWI with clinical data and PI (see below) clearly increases the reliability of the prediction.

Limitations of the DWI in stroke imaging include possible overestimation of $ADC_{av}$ values due to risk of contamination of ischemic lesions with the CSF (Latour and Warach, 2002). This can be counteracted with the use of a CSF suppression technique (Latour and Warach, 2002) or with special care taken in selecting the regions of interest (ROI) near CSF spaces. In addition to the contamination risk, the ischemic lesions are heterogeneous, containing layers of decreased, pseudonormal, and increased pixels of $ADC_{av}$ values.

### IMAGING OF CAROTID STENOSIS AND ENDARTERECTOMY

DWI has a role in the imaging of CS and carotid occlusion patients, although its applicability to changes induced by these circumstances has been tested only recently and in a fairly small number of studies (Szabo et al., 2001; Kang et al., 2002; Kastrup et al., 2002). In these studies, the primary interest was on stroke patterns and visually detected ischemic lesions of such patients. Its role in investigating changes in diffusion parameters over time and its possibilities in differentiating ACS patients from SCS patients have not been studied. The stroke patterns of CS and occlusion patients are heterogeneous, but certain patterns seem to be more common (Szabo et al, 2001; Kang et al, 2002; Kastrup et al, 2002). Especially multiple embolic lesions and additional hemodynamic alterations within border zone regions appear to be overrepresented in these patient groups (Szabo et al, 2001; Kang et al, 2002; Kastrup et al, 2002).

The detection of minor and silent infarctions after CEA or carotid stent implantation is possible with DWI (Müller et al, 2000; Feiwell et al, 2001; Jaeger et al, 2002), but its ability to detect other changes induced by CEA has not been previously tested. CEA is known to be associated with the risk of cerebral embolization and hypoperfusion, and thus, is accompanied by a substantial number of small areas of brain

tissue-at-risk for irreversible ischemia (Müller et al, 2000). However, the incidence of silent ischemic lesions of embolic origin in DW images is low, confirming CEA to be a safe procedure for CS patients, when appropriately performed (Barth et al., 2000; Feiwell et al, 2001).

### IMAGING OF LEUKOARAIOSIS

DWI provides information on the extent and formation of LA and elucidates the mechanism of LA in vivo (Okada et al, 1999). On DW images, leukoaraiotic regions are hypointense and are therefore hyperintense on $ADC_{av}$ maps (Okada et al, 1999; Mascalchi et al., 2002a). Fractional anisotropy is decreased and $ADC_{av}$ values increased in these regions (Jones et al., 1999). Additionally, the whole brain ADC histogram seems to correlate with the severity of LA (Mascalchi et al., 2002b). As discussed earlier, LA is characterized by axonal loss and proliferation of glial cells (Pantoni and Garcia, 1997). Especially axonal loss, leading to an increase in water content of the tissue, may contribute to the $ADC_{av}$ increase since axons produce significant hindrance to water diffusion. The $ADC_{av}$ values of leukoaraiotic regions have been found to be around 1.2 $x10^{-3}$ $mm^2/s$ (Jones et al, 1999; O'Sullivan et al., 2001), but these values have not been extensively studied.

Besides the visually detected leukoaraiotic regions, DWI reveals changes in normal-appearing WM of subjects with LA (Jones et al, 1999; O'Sullivan et al, 2001; Mascalchi et al, 2002a). A change in the normal-appearing WM may be due to primary phases of relative hypoperfusion and chronic ischemia, even though these cannot be visually detected on conventional MR images. $ADC_{av}$ values of normal-appearing WM in patients with LA or another WM disease, multiple sclerosis (MS), range between 0.74 and 0.84 $x10^{-3}$ $mm^2/s$, and may even reach 1.1 $x10^{-3}$ $mm^2/s$, although in the case of very high $ADC_{av}$ values, one may suspect contamination of the ROIs with the leukoaraiotic lesions (Droogan et al., 1999; Jones et al, 1999; Cercignani et al., 2001; O'Sullivan et al, 2001; Caramia et al., 2002; Guo et al., 2002). $ADC_{av}$ values of normal-appearing WM of LA and MS patients were found to be substantially higher than those of healthy subjects (Table 3).

$ADC_{av}$ values of acute ischemic lesions of the brain are lower than those of normal-appearing WM or leukoaraiotic regions. As $ADC_{av}$ values of chronic brain infarcts are clearly higher than those of normal brain tissue and regions of LA, it seems

| Reference | N | Age (Years) | | | |
|---|---|---|---|---|---|
| | P / C | P / C | Disease | Patients | Controls |
| Caramia et al., 2002 | 19 /12 | 30 /30 | MS | 0.77±0.02 | 0.75±0.02 |
| Cercignani et al., 2001 | 30 /18 | 38 /38 | MS | 0.84±0.04 | 0.82±0.04 |
| Droogan et al., 1999 | 35 /12 | 44 /34 | MS | 0.78±na | 0.76±na |
| Guo et al., 2002 | 26 /26 | 40 /40 | MS | 0.74±0.04 | 0.73±0.04 |
| Jones et al., 1999 | 9 /10 | 62 /66 | LA | 1.1±0.3 | 0.75±0.1 |
| O'Sullivan et al., 2001 | 30 /17 | 70 /72 | LA | 0.79±0.04 | 0.75±0.04 |

**Table 3.** $ADC_{av}$ values ($x10^{-3}$ $mm^2/s$) ± SDs of normal-appearing WM in subjects with LA or multiple sclerosis. LA=leukoaraiosis, MS=multiple sclerosis, P=patients, C=controls, na=data not available.

that DWI may be useful in distinguishing ischemic stroke lesions of acute and chronic stage from regions of LA. Comparative studies are, however, rare in the literature (Calli et al., 2003).

### IMAGING OF OTHER DISEASES

Utility of DWI has been investigated in several diseases besides ischemic disorders. It has been found to be an especially useful method for the study of MS, a devastating progressive neurological disease of young adulthood (Droogan et al, 1999; Cercignani et al., 2000; Nusbaum et al., 2000; Schaefer et al, 2000; Cercignani et al, 2001; Guo et al., 2001; Caramia et al, 2002; Guo et al, 2002; Rovaris et al., 2002). Various dementias (Hanuy et al., 1998; Hanuy et al., 1999; Yoo et al., 2002), epilepsy (Helpern and Huang, 1995; Hugg et al., 1999), Parkinson's disease (Adachi et al., 1999), cerebral infections (Demaerel et al., 1999; Na et al., 1999; Schaefer et al, 2000), cystic abscesses, trauma (Schaefer et al, 2000; Arfanakis et al., 2002), tumors (Le Bihan et al, 1992; Kono et al., 2001), venous thrombosis (Chu et al., 2001), Creutzfeldt-Jakob disease (Demaerel et al., 2003), and hemorrhages (Schaefer et al, 2000) have also increasingly been studied with

DWI, and the results have been promising. DWI is an appropriate tool for neuropathological investigations in vivo, as it detects changes which have previously only been diagnosed at autopsy.

### DIFFUSION TENSOR IMAGING

As briefly discussed earlier, diffusion is a three-dimensional process, and molecular mobility is not the same in all directions in biological tissues. This phenomenon is called diffusion anisotropy. In the GM, diffusion is relatively isotropic, whereas diffusion in the WM is highly anisotropic due to the specific organization of the WM in bundles of more or less myelinated axonal fibers running in parallel. Since only the molecular displacement that occurs along the direction of gradient pulses is visible, the effect of diffusion anisotropy can easily be detected by observing variations in diffusion measurements after the direction of gradient pulses is changed. With diffusion tensor imaging, anisotropy effects can be extracted, characterized, and exploited, which provides more detailed information on tissue microstructure in healthy and diseased brains (Shimony et al., 1999; Sorensen et al., 1999b; Le Bihan et al., 2001). WM tracts can be followed from the cerebral cortex to the spinal cord, and the diseases involving these tracts can be studied (Pierpaoli et al., 1996; Conturo et al., 1999; Eriksson et al., 2002; Mamata et al., 2002). Diffusion tensor imaging makes the imaging of the diffusional changes in the brain even more accurate.

## PERFUSION MAGNETIC RESONANCE IMAGING (PI)

### METHODOLOGY

Brain perfusion refers to the microcirculation of the brain. Microcirculation comprises the blood circulation in capillary networks and the exchange of oxygen and nutrients between the blood and the brain tissue. The effectiveness of brain perfusion depends on blood pressure, blood velocity, characteristics of the capillary network, capillary wall permeability, and diffusion rates of oxygen and nutrients. In the healthy brain, perfusion is symmetrical, and higher in the GM than in the WM. Brain perfusion is usually quantified in terms of mL/100 g (CBV) (Belliveau et al, 1990; Rosen et al, 1991), mL/100 g/min (CBF) (Østergaard et al, 1996a; Østergaard et al, 1996b), or seconds (MTT, the CBV:CBF ratio) (Meier and Zierler, 1954; Stewart, 1984).

PI can be performed using susceptibility-based techniques (DSC MRI and blood oxygenation-level dependent imaging, BOLD) or arterial spin-labeling (Siewert et al.,

1997; Calamante et al., 1999; Vonken et al., 1999; Li et al., 2000; Barbier et al., 2001; Hoehn et al, 2001; Wang et al., 2002). DSC MRI with either SE- or GE-based sequences is mostly used clinically (Boxerman et al., 1995; Simonsen et al., 2000; Speck et al., 2000; Yamada et al., 2002), whereas BOLD imaging is largely utilized for cortical activation studies.

DSC MRI has shown promise in assessing cerebral perfusion since it is widely available, offers a good spatial and temporal resolution, does not expose subjects to ionizing radiation, is minimally invasive, and covers a large spatial volume. It is performed by combining the simultaneous use of Gd-DTPA, preferably in higher doses (>0.15 mmol/kg) than those used clinically (Griffiths et al., 2001), and a rapid collection of the MR signal during the passage of the Gd-DTPA bolus through the brain (Villringer et al, 1988). Gd-DTPA produces a strong susceptibility effect, extending approximately 5 μm from the capillaries to the brain tissue, and causes dephasing of the spins. The susceptibility difference between Gd-DTPA and the brain tissue sets up local magnetic field gradients, creating a loss of phase coherence and a decrease in signal intensity in the tissue surrounding the capillaries. This results in darkening of the images. In healthy brains, the signal intensity declines as Gd-DTPA reaches the brain, whereas in brain ischemia, the ischemic lesion remains bright, and a sharp contrast between normally perfused and hypoperfused regions can be seen. After a few seconds, Gd-DTPA is flushed away from the brain tissue, and the entire brain appears bright on subsequent images (Le Bihan, 1990; Hossmann and Hoehn-Berlage, 1995; Barbier et al, 2001; Cha et al, 2002).

The raw images obtained with DSC MRI have to be postprocessed for the determination of the absolute hemodynamic parameters, CBV, CBF, and MTT. Extensive postprocessing is needed for the more accurate measurement of perfusion changes in quantitative terms (Calamante et al, 1999); several methods to accomplish this have been tested (Perkiö et al., 2002). One of the most common of these is the deconvolution approach, described in detail in the Subjects and Methods section. The term deconvolution refers to the determination of CBF and MTT from arterial and tissue concentration time curves (Østergaard et al, 1996a). Different posprocessing methods give slightly different perfusion values (Smith et al., 2000; Wirestam et al., 2000), which have to be considered when comparing the results between centers and studies (Calamante et al, 1999; Vonken et al, 1999; Vonken et al., 2000).

DSC MRI data analysis for producing quantitative results has inherent limitations and thus far has not fulfilled the criteria of strict quantification (Weisskoff et al., 1993; Calamante et al., 2000; Kiselev, 2001; Sorensen, 2001; Calamante et al., 2002). For one thing, the quantitative analysis of perfusion data is based entirely on determining an arterial input function (AIF), which cannot accurately be determined by DSC MRI

(Perthen et al., 2002). Whereas the shape of the function can be determined with rather good accuracy, the height of the function remains arbitrary (Østergaard et al, 1996b). The proportionality factor relating MR signal change to concentration of Gd-DTPA is not equal in brain tissue and larger vessels. Therefore, the size of the AIF has to be normalized to the injected dose of Gd-DTPA to produce quantitative results. Further, the microvascular hematocrit is approximated to be two-thirds of the systemic blood hematocrit (Østergaard et al, 1996b). However, as a complex function of vessel size and physiological conditions is needed to calculate it, it may be subject-dependent. Since the hematocrit ratio is directly associated with the scale factor relating tissue first-pass area to the CBV, any errors in the hematocrit ratio are directly seen in the quantitative value of the CBV. In addition, the orientation of the MCA with respect to the main magnetic field has a major effect on the signal. Finally, a normalization factor for producing absolute CBF by DSC MRI has been introduced which compares MR CBF with PET CBF among normal subjects (Østergaard et al., 1998a; Østergaard et al., 1998b). However, the assumption that the same fraction of cardiac output reaches the brain of all subjects may not hold true with aging.

### IMAGING OF THE HEALTHY BRAIN

Brain perfusion of the normal human brain has been investigated for decades with different imaging techniques and variable results. Quantitative values have traditionally been studied with PET, a golden standard for absolute perfusion parameters, whereas relative values of the brain perfusion have been measured with DSC MRI and SPECT. One of the goals in DSC MRI methodology has, however, been the technical development for obtaining these absolute values. These values for healthy brain perfusion according to the literature concerning DSC MRI, PET, and $^{133}$Xe inhalation methods are as outlined in the next three paragraphs (Tables 4a-c). As seen in these paragraphs, the results are highly variable, and no method can be considered better than the others in determining these parameters.

The CBV in units of mL/100 g in the GM has been found to range between 4.1 and 6.5, and in the WM between 2.5 and 3.6, the ratio of GM to WM being 1.4-2.4 (Yamaguchi et al., 1986; Leenders et al., 1990; Nighoghossian et al., 1997; Petrella et al., 1998; Schreiber et al., 1998; Koshimoto et al., 1999; Vonken et al, 1999; Hunsche et al., 2002) (Table 4a).

The CBF in units of mL/100 g/min in the GM ranges between 37.3 and 89.1, and in the WM between 16.0 and 35.8, with the ratio of GM to WM being 1.7-5.2 (McHenry et al., 1978; Naritomi et al., 1979; Pantano et al., 1984; Yamaguchi et al, 1986;

| Reference | N M/N | Age Years | Modality | GM | WM | GM:WM |
|---|---|---|---|---|---|---|
| Hunsche et al., 2002 | 7 / 3 | 57±13 | DSC MRI | na | na | 2.0±0.3 |
| Koshimoto et al., 1999 | 8 /11 | 25-73 | DSC MRI | 4.1±0.8 | 2.9±0.4 | 1.4±na |
| Leenders et al., 1990 | 18 /16 | 22-82 | PET | 4.6±1.0 | 2.6±0.4 | 1.8±na |
| Nighoghossian et al., 1997 | 8 / 2 | 31-79 | DSC MRI | na | na | 2.4±na |
| Petrella et al., 1998 | 30 / 0 | 23-82 | DSC MRI | na | na | 1.9±na |
| Schreiber et al., 1998 | 13 / 0 | 24-68 | DSC MRI | 5.3±0.9 | 2.5±0.4 | 2.1±na |
| Vonken et al., 1999 | 41 / 0 | 40-86 | DSC MRI | 6.5±1.0 | 3.6±0.9 | 1.8±na |
| Yamaguchi et al., 1986 | 17 / 5 | 26-64 | PET | 4.1±0.5 | na | na |

**Table 4a.** CBV (mL/100 g) ± SDs of the healthy human brain. GM=gray matter, WM=white matter, GM:WM=the ratio of GM to WM, M=males, F=females, na=data not available, DSC MRI= dynamic susceptibility contrast MRI, PET=positron emission tomography.

Leenders et al, 1990; Herzog et al., 1996; Østergaard et al, 1996a; Nighoghossian et al, 1997; Schreiber et al, 1998; Koshimoto et al, 1999; Vonken et al, 1999; Meltzer et al., 2000; Wirestam et al, 2000; Hunsche et al, 2002) (Table 4b).

The MTT in units of seconds in the GM ranges between 2.6 and 6.8, and in the WM between 3.2 and 7.8, the ratio of GM to WM being 0.8-1.1 (Østergaard et al, 1996a; Nighoghossian et al, 1997; Schreiber et al, 1998; Koshimoto et al, 1999; Vonken et al, 1999; Hunsche et al, 2002) (Table 4c).

Age-and gender-related changes in perfusion parameters and cerebral hemodynamics in general have been found to be as variable as the absolute values. No firm conclusions can therefore be made, especially in connection with gender-related changes. However, some patterns in the changes with age do emerge. The CBV, both in the GM and in the WM, either decrease (Leenders et al, 1990; Marchal et al., 1992;

| Reference | N M/N | Age Years | Modality | GM | WM | GM:WM |
|---|---|---|---|---|---|---|
| Herzog et al., 1996 | 20 / 7 | 26±4 | PET | 83±20 | 16±3 | 5.2±na |
| Hunsche et al., 2002 | 7 / 3 | 57±13 | DSC MRI | na | na | 2.4±0.4 |
| Hunsche et al., 2002 | 7 / 3 | 57±13 | FAIR | na | na | 2.9±0.4 |
| Koshimoto et al., 1999 | 8 /11 | 25-73 | DSC MRI | 37.3±8.4 | 22±na | 1.7±na |
| Leenders et al., 1990 | 18/16 | 22-82 | PET | 52.1±11 | 20.3±3.7 | 2.6±na |
| McHenry et al., 1978 | 15 / 0 | 20-36 | Xe | 77.6±10.4 | 18.2±2.7 | 4.3±na |
| Meltzer et al., 2000 | 5 /13 | 29±7 | PET | 62±10 | na | na |
| Naritomi et al., 1979 | 26/20 | 21-63 | Xe | 89.1±7.3 | na | na |
| Nighoghossian et al., 1997 | 8 / 2 | 31-79 | DSC MRI | na | na | 2.4±na |
| Pantano et al., 1984 | 19 / 8 | 19-76 | PET | 50.7±10.3 | 24.5±4.1 | 2.1±na |
| Schreiber et al., 1998 | 13 / 0 | 24-68 | DSC MRI | 67.1±16.3 | 23.7±4.9 | 2.8±na |
| Wirestam et al., 2000 | 25/19 | 42-88 | DSC MRI | 68±28 | 36±13 | 1.9±na |
| Vonken et al., 1999 | 41 / 0 | 40-86 | DSC MRI | 66±20 | 34±11 | 1.9±na |
| Yamaguchi et al., 1986 | 17 / 5 | 26-64 | PET | 42.4±7.8 | na | na |
| Østergaard et al,1996 | 6 / 0 | 29±4 | DSC MRI | 58.9±na | 22±na | 2.7±na |

**Table 4b.** CBF (mL/100 g/min) ± SDs of the healthy human brain. GM=gray matter, WM=white matter, GM:WM= the ratio of GM to WM, M=males, F=females, na=data not available, DSC MRI= dynamic susceptibility contrast MRI, FAIR=flow-sensitive alternating inversion recovery, PET=positron emission tomography, Xe=$^{133}$Xe inhalation methods.

| Reference | N M/N | Age Years | Modality | GM | WM | GM:WM |
|---|---|---|---|---|---|---|
| Hunsche et al., 2002 | 7 / 3 | 57±13 | DSC MRI | na | na | 0.9±0.1 |
| Koshimoto et al., 1999 | 8 /11 | 25-73 | DSC MRI | 6.8±1.3 | 7.8±1.1 | 0.8±na |
| Nighoghossian et al., 1997 | 8 / 2 | 31-79 | DSC MRI | na | na | 1.1±na |
| Schreiber et al., 1998 | 13 / 0 | 24-68 | DSC MRI | 4.7±0.8 | 5.4±1.1 | 0.9±na |
| Vonken et al., 1999 | 41 / 0 | 40-86 | DSC MRI | 6.4±1.8 | 6.9±2.3 | 0.9±na |
| Østergaard et al.,1996 | 6 / 0 | 29±4 | DSC MRI | 2.62±0.6 | 3.19±0.93 | 0.8±na |

**Table 4c.** MTT (seconds) ± SDs of the healthy human brain. GM=gray matter, WM=white matter, GM:WM=ratio GM versus WM, M=males, F=females, na=data not available, DSC MRI= dynamic susceptibility contrast MRI.

Petrella et al, 1998; Koshimoto et al, 1999) or remain fairly constant (Yamaguchi et al, 1986; Marchal et al, 1992; Koshimoto et al, 1999) with age. The same tendency has been seen in the CBF of the GM, the CBF either decreasing (Naritomi et al, 1979; Pantano et al, 1984; Leenders et al, 1990; Martin et al., 1991; Marchal et al, 1992; Krausz et al., 1998; Koshimoto et al, 1999; Wirestam et al, 2000) or remaining fairly constant (Fujishima and Omae, 1980; Yamaguchi et al, 1986; Waldemar et al., 1991; Meltzer et al, 2000). The CBF of the WM, by contrast, either remains fairly constant (Pantano et al, 1984; Leenders et al, 1990; Marchal et al, 1992) or increases (Wirestam et al, 2000). The MTT has been the least studied parameter; however, it appears to increase with age (Fujishima and Omae, 1980).

### IMAGING OF ISCHEMIC STROKE

In DSC MRI, acute ischemic changes can be seen within minutes after induction of focal ischemia in experimental models (Hoehn et al, 2001). It is thought to be even more sensitive to these changes than DWI (Tong et al., 1998; Ueda et al., 1999b), to correlate

more closely with the acute neurological deficit (Tong et al, 1998), and to predict more accurately the size of final lesion (Fiehler et al., 2002c). Serial imaging with DSC MRI can document the evolution of perfusion lesion over time in experimental as well as in human studies (Barber et al, 1998; Beaulieu et al., 1999; Marks et al., 1999; Karonen et al., 2000). Perfusion deficit typically diminishes over time, in contrast to diffusion deficit (Barber et al, 1998).

By combining DWI with DSC MRI, the diagnosis of acute stroke becomes more accurate (Warach et al., 1996; Baird and Warach, 1998; Fisher and Albers, 1999; Karonen et al., 1999; Sorensen et al., 1999a; Ueda et al., 1999a; Neumann-Haefelin et al., 2000a; Fiehler et al., 2001; Wittsack et al., 2002; Schellinger et al, 2003). Typically, an early perfusion lesion is larger than an early diffusion lesion, a phenomenon called diffusion-perfusion mismatch (Baird et al., 1997; Barber et al, 1998; Rordorf et al., 1998; Tong et al, 1998). However, other patterns of acute lesions can also be seen. A perfusion deficit may sometimes be smaller or equal to the diffusion deficit (Barber et al, 1998). Thus, early identification of the clinically relevant lesion and differentiation between various stroke types are feasible with the analysis of diffusion-perfusion lesion patterns (Darby et al., 1999; Neumann-Haefelin et al, 2000a). DWI combined with DSC MRI facilitates the decision between management with and without thrombolytic therapy (Neumann-Haefelin et al., 1999; Sunshine et al., 1999; Warach, 2001; Parsons et al., 2002; Schellinger et al, 2003), even after the three-hour time window for thrombolysis (Barber et al, 1998; Albers, 1999; Parsons et al, 2002; Röther et al, 2002; Schellinger et al, 2003). While the diffusion deficit represents the ischemic core, which reflects irreversible damage in most cases, the more extensive perfusion deficit typically represents the penumbra, in which the neurons are functionally silent but structurally intact and therefore potentially salvageable with recanalization (Albers, 1999; Parsons et al, 2002; Schellinger et al, 2003). However, chronic hypoperfusion due to CS in the setting of acute ischemia may erroneously be attributed to acute thrombosis and be regarded as tissue-at-risk (Neumann-Haefelin et al., 2000b). In such cases, MRA demonstrating a tight CS without intracranial arterial occlusions should raise the suspicion of a chronic hypoperfusive state.

Studies of quantitative values for brain perfusion in ischemic lesions have been scarce and the results highly variable. Therefore, the relative values between the hypoperfused area and the normal-appearing contralateral region may be more reliable. The use of the contralateral region as a reference may, however, have limitations because of possible earlier ischemic or other lesions in these patients. Mean ratios for the ischemic lesion of the CBV have been found to vary between 0.69 and 0.89, of the CBF between 0.12 and 0.29, and of the MTT between 1.82 and 2.31 (Schlaug et al., 1999; Hunsche et al, 2002). The regions of hypoperfusion seen on the MTT maps are larger than on other

maps (Ueda et al, 1999b), and the MTT map is considered to be the most sensitive parameter for detecting the ischemic penumbra.

### IMAGING OF CAROTID STENOSIS AND ENDARTERECTOMY

CS and occlusion may compromise cerebral perfusion (Chaves et al., 2003; Kajimoto et al., 2003). However, the findings of several studies with different imaging methods (DSC MRI, PET, SPECT, $^{133}$Xe inhalation, and transcranial Doppler sonography) have varied markedly (Powers et al, 1987; Powers, 1991; Nighoghossian et al, 1994; Nighoghossian et al., 1996; Klijn et al, 1997; Derdeyn et al., 1998; Kluytmans et al., 1998b; Derdeyn et al, 1999; Maeda et al., 1999; Lin et al., 2001; Derdeyn et al., 2002; Chaves et al, 2003; Vanninen et al., 2003). This might be due to variability in patient selection or differences in the ability of imaging methods to detect hemodynamic changes. Generally, the risk for stroke in patients with tight CS and occlusion is increased (Silvestrini et al, 1996; Yamauchi et al, 1996; Markus and Cullinane, 2001; Vernieri et al, 2001), but the role of the degree of stenosis in increasing the risk in the ACS patients is debatable (see above).

CS or occlusion may interfere with the diffusion-perfusion mismatch of an acute stroke patient (Neumann-Haefelin et al, 2000b; Szabo et al, 2001). Proper management in such cases would depend on the suspicion of stenosis or occlusion behind the diffusion-perfusion mismatch by the physician, and imaging with MRA. An acute stroke patient who does not benefit from thrombolytic therapy thus receives it in vain and is exposed to possible complications.

When appropriately performed, CEA improves outcome of SCS patients, but its role in ASC is less beneficial, and its effect on cerebral hemodynamics over the long term is less clear. It seems to improve hemodynamic state, as suggested by postoperative improvement in CBF and cerebrovascular reactivity (Hartl et al, 1994; Vanninen et al, 1995; Kluytmans et al, 1998a; Wiart et al, 2000; Markus and Cullinane, 2001; Rutgers et al, 2001; Vanninen et al, 2003). However, some findings suggest that differences exist in hemodynamics between these patient populations (Silvestrini et al, 1996; Derdeyn et al, 1999), but heterogeneity in patient selection makes it difficult to draw definitive conclusions (Gillard et al., 1998).

DSC MRI seems to be a reasonable imaging method for detecting the changes caused by CS, carotid occlusion, and CEA (Nighoghossian et al, 1996; Reith et al., 1997; Schreiber et al, 1998; Lythgoe et al., 2000; Apruzzese et al., 2001; Doerfler et al., 2001; Lin et al, 2001; van Osch et al., 2002; Chaves et al, 2003; Kajimoto et al, 2003). It may even be possible to receive absolute perfusion parameters of changes induced by these disease states and the operation. However, DSC MRI may be more useful and reliable in relative measures, as could be expected on the grounds of earlier discussion.

### IMAGING OF LEUKOARAIOSIS

As the primary hypothesis for the etiology of LA is chronic ischemia of the brain, PI appears to be a suitable tool for investigating this state. Studies of LA with DSC MRI are few, but some preliminary conclusions can be drawn. The CBF seems to be the most sensitive perfusion parameter for leukoaraiotic changes. It is consistently lower both in leukoaraiotic regions and in normal-appearing WM of subjects with LA than in healthy controls (Markus et al., 2000; O'Sullivan et al., 2002), supporting hypoperfusion and chronic ischemia being involved in the pathogenesis of LA. Findings in other perfusion parameters have, however, been more variable (Oppenheimer et al., 1995; Markus et al, 2000). CS leading to hypoperfusion and thus to chronic ischemia of the brain has been suspected of inducing LA, and some studies support this expectation (Oppenheimer et al, 1995; Yamauchi et al., 1999). However, DSC MRI on LA is still in its early days, and further studies are needed.

### IMAGING OF OTHER DISEASES

DSC MRI detects changes in the microcirculation of brain tissue. Therefore, it is a suitable imaging method in studying diseases with disturbance in the cerebral circulation. Ischemic stroke is by far the most studied disease, but utility of DSC MRI in imaging other diseases, such as neoplasms (Cha et al, 2002), migraine (Cutrer et al., 1998; Sanchez del Rio et al., 1999), cerebral infections (Cha et al, 2002), and various dementias (Sandson et al., 1996; Alsop et al., 2000), has been reported. In neoplasms, DSC MRI may even preoperatively differentiate high- and low-grade tumors (Knopp et al., 1999), thus aiding in prognostic evaluation and management. It also seems to be useful in the study of MS, distinguishing active lesions from chronic ones (Haselhorst et al., 2000). As the methodology develops, DSC MRI may become a more attractive imaging method in studying various diseases of the brain, as it has the potential to provide physiologic information to complement the anatomic information provided by conventional MRI.

## AIMS OF THE STUDY

The purpose of this thesis was to test the feasibility of DWI and DSC MRI in studying the healthy human brain and in detecting changes induced by ischemic stroke, CS, CEA, and LA. The more detailed aims were:

1. To evaluate whether $ADC_{av}$ values, CBV, CBF, and MTT in selected regions of the healthy human brain differ with age, gender, or hemisphere, and to establish reference values for further studies of DWI and DSC MRI (Studies I and II).

2. To investigate $ADC_{av}$ values, CBV, CBF, and MTT before CEA, and 3 and 100 days afterwards to determine whether these values differ between hemispheres over time, and in ASC and SCS patient groups (Studies III and IV).

3. To assess whether $ADC_{av}$ values of leukoaraiotic regions or normal-appearing WM vary according to the severity of LA, and whether these values can be used to distinguish leukoaraiotic regions from normal-appearing WM and from ischemic strokes of various ages (Study V).

# SUBJECTS AND METHODS

## SUBJECT CHARACTERISTICS

The Ethics Committees of the Departments of Neurology and Radiology at Helsinki University Central Hospital approved all study protocols. Principles of the Declaration of Helsinki and institutional guidelines were followed. The subjects provided written informed consent before enrollment, after which they underwent thorough clinical assessment and detailed questioning regarding any symptoms. Those for whom MRI was contraindicated (Shellock et al, 1993) were excluded.

### HEALTHY SUBJECTS

Eighty volunteer subjects (40 males and 40 females) were chosen from a healthy adult population of the Helsinki region. They were 22 to 85 years of age, with a mean age of 50.0±17.4 years in Study I, and 49.9±17.4 years in Study II [49.9±17.2 (49.8±17.1), range 22-85 years for males and 50.1±17.9, range 22-82 years for females]. Their age distribution was uniform within each of the four age groups (10 males and 10 females per group): Group I: 20 to 34 years (mean 26.8±4.1, range 22-34 years), Group II: 35 to 49 years (mean 43.6±4.4, range 36-49 years), Group III: 50 to 64 years [mean 57.4±3.5 (57.3±3.8), range 52-64 (51-64) years], and Group IV: 65+ years (mean 72.2±5.2 (72.1±5.3), range 65-85 years]. Eight of the volunteers were left-handed, and 72 were right-handed.

None of the subjects had symptoms, signs, or history of any neurological or systemic disease that might have affected the brain (e.g. diabetes, chronic obstructive pulmonary disease, hypertension, or metabolic disorders), nor did they have a family history of dementia or MS. None was taking medication regularly, except for female hormones for replacement therapy or topical drugs. Subjects in whom MRI revealed an unexpected cerebral lesion (one meningeoma and one arteriovenous malformation) were excluded. WM changes (n=22, 16 in Group IV, and 6 in Group III) found in the conventional MR images of older subjects were regarded as a part of normal aging. All of the subjects were white and all except two were of Finnish origin.

In Study III, 45 individuals (28 males, aged 59.1±11.1, range 42-85 years, and 17 females, aged 66.9±8.5, range 52-82 years) with or without LA, and in Study V, 22

individuals (12 males, aged 59.9±6.3, range 52-70 years, and 10 females, aged 60.7±6.9, range 52-73 years) without LA on conventional MR images were chosen from the 80 healthy subjects described above for the comparative analyses.

## ISCHEMIC STROKE PATIENTS

Ten acute ischemic stroke patients (5 males, aged 64.4±17.9, range 48-88 years, and 5 females, aged 73.8±4.6, range 67-78 years) without thrombolytic therapy were serially imaged less than 6 hours (mean 4.4±1.0, range 2.7-5.9 hours, n=10), 24 hours (mean 28±2.7, range 23.8-31 hours, n=10), one week (mean 6.6±0.6, range 5.8-7.3 days, n=10), one month (mean 33±2.9, range 30-36 days, n=4), and 3 months (mean 90±5.8, range 80-95 days, n=6) after the insult. The mean infarct volume measured on the one-week images was 16.2±19 $cm^3$. Four of the infarcts were cortical and six were subcortical. According to the TOAST criteria (Adams et al, 1993), four of the infarcts were due to atherosclerosis, three were cardioembolic, two were caused by small vessel disease, and in one patient the etiology could not be determined. Five of them were left-sided and five right-sided.

## CAROTID STENOSIS AND ENDARTERECTOMY PATIENTS

Studies III and IV were conducted as part of the larger Helsinki Carotid Endarterectomy Study, which included 102 patients with high-grade CS. The patients of these two studies were independent in their daily lives (modified Rankin scale $\leq$ 2). They did not have emboli of cardiogenic origin or a history of previous CEA or radiotherapy for the neck or cervical region. They had a surgically accessible unilateral CS measuring 70% or more in digital subtraction angiography according to the NASCET criteria (North American Symptomatic Carotid Endarterectomy Trial, 1991). Due to artifacts in $ADC_{av}$ (n=2) or perfusion (n=2) maps, minor differences exist between patient populations of Studies III (n=45) and IV (n=46).

Of the 46 (45) [29 (28) males, 17 females] patients (mean age 64.6±8.6, range 48-78 years), 23 (22) [12 (11) males, 11 females; 65.0±8.6 (65.6±8.3), range 52-78 years] were asymptomatic, and 23 [17 males, 6 females; mean age 63.2±9.1 (63.7±9.0), range 48-78 years] had had recent cerebrovascular symptoms (average 39 days) ascribed to the territory of the stenotic artery. In the asymptomatic group, stenosis was on average 77±7.6%, and in the symptomatic group 80±10.9%, as measured from digital subtraction carotid artery angiograms by an experienced neuroradiologist (OS) blinded to the clinical

| | ACS | SCS | p value |
|---|---|---|---|
| **Age (years)** | 65.0±8.6 | 63.2±9.1 | 0.53 |
| **Degree of CS (%)** | 77±7.8 | 80±10.9 | 0.33 |
| **Cerebrovascular events:** | | | |
| Stroke | 0 | 11 | |
| TIA | 0 | 12 | |
| **Gender (males/females)** | 12 / 11 | 17 / 6 | 0.22 |
| **Arterial hypertension** | 14 | 16 | 0.56 |
| **Coronary heart disease** | 12 | 9 | 0.39 |
| **Diabetes** | 4 | 8 | 0.44 |
| **Peripheral arterial disease** | 9 | 7 | 0.59 |
| **Smoking** | | | |
| Never | 3 | 4 | |
| former | 15 | 13 | |
| Current | 5 | 6 | 0.78 |
| **Blood viscosity (fibr x(hcr)$^3$)** | 0.24±0.07 | 0.28±0.08 | 0.04 |
| **Total cholesterol (mmol/L)** | 5.3±1.1 | 5.3±1.1 | 0.90 |
| **Triglycerides (mmol/L)** | 1.7±0.9 | 1.6±0.8 | 0.64 |
| **Anticoagulation** | 4 | 10 | 0.10 |
| **Antiaggregation** | 16 | 12 | 0.58 |

**Table 5.** Demographic and risk factor profiles of ACS and SCS patients (±SD). For clarity, only profiles of subgroups of Study IV are included.

data. None of the patients had significant stenoses in intracranial arteries. Demographic and risk factor profiles were uniform in ACS and SCS patient groups (Table 5).

The first imaging was performed in the evening of the preoperative day, and the scanning was repeated at three days (postoperative) (n=42) and 100 days (chronic) (n=37) after CEA. Ipsilateral silent lacunar infarcts were detected in two (three) ACS patients. In the SCS group, relevant infarcts were detected in 11 patients. As perioperative complications, three patients had new minor brain infarcts, and one had an asymptomatic intracerebral hemorrhage. All infarcts and the intracerebral hemorrhage were detected on DWI, T2*-weighted, and conventional MR images by an experienced neuroradiologist.

### SUBJECTS WITH LEUKOARAIOSIS

In the imaging studies of healthy subjects, ischemic stroke patients, and CS patients, altogether 85 subjects with LA were identified. Twenty-two of these were healthy (9 males, aged 71.2±6.7, range 62-85 years, and 13 females, aged 66.5±11.0, range 42-82 years), 53 were either unilateral or bilateral CS patients (33 males, aged 64.0±8.9, range 47-77 years, and 20 females, aged 65.1±7.8, range 52-77 years), and 10 were the acute ischemic stroke patients described above.

## METHODS

### IMAGING TECHNIQUES

All studies were performed with a Siemens Magnetom Vision imager (Siemens Medical Systems, Erlangen, Germany) operating at 1.5 T. A standard head coil was used. Axial DW images, DSC MRI, fluid-attenuated inversion recovery, T1-weighted, T2-weighted, and proton density-weighted imaging as well as MRA were obtained. All imaging studies were completed without adverse events or complications. In the studies of healthy subjects (Studies I and II), however, due to malfunction of the imager (n=3) or artifacts in perfusion images (n=2), extra imaging sessions had to be arranged.

#### DIFFUSION-WEIGHTED IMAGING

DWI was performed with a SE EPI sequence that had a TR of 4000 ms, an TE of 103 ms, and a gradient strength of 25 mT/m covering 19 five-mm-thick slices (interslice gap 1.5 mm, field of view (FOV) 230x230 $mm^2$, and matrix size 96*128 interpolated to 256*256). Diffusion was measured in three orthogonal directions (x, y, and z) with two b values (b=0 and b=1000 $s/mm^2$).

#### DYNAMIC SUSCEPTIBILITY CONTRAST IMAGING

In Study II, DSC MRI was performed with a lipid-suppressed SE EPI sequence (TR 1500 ms, TE 78 ms, FOV 230x230 $mm^2$, matrix size 96*128) covering 7 five-mm-thick slices with an interslice gap of 1.5 mm. The seven slices were imaged 40 times at 1.5-second intervals.

In Study IV, a GE EPI sequence (TR 1.2 ms, TE 42.1 ms, FOV 230x230 $mm^2$, matrix size 96*128) covering 5 five-mm-thick slices with an interslice gap of 1.5 mm was used. The five slices were imaged 60 times at 1.5-second intervals.

After the collection of seven baseline images, Gd-DTPA (Magnevist, Schering AG, Berlin, Germany) 0.2 mmol/kg (Study II) or 0.15 mmol/kg (Study IV) was injected into the antecubital vein using an 18-gauge catheter. The injection was performed at a speed of 5 mL/s using an MR-compatible power injector (Spectris, Medrad, Pittsburg, PA, USA). The bolus of Gd-DTPA was followed by a 10-mL bolus of saline at the same injection rate to flush the remaining contrast agent into the bloodstream. The intravenous line was kept open until the actual injection by flushing it with saline at a rate of 0.25 mL/min.

## DATA ANALYSES

### DIFFUSION-WEIGHTED IMAGING

After the imaging session, the DW images were transferred to a separate workstation for calculation of the $ADC_{av}$ maps. The calculation was performed with a commercially available software program (MatLab, Mathsoft Inc., Natick, MA, USA). First, the DW images in the three orthogonal directions were co-registered. Then, natural logarithms of the images were averaged to form a rotationally invariant resultant image. Using a linear least-square regression on a pixel-by-pixel basis, the resultant image and the natural logarithm of the reference T2-weighted image were fitted to the b values (b=0 and b=1000). The negative slope of the fitted line was the $ADC_{av}$ (Figure 1).

### DYNAMIC SUSCEPTIBILITY CONTRAST IMAGING

The postprocessing of the perfusion data was also performed on a separate workstation. Spatial filtering was performed on the raw images by a 3-by-3 pixel uniform smoothing kernel before the calculation of the perfusion maps. Tissue and arterial concentration levels were determined from the perfusion raw images assuming a linear relationship between intravascular concentration of Gd-DTPA and the change in transverse relaxation rate (Fisel et al., 1991; Weisskoff et al., 1994):

$$C(t) \propto \Delta R_2 = -\frac{1}{TE}\ln(\frac{S(t)}{S_0})$$

where C(t) is the tissue concentration-time curve, $\Delta R_2$ is the change in transverse relaxation rate, TE is the echo time, $S_0$ is the baseline signal intensity, and S(t) is the tissue signal intensity with Gd-DTPA present (Belliveau et al, 1990; Østergaard et al, 1996a). T1 was assumed to be unchanged during the bolus injection (Østergaard et al, 1996a). Then, the CBV, CBF, and MTT (Figure 2) were determined from the concentration curves on a pixel-by-pixel basis.

For the calculation of the CBV, the area under the first pass of the tissue concentration-time curve was determined on a pixel-by-pixel basis using numerical integration (Perkiö et al, 2002). The lower and upper limits of the integration of the tissue concentration time were determined based on inspection of the whole brain concentration-time curve, i.e. the first pass of the Gd-DTPA bolus was set to begin and end at the same time for all pixels. For quantification purposes, an AIF was determined from 2-5 pixels located in small vessels supplied by the MCA (Østergaard, 1998). CBV was determined as the area under the first pass of the tissue concentration-time curve normalized with the area of the AIF and the injected dose of Gd-DTPA (Rosen et al, 1991) and taking into account the hematocrit difference of 2/3 between the micro- and macrovasculature (Østergaard et al, 1998b).

For the calculation of the CBF, the tissue concentration-time curve was first deconvolved with the AIF by singular value decomposition to determine the tissue impulse response functions on a pixel-by-pixel basis. Then, the CBF was determined as the height of the deconvolved tissue impulse response (Østergaard et al, 1996b).

For the calculation of the MTT in units of seconds, the ratio CBV:CBF was determined (Meier and Zierler, 1954; Stewart, 1984).

### RATING SCALE FOR LEUKOARAIOSIS

T2-weighted, proton density-weighted, and fluid-attenuated inversion recovery images were evaluated for leukoaraiotic regions according to a previously validated rating scale (Mäntylä et al, 1999a) by a neuroradiologist blinded to subjects' clinical data. Ischemic and other lesions were also evaluated. Subjects with unexpected cerebral lesions (meningioma, n=1, and arteriovenous malformation, n=1) were excluded from the studies of healthy subjects (Studies I and II).

Periventricular hyperintensities (PVH) were classified based on size and shape into the following three groups: PVH 1 (small cap/thin lining, <5 mm, n=47), PVH 2 (large cap/smooth halo, 6 to 10 mm, n=22), and PVH 3 (extending cap/irregular halo, >10 mm, n=16).

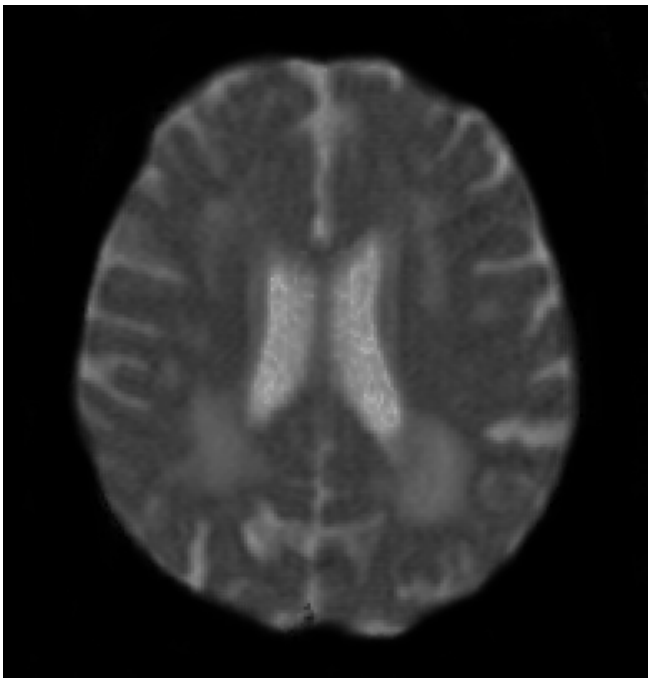

**Figure 1.** $ADC_{av}$ map of a male subject with LA. Note that leukoaraiotic regions and CSF are hyperintense. In DW images, the same regions are hypointense.

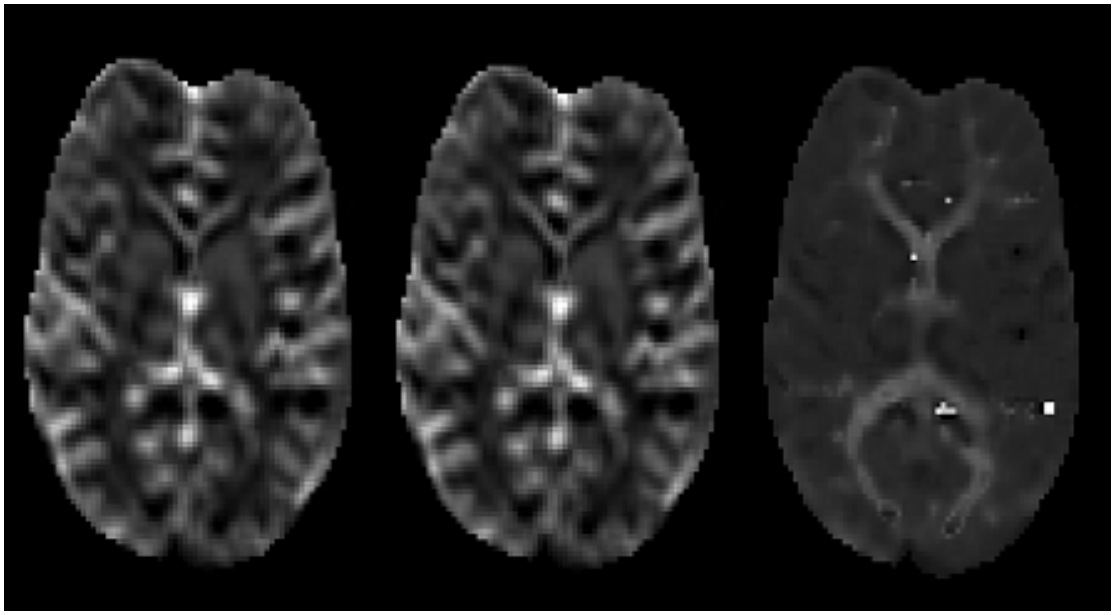

**Figure 2.** CBV, CBF, and MTT maps of a healthy female.

Hyperintensities (HI), the WM lesions situated far from the periventricular area, were classified into five groups: HI 1 (small focal, <5 mm, n=41), HI 2 (large focal, 6 to 10 mm, n=25), HI 3 (focal confluent, 11 to 25 mm, n=13), HI 4 (diffusely confluent, >25 mm, n=6), and HI 5 (diffuse lesions affecting most of the WM area, n=0).

### Region of Interest (ROI) Analysis

The ROI analysis varied slightly between studies due to differences in imaging methods (DWI and DSC MRI) or patient groups (healthy volunteers and patients with cerebral lesions) used. The following was, however, uniform in all studies: ROIs were manually drawn on their respective maps after the lesions were carefully analyzed on the conventional images. The surface area was measured in pixels, and the mean, standard deviation (SD), and range of the given values were obtained. The ROI analysis was performed with a commercially available image analysis software (Alice, Hayden Image Processing Group, Perceptive Systems Inc., Boulder, CO, USA).

In healthy subjects and in CS patients, 20 to 36 distinct structures – the exact number of structures depending on the imaging method (DWI and DSC MRI) or the given study (healthy subjects or CS patients) – were selected for the analysis. These structures were the frontal, parietal, temporal, occipital, and cerebellar GM and WM, watershed regions (WsR) between the territories of MCA and ACA or MCA and PCA, the caudate nucleus, putamen, thalamus, internal capsule, pons, and the CSF in lateral ventricles (frontal horn, middle part, posterior horn). Special care was taken to avoid contamination of normal-appearing WM ROIs with the regions of LA, ischemic lesions, or CSF.

In ischemic stroke patients, 2 to 6 ROIs covering the ischemic lesions, 8 to 14 ROIs of the leukoaraiotic regions, and 4 normal-appearing WM ROIs from the frontal and occipital lobes were analyzed.

In the analysis of LA subjects, 8 to 14 ROIs of leukoaraiotic regions were selected from both hemispheres covering the entire surface area of LA in the brain, and compared with 4 ROIs of the normal-appearing WM from the frontal and occipital lobes.

In addition to the ROI analysis, the baseline and postoperative MTT maps of Study IV were analyzed visually for the presence of a perfusion deficit.

## STATISTICAL ANALYSES

The normality of distributions was tested with Shapiro-Wilk's test. In Studies I-IV, the values were normally distributed and therefore parametric tests were used. Interhemispheric and regional variation in healthy subjects and in CS patients as well as the comparison between ACS and SCS patient groups were studied with one-way or two-way and repeated-measures analyses of variance (or covariance), as appropriate, using symptomaticity (Studies III and IV) as the between-subjects variable. Comparison between the groups representing different age cohorts and different genders was performed using multivariate analysis of variance or covariance, with within-subject and between-subjects designs, as appropriate. Bivariate regression analysis was used to further test age dependence (Studies I and II). Pairwise comparisons were made with Student's t test, either for independent or dependent samples, as appropriate. The univariate results were corrected for multiple comparisons. Chi-square test or Fisher's exact test was applied to univariate dichotomous variables. The homogeneity of the variances was studied using Box M test or Levene's test, sphericity was evaluated with Greenhouse-Geisser values, and the Scheffé test was applied for post-hoc comparisons. Correlations were studied with Pearson's product-moment correlation or Spearman's rank correlation, as appropriate.

Since $ADC_{av}$ values and group sizes in Study V deviated significantly from normal distribution, nonparametric tests were used. The $ADC_{av}$ values of LA, ischemic stroke, and normal-appearing WM were compared using Kruskal-Wallis one-way analysis of variance, as were the groups of varying degrees of LA and stroke. Groupwise comparison between any two groups was made using the Mann-Whitney U test.

The values are given as means ± SDs and 95% confidence intervals. A two-tailed value of $p<0.05$ was considered to be significant.

# RESULTS

## DIFFUSION-WEIGHTED IMAGING

All $ADC_{av}$ values are given as $x10^{-3}$ $mm^2/s$. The values are means ± SDs and (95% confidence intervals) in the text, and means ± SDs or (95% confidence intervals) in the tables and figures.

### HEALTHY BRAIN

For the whole brain of all healthy subjects (n=80), the mean $ADC_{av}$ values were 0.89±0.04 (0.88-0.90) for the cortical GM, 0.70±0.03 (0.69-0.71) for the WM vs. 0.63±0.02 (0.63-0.64) for the WM of the subjects in Study III (n=45), 0.65±0.04 (0.64-0.66) for the WsR (n=45), 0.75±0.03 (0.74-0.75) for the basal ganglia, 0.73±0.03 (0.73-0.74) for the thalamus, 0.51±0.07 (0.50-0.53) for the internal capsule, 0.60±0.06 (0.59-0.62) for the pons, 0.82±0.11 (0.79-0.84) for the cerebellar GM, 0.59±0.05 (0.58-0.60) for the cerebellar WM, and 2.86±0.22 (2.8-2.9) for the lateral ventricles. More detailed values for various age groups and for males and females separately are presented in Table 6.

The $ADC_{av}$ values of the cortical GM were consistently higher than those of the WM in all subjects ($p<0.001$) and in all subgroups ($p<0.001$). The $ADC_{av}$ values of the basal ganglia and thalamus were higher than those of the WM ($p<0.001$) but lower than those of the cortical GM ($p<0.001$) (Table 6). The $ADC_{av}$ values of the WM in the brain lobes did not differ from each other in Study I subjects. However, the $ADC_{av}$ values of the frontal WM were higher than those of the other three lobes in Study III subjects, since the ROI analysis in this study slightly differed from that of Study I. No significant differences were found in the lobular GM $ADC_{av}$ values or between the hemispheres, except in the cerebellar GM, where the left hemisphere had $ADC_{av}$ values of 0.84±0.12 (0.81-0.86) and the right 0.80±0.14 (0.77-0.83) ($p<0.02$).

The $ADC_{av}$ values of the lateral ventricles increased with age ($p<0.001$) (Table 6). The homogeneity of the variances was normal in all of the other brain regions, except in the thalami ($p<0.002$ for the left and $p<0.001$ for the right thalamus), where the $ADC_{av}$ values in Group IV were significantly higher than in the other age groups (Table 6). No other age-related changes were found (Figure 3).

No differences were observed between males and females in any region of the brain (Figure 3 and Table 6).

| | Genders | | | Age Groups | | | |
|---|---|---|---|---|---|---|---|
| **ROI** | **All** | **Males** | **Females** | **I** | **II** | **III** | **IV** |
| **GM** | 0.89±0.04 | 0.89±0.03 | 0.89±0.05 | 0.90±0.03 | 0.89±0.04 | 0.90±0.06 | 0.89±0.03 |
| **WM** | 0.70±0.03 | 0.70±0.03 | 0.71±0.03 | 0.70±0.02 | 0.70±0.04 | 0.70±0.03 | 0.71±0.04 |
| **BG** | 0.75±0.03 | 0.75±0.03 | 0.75±0.04 | 0.74±0.03 | 0.74±0.02 | 0.75±0.03 | 0.76±0.04 |
| **TH** | 0.73±0.03 | 0.73±0.03 | 0.74±0.03 | 0.73±0.02 | 0.72±0.03 | 0.73±0.03 | 0.76±0.05 |
| **IC** | 0.51±0.07 | 0.51±0.07 | 0.52±0.06 | 0.52±0.06 | 0.50±0.08 | 0.51±0.07 | 0.53±0.06 |
| **PO** | 0.60±0.06 | 0.60±0.06 | 0.60±0.06 | 0.61±0.07 | 0.57±0.04 | 0.62±0.05 | 0.60±0.07 |
| **CG** | 0.82±0.11 | 0.80±0.11 | 0.83±0.11 | 0.80±0.10 | 0.78±0.12 | 0.85±0.12 | 0.83±0.10 |
| **CW** | 0.59±0.05 | 0.59±0.05 | 0.59±0.06 | 0.60±0.04 | 0.59±0.06 | 0.59±0.07 | 0.59±0.04 |
| **CS** | 2.86±0.22 | 2.86±0.20 | 2.87±0.24 | 2.78±0.22 | 2.78±0.21 | 2.88±0.20 | 3.01±0.16 |

**Table 6.** $ADC_{av}$ values ($x10^{-3}$ $mm^2/s$) ± SDs of healthy subjects for males and females and for age groups. GM=gray matter, WM=white matter, BG=basal ganglia, TH=thalamus, PO=pons, IC=internal capsule, CG=cerebellar gray matter, CW=cerebellar white matter, CS=cerebrospinal fluid in lateral ventricles.

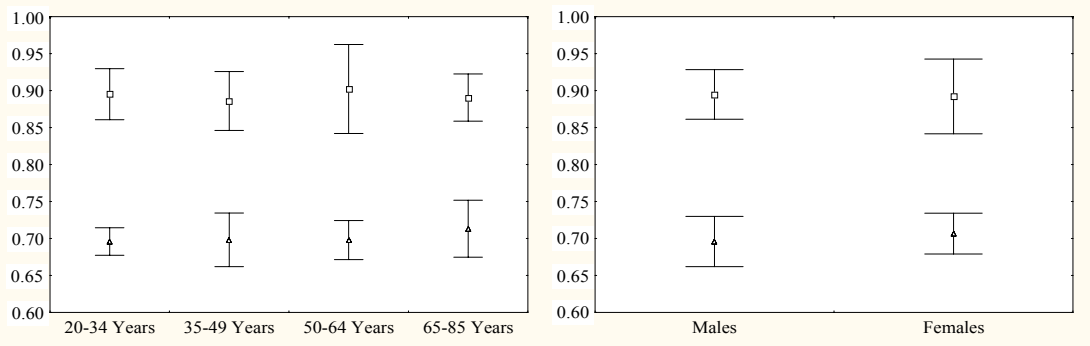


**Figure 3.** $ADC_{av}$ values ($x10^{-3}$ $mm^2/s$) ± SDs of gray and white matter of the healthy brain in age groups I to IV and in males and females separately. Squares=gray matter, and triangles=white matter.

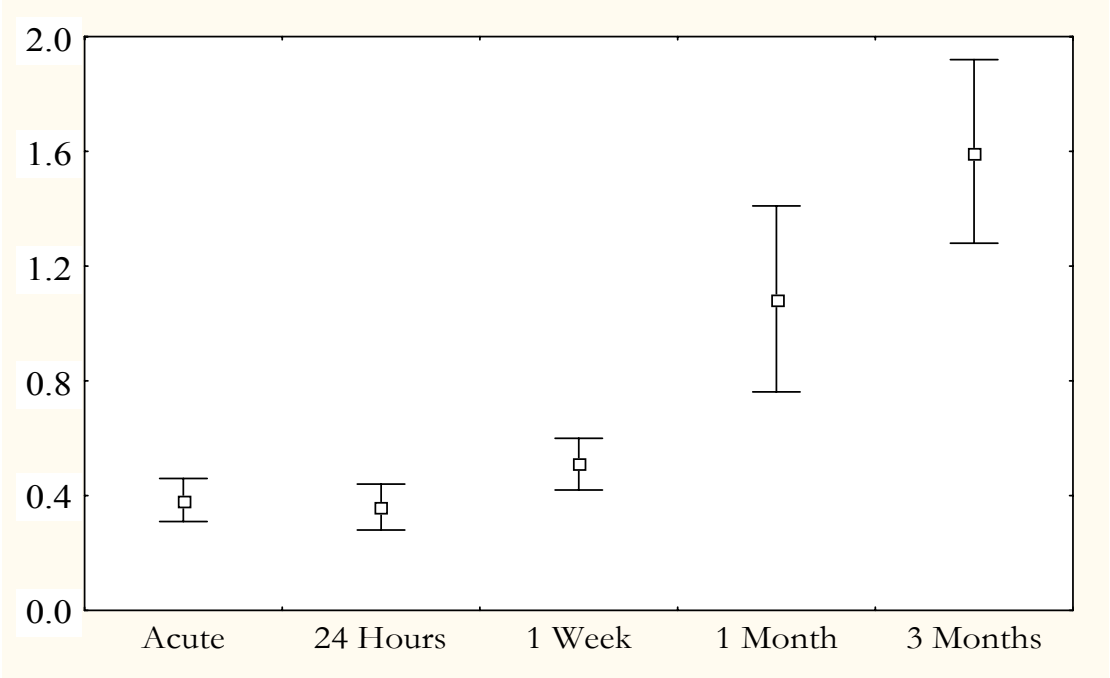


**Figure 4.** Stroke $ADC_{av}$ values ($x10^{-3}$ $mm^2/s$) ± SDs from the hyperacute to the chronic phase.

ISCHEMIC STROKE

The $ADC_{av}$ values of the ischemic stroke lesions were 0.38±0.08 (0.33-0.44) at hyperacute stage, 0.36±0.08 (0.31-0.42) at 24-hour stage, and 0.51±0.09 (0.45-0.57) at one-week stage (n=10 for each imaging time). At one month, the $ADC_{av}$ values of the ischemic lesions were 1.08±0.33 (0.56-1.60) (n=4) and at chronic stage 1.59±0.32 (1.26-1.93) (n=6) (Figure 4).

| | All | ACS | SCS | All | ACS | SCS |
|---|---|---|---|---|---|---|
| **Gray Matter** | | | | **Thalamus** | | |
| Stenotic | | | | Stenotic | | |
| Preoperative | 0.91±0.03 | 0.90±0.03 | 0.92±0.03 | 0.76±0.06 | 0.75±0.06 | 0.77±0.06 |
| Postoperative | 0.90±0.03 | 0.89±0.03 | 0.90±0.03 | 0.77±0.06 | 0.76±0.06 | 0.78±0.07 |
| Chronic | 0.90±0.03 | 0.89±0.03 | 0.90±0.03 | 0.76±0.06 | 0.74±0.06 | 0.77±0.06 |
| Contralateral | | | | Contralateral | | |
| Preoperative | 0.90±0.03 | 0.90±0.02 | 0.90±0.03 | 0.77±0.07 | 0.76±0.07 | 0.77±0.06 |
| Postoperative | 0.89±0.03 | 0.88±0.02 | 0.89±0.03 | 0.76±0.06 | 0.75±0.06 | 0.76±0.06 |
| Chronic | 0.89±0.03 | 0.88±0.02 | 0.90±0.03 | 0.76±0.07 | 0.73±0.05 | 0.78±0.09 |
| **White Matter** | | | | **Watershed** | | |
| Stenotic | | | | Stenotic | | |
| Preoperative | 0.69±0.04 | 0.69±0.04 | 0.69±0.04 | 0.74±0.05 | 0.73±0.05 | 0.74±0.05 |
| Postoperative | 0.67±0.04 | 0.67±0.04 | 0.68±0.04 | 0.70±0.05 | 0.70±0.04 | 0.70±0.06 |
| Chronic | 0.67±0.04 | 0.66±0.03 | 0.67±0.04 | 0.69±0.05 | 0.68±0.04 | 0.70±0.06 |
| Contralateral | | | | Contralateral | | |
| Preoperative | 0.65±0.04 | 0.66±0.04 | 0.65±0.03 | 0.70±0.04 | 0.70±0.05 | 0.70±0.04 |
| Postoperative | 0.67±0.04 | 0.67±0.04 | 0.67±0.04 | 0.70±0.06 | 0.71±0.06 | 0.69±0.06 |
| Chronic | 0.67±0.04 | 0.67±0.04 | 0.67±0.04 | 0.69±0.06 | 0.71±0.06 | 0.68±0.06 |

**Table 7.** $ADC_{av}$ values ($x10^{-3}$ $mm^2/s$) ± SDs of CS patients for ACS and SCS patient groups separately at three imaging stages. ACS=asymptomatic carotid stenosis, SCS=symptomatic carotid stenosis.

CAROTID STENOSIS AND ENDARTERECTOMY

Preoperatively, the $ADC_{av}$ values of the WM and the WsR in the lobes of the hemisphere ipsilateral to the CS were higher than those of the contralateral side ($p<0.001$). Such an asymmetry was not detected in the GM ($p=0.2$) or the thalamus ($p=0.8$) (Table 7).

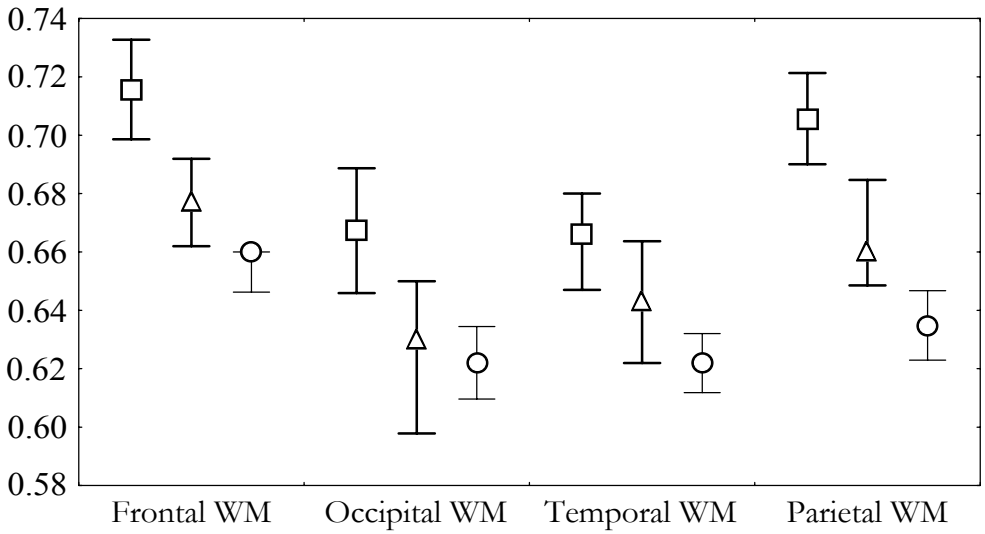


**Figure 5.** Lobular WM $ADC_{av}$ values ($x10^{-3}$ $mm^2/s$) ± 95% confidence intervals of ipsilateral and contralateral sides compared with lobular WM $ADC_{av}$ values of control subjects. Squares=ipsilateral means, triangles=contralateral means, and circles=control means.

At the postoperative and chronic stages, the ipsilateral WM and WsR had resumed lower $ADC_{av}$ levels that were not significantly different from those of the contralateral hemisphere (postoperatively, WM: p=0.5 and WsR: p=0.9; at the chronic stage, WM: p=0.5 and WsR: p=0.4) (Table 7).

In comparing ACS and SCS patient groups, no significant differences were found, although SCS patients tended to have slightly higher $ADC_{av}$ values in the WM and WsR (Table 7).

The lobar $ADC_{av}$ values in the WM were different in each of at the three imaging stages. At the preoperative stage, the frontal and parietal lobes displayed higher values than the occipital and temporal ($p<0.05$) (Figure 5). The lobar differences at the postoperative and chronic stages persisted.

| | Leukoaraiosis | | | | NAWM |
|---|---|---|---|---|---|
| | All Subjects | Healthy Volunteers | CS Patients | Stroke Patients | All Subjects |
| **PVH 1** | 0.92±0.04 | 0.95±0.03 | 0.91±0.04 | 0.91±0.01 | 0.69±0.03 |
| **PVH 2** | 0.99±0.08 | 0.93±0.04 | 1.02±0.08 | 1.06±0.00 | 0.69±0.04 |
| **PVH 3** | 1.16±0.13 | 1.15±0.13 | 1.13±0.17 | 1.21±0.08 | 0.74±0.02 |
| **HI 1** | 0.92±0.04 | 0.92±0.04 | 0.92±0.04 | 0.91±0.01 | 0.69±0.04 |
| **HI 2** | 0.97±0.08 | 0.98±0.07 | 0.96±0.09 | na | 0.70±0.04 |
| **HI 3** | 1.09±0.10 | 1.05±0.12 | 1.10±0.11 | 1.11±0.07 | 0.72±0.04 |
| **HI 4** | 1.27±0.04 | 1.28±0.07 | 1.31±0.00 | 1.26±0.01 | 0.74±0.02 |

**Table 8.** $ADC_{av}$ values ($x10^{-3}$ $mm^2/s$) ± SDs of the leukoaraiotic regions and the normal-appearing WM in subjects with LA. CS=carotid stenosis, PVH=periventricular hyperintensity, HI=hyperintensity, NAWM=normal-appearing WM, na=data not available.

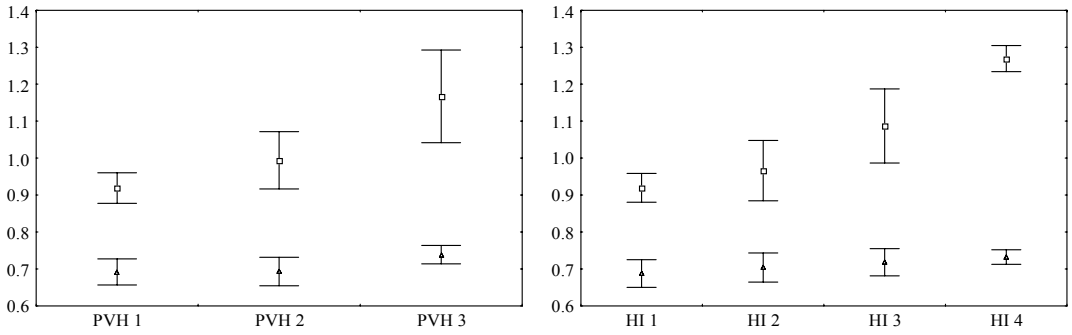


**Figure 6.** $ADC_{av}$ values ($x10^{-3}$ $mm^2/s$) ± SDs in the regions of leukoaraiosis and normal-appearing WM in PVH 1 to 3 and HI 1 to 4. Squares=leukoaraiosis and tringles=white matter.

## LEUKOARAIOSIS

As the severity of LA increased from PVH 1 to PVH 3, and from HI 1 to 4, the $ADC_{av}$ values of both the leukoaraiotic regions and the normal-appearing WM showed a directly proportional increase ($p<0.01$ for both PVH and HI) (Table 8, and Figure 6).

The regions of LA showed significantly higher $ADC_{av}$ values than the normal-appearing WM in all subgroups (healthy subjects, CS patients, and ischemic stroke patients) ($p<0.01$ for each) (Table 8).

The surface area of the regions of LA in unilateral CS patients was slightly larger in the ipsilateral than in the contralateral hemisphere ($p<0.04$), but the $ADC_{av}$ values of these regions were not different between hemispheres ($0.95\pm0.12$ vs. $0.95\pm0.11$, $p=1.0$).

## COMPARISONS BETWEEN GROUPS

Healthy controls had lower $ADC_{av}$ values in the WM and the WsR than CS patients in their preoperative ipsilateral WM and WsR ($p<0.001$), whereas no difference was detected in the GM or the thalamus. Despite the higher $ADC_{av}$ levels of CS patients, the relative differences between various brain lobes in their WM were identical to those of controls (Figure 5). The $ADC_{av}$ values of the anterior WsR were higher than the posterior WsR, on both the ipsilateral ($0.76\pm0.05$ vs. $0.71\pm0.07$; $p<0.001$) and the contralateral ($0.73\pm0.05$ vs. $0.67\pm0.06$; $p<0.001$) sides, and in controls ($0.66\pm0.04$ vs. $0.64\pm0.04$; $p<0.01$). In the period following the operation, the $ADC_{av}$ values decreased considerably, but nonetheless remained significantly higher among patients than controls for the WM and the WsR ($p<0.001$).

Overall, the $ADC_{av}$ values of the normal-appearing WM of subjects with LA did not significantly differ from those of healthy subjects with no LA. However, with more detailed analysis within the subject group with LA, the $ADC_{av}$ values of the normal-appearing WM were found to vary according to the severity of LA, being highest in the most severe LA patient groups ($p<0.01$ for all) (Figure 6).

At hyperacute stage, 24-hour stage, and one-week stage, the $ADC_{av}$ values of ischemic lesions were lower than those of the leukoaraiotic lesions ($p<0.01$ for all). At one month, the ischemic lesions showed similar $ADC_{av}$ values to those of the regions of LA. At chronic stage, by contrast, the ischemic lesions had significantly higher $ADC_{av}$ values than the regions of LA ($p<0.01$).

## DYNAMIC SUSCEPTIBILITY CONTRAST IMAGING

The values given are means ± SDs and (95% confidence intervals) in the text, and means ± SDs or (95% confidence intervals) in the tables and figures.

### HEALTHY BRAIN

For the analyzed regions of healthy subjects, the cortical GM showed the following perfusion values: CBV (4.6±1.0, 4.3-4.8 mL/100 g), CBF (94.2±23.0, 89.1-99.3 mL/100 g/min), and MTT (3.0±0.6, 2.8-3.1 s), and the cortical WM: CBV (1.3±0.4, 1.2-1.4 mL/100 g), CBF (19.6±5.8, 18.3-20.8 mL/100 g/min), and MTT (4.3±0.7, 4.2-4.5 s). More detailed analyses can be found in Tables 9a-c.

No differences between hemispheres were found in any perfusion parameter. However, differences between brain lobes were found in all three perfusion parameters ($p<0.02$), the temporal lobes having the highest perfusion rates. The cortical GM had the highest perfusion rate, followed by the deep GM and the WM ($p<0.01$). The caudate nucleus showed higher CBV and CBF than the thalamus ($p<0.01$). No difference between the caudate nucleus and the thalamus was found in the MTT (Tables 9a-c).

Generally, no change with age was found in any perfusion parameter, except for an increase in the MTT of the frontal and parietal GM ($p<0.02$). Although not significant, a tendency for an increase was also found in the mean GM MTT and CBV (Tables 9a-c, and Figures 7a-c).

Males had higher CBV and MTT in the cortical and in the deep GM than females ($p<0.04$). In the WM, the MTT was also higher in males than in females ($p<0.03$), but no difference was detected in the CBV of the WM. No differences between genders were found in the CBF in any region (Tables 9a-c, and Figures 7a-c).

| | | Gender | | | Age Groups | | | |
|---|---|---|---|---|---|---|---|---|
| **ROIs** | **All** | **Males** | **Females** | | **I** | **II** | **III** | **IV** |
| **GRAY MATTER** | | | | | | | | |
| Frontal | 4.2±1.0 | 4.5±1.0 | 3.9±0.9 | * | 3.9±1.0 | 4.0±0.9 | 4.3±0.9 | 4.6±1.1 |
| Occipital | 4.5±1.1 | 4.9±1.1 | 4.2±1.1 | * | 4.5±1.2 | 4.4±1.2 | 4.8±1.2 | 4.6±1.0 |
| Temporal | 5.1±1.3 | 5.6±1.4 | 4.6±1.0 | * | 4.8±1.3 | 4.7±1.0 | 5.5±1.2 | 5.4±1.6 |
| Parietal | 4.4±1.1 | 4.8±1.1 | 3.9±0.9 | * | 4.1±1.0 | 4.3±0.9 | 4.5±1.2 | 4.6±1.2 |
| **WHITE MATTER** | | | | | | | | |
| Frontal | 1.4±0.4 | 1.5±0.5 | 1.4±0.3 | | 1.2±0.4 | 1.3±0.4 | 1.6±0.5 | 1.6±0.4 |
| Occipital | 1.4±0.6 | 1.5±0.6 | 1.4±0.5 | | 1.2±0.4 | 1.3±0.4 | 1.7±0.6 | 1.5±0.7 |
| Temporal | 1.5±0.7 | 1.6±0.8 | 1.3±0.5 | | 1.5±0.7 | 1.4±0.7 | 1.4±0.7 | 1.5±0.8 |
| Parietal | 1.0±0.4 | 1.1±0.4 | 0.9±0.3 | | 0.9±0.3 | 1.0±0.3 | 1.2±0.5 | 1.0±0.4 |
| **DEEP GRAY MATTER** | | | | | | | | |
| Caudatus | 4.2±1.1 | 4.4±1.3 | 4.0±0.9 | * | 3.9±1.1 | 3.8±0.9 | 4.2±1.0 | 4.8±1.3 |
| Thalamus | 3.9±1.1 | 4.2±1.1 | 3.5±0.9 | * | 3.4±0.8 | 3.5±1.1 | 4.2±1.0 | 4.3±1.2 |
| **MEAN VALUES** | | | | | | | | |
| Gray Matter | 4.6±1.0 | 4.9±1.0 | 4.2±0.8 | * | 4.3±1.0 | 4.3±0.9 | 4.8±1.0 | 4.8±1.1 |
| White Matter | 1.3±0.4 | 1.4±0.5 | 1.2±0.3 | | 1.2±0.3 | 1.3±0.3 | 1.5±0.5 | 1.4±0.4 |

**Table 9a.** CBV (mL/100 g) ± SDs of all subjects for genders and age groups separately. Significant findings between subgroups have been marked with asterisks.

| | | Gender | | Age Groups | | | |
|---|---|---|---|---|---|---|---|
| **ROIs** | **All** | **Males** | **Females** | **I** | **II** | **III** | **IV** |
| **GRAY MATTER** | | | | | | | |
| Frontal | 89±24 | 91±27 | 86±19 | 93±28 | 83±23 | 91±25 | 88±18 |
| Occipital | 93±24 | 94±26 | 91±23 | 98±29 | 86±20 | 95±27 | 91±19 |
| Temporal | 105±28 | 109±32 | 101±24 | 109±31 | 96±20 | 111±33 | 105±26 |
| Parietal | 90±24 | 94±27 | 86±19 | 95±27 | 88±18 | 91±29 | 87±19 |
| **WHITE MATTER** | | | | | | | |
| Frontal | 23±8 | 23±9 | 23±6 | 20±6 | 21±7 | 25±9 | 24±6 |
| Occipital | 20±8 | 20±9 | 20±7 | 17±7 | 18±6 | 24±9 | 20±9 |
| Temporal | 21±9 | 22±10 | 20±7 | 21±10 | 20±6 | 22±9 | 21±9 |
| Parietal | 15±6 | 15±7 | 15±6 | 14±5 | 14±6 | 18±8 | 15±5 |
| **DEEP GRAY MATTER** | | | | | | | |
| Caudatus | 94±29 | 95±34 | 93±23 | 99±36 | 87±25 | 93±31 | 97±24 |
| Thalamus | 84±22 | 85±24 | 83±21 | 83±23 | 78±20 | 89±28 | 88±17 |
| **MEAN VALUES** | | | | | | | |
| Gray Matter | 94±23 | 97±26 | 91±20 | 99±27 | 89±19 | 97±27 | 93±18 |
| White Matter | 20±6 | 20±7 | 19±4 | 18±5 | 18±5 | 22±7 | 20±5 |

**Table 9b.** CBF (mL/100 g/min) ± SDs of all subjects for genders and age groups separately. No differences between subgroups were found.

| | | Gender | | | Age Groups | | | |
|---|---|---|---|---|---|---|---|---|
| **ROIs** | **All** | **Males** | **Females** | | **I** | **II** | **III** | **IV** |
| **GRAY MATTER** | | | | | | | | |
| Frontal | 2.9±0.6 | 3.1±0.7 | 2.7±0.4 | * | 2.6±0.4 | 3.0±0.7 | 3.0±0.7 | 3.1±0.5 * |
| Occipital | 3.0±0.7 | 3.2±0.8 | 2.8±0.5 | * | 2.8±0.6 | 3.1±0.6 | 3.2±0.9 | 3.0±0.5 |
| Temporal | 3.0±0.6 | 3.2±0.7 | 2.8±0.4 | * | 2.7±0.4 | 3.0±0.7 | 3.1±0.7 | 3.0±0.6 |
| Parietal | 3.0±0.7 | 3.2±0.8 | 2.8±0.4 | * | 2.7±0.4 | 3.0±0.7 | 3.2±0.9 | 3.2±0.5 * |
| **WHITE MATTER** | | | | | | | | |
| Frontal | 4.0±0.8 | 4.3±0.9 | 3.7±0.6 | * | 3.9±0.7 | 4.1±0.8 | 4.0±0.8 | 4.3±0.9 |
| Occipital | 4.6±1.0 | 4.9±1.1 | 4.3±1.0 | * | 4.6±0.9 | 4.5±1.2 | 4.6±1.2 | 4.7±0.8 |
| Temporal | 4.3±1.1 | 4.7±1.0 | 4.0±1.1 | * | 4.2±1.1 | 4.4±1.2 | 4.1±1.1 | 4.5±1.2 |
| Parietal | 4.3±1.0 | 4.7±1.0 | 4.0±0.8 | * | 4.2±0.6 | 4.5±1.1 | 4.2±0.9 | 4.4±1.1 |
| **DEEP GRAY MATTER** | | | | | | | | |
| Caudatus | 2.8±0.6 | 3.0±0.7 | 2.6±0.5 | * | 2.5±0.5 | 2.7±0.7 | 2.9±0.9 | 3.0±0.6 |
| Thalamus | 2.8±0.7 | 3.1±0.8 | 2.6±0.5 | * | 2.5±0.6 | 2.8±0.8 | 3.0±0.7 | 2.9±0.6 |
| **MEAN VALUES** | | | | | | | | |
| Gray Matter | 3.0±0.6 | 3.2±0.7 | 2.8±0.4 | * | 2.7±0.4 | 3.0±0.7 | 3.1±0.7 | 3.1±0.5 |
| White Matter | 4.3±0.8 | 4.6±0.8 | 4.0±0.6 | * | 4.2±0.6 | 4.4±0.9 | 4.2±0.8 | 4.5±0.7 |

**Table 9c.** MTT (seconds) ± SDs of all subjects for genders and age groups separately. Significant findings between subgroups have been marked with asterisks.

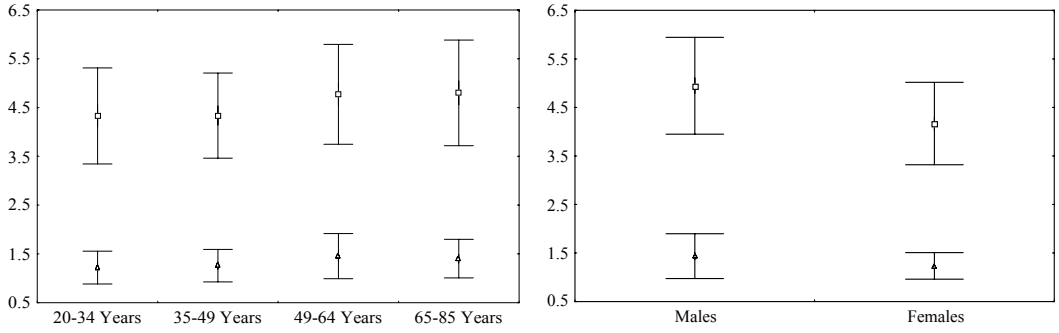


**Figure 7a.** CBV (mL/100 g) ± SDs of gray and white matter of the healthy brain in age groups I to IV and in males and females separately. Squares=gray matter and triangles=white matter.

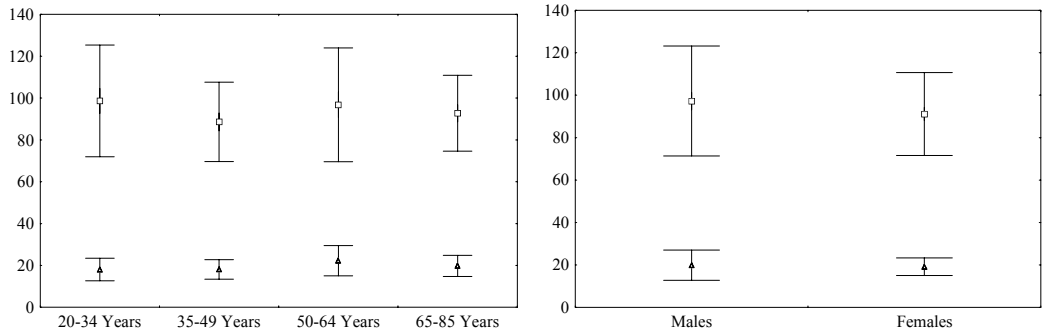


**Figure 7b.** CBF (mL/100 g/min) ± SDs of gray and white matter of the healthy brain in age groups I to IV and in males and females separately. Squares=gray matter and triangles=white matter.

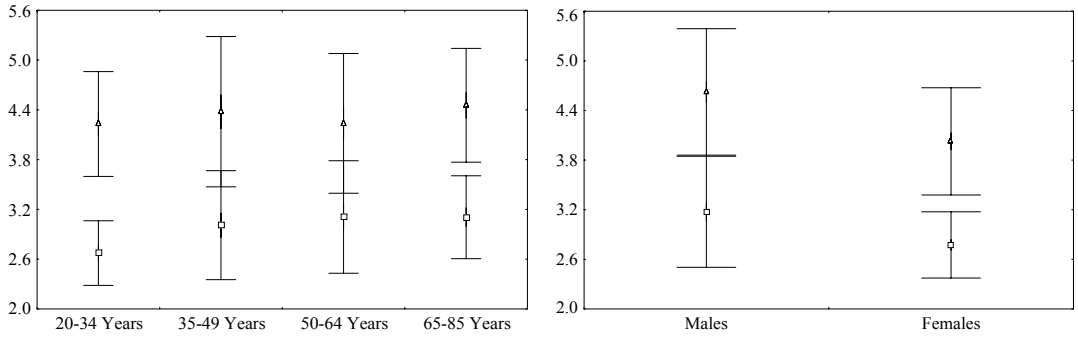


**Figure 7c.** MTT (seconds) ± SDs of gray and white matter of the healthy brain in age groups I to IV and in males and females separately. Squares=gray matter and triangles=white matter.

| | Stenotic Side | | Contralateral Side | |
|---|---|---|---|---|
| | **ACS** | **SCS** | **ACS** | **SCS** |
| **Gray Matter** | | | | |
| Preoperative | 4.6 (4.0-5.2) | 4.6 (4.1-5.1) | 4.6 (4.1-5.1) | 4.6 (4.1-5.1) |
| Postoperative | 4.5 (4.0-5.0) | 4.7 (4.4-5.1) | 4.3 (3.9-4.7) | 5.0 (4.6-5.3) |
| Chronic | 4.6 (4.2-5.0) | 4.3 (3.8-4.8) | 4.6 (4.2-5.1) | 4.3 (3.9-4.6) |
| **White Matter** | | | | |
| Preoperative | 1.9 (1.6-2.2) | 1.9 (1.6-2.1) | 1.9 (1.6-2.1) | 1.8 (1.6-2.0) |
| Postoperative | 1.7 (1.5-1.9) | 1.8 (1.5-2.1) | 1.6 (1.4-1.8) | 1.8 (1.5-2.1) |
| Chronic | 1.7 (1.5-2.0) | 1.6 (1.4-1.8) | 1.7 (1.5-2.0) | 1.7 (1.4-1.9) |
| **Watershed** | | | | |
| Preoperative | 2.0 (1.8-2.3) | 1.9 (1.6-2.2) | 2.0 (1.7-2.3) | 1.9 (1.6-2.1) |
| Postoperative | 1.8 (1.6-2.1) | 1.8 (1.5-2.1) | 1.8 (1.6-2.1) | 1.8 (1.5-2.0) |
| Chronic | 1.8 (1.5-2.0) | 1.7 (1.4-1.9) | 1.8 (1.6-2.1) | 1.7 (1.4-2.0) |

**Table 10a.** CBV (mL/100 g) of CS patients (95% confidence interval) for ACS and SCS patient groups separately at three imaging stages. ACS=asymptomatic carotid stenosis, SCS=symptomatic carotid stenosis.

CAROTID STENOSIS AND ENDARTERECTOMY

In comparing ASC and SCS patient groups separately, the following was found. In SCS patients, the preoperative MTT was higher in the ipsilateral WM ($p<0.001$) and WsR ($p<0.001$), and marginally higher in the GM ($p=0.05$), in comparison with the contralateral hemisphere (Table 10c). In the postoperative value and in the ACS patient group, no differences were detected on the MTT ($p>0.05$). No interhemispheric differences in the CBV were detected at any stage and in any subgroup ($p>0.05$) (Table 10a). In SCS patients, the preoperative CBF was lower in the ipsilateral WM ($p<0.01$) and WsR ($p<0.01$), and marginally lower in the GM ($p=0.05$). By contrast, in ACS patients, only the ipsilateral CBF of the GM was lower than in the contralateral hemisphere ($p<0.05$) (Table 10b). The interhemispheric ratio showed the abolition of asymmetry by

| | Stenotic Side | | Contralateral Side | |
|---|---|---|---|---|
| | **ACS** | **SCS** | **ACS** | **SCS** |
| **Gray Matter** | | | | |
| Preoperative | 64 (61-68) | 58 (54-63) | 68 (64-72) | 65 (61-68) |
| Postoperative | 70 (66-74) | 65 (61-69) | 70 (67-74) | 68 (63-73) |
| Chronic | 69 (66-73) | 65 (59-71) | 69 (66-73) | 66 (60-72) |
| **White Matter** | | | | |
| Preoperative | 22 (19-25) | 19 (16-21) | 23 (20-26) | 22 (20-25) |
| Postoperative | 24 (20-27) | 20 (18-23) | 24 (20-27) | 22 (19-25) |
| Chronic | 21 (20-23) | 21 (17-25) | 21 (18-24) | 23 (19-26) |
| **Watershed** | | | | |
| Preoperative | 25 (22-29) | 19 (16-22) | 24 (21-28) | 23 (19-26) |
| Postoperative | 25 (22-29) | 20 (17-23) | 26 (22-30) | 22 (18-25) |
| Chronic | 22 (19-24) | 22 (18-26) | 22 (19-24) | 23 (19-27) |

**Table 10b.** CBF (mL/100 g/min) of CS patients (95% confidence interval) for ACS and SCS patient groups separately at three imaging stages. ACS=asymptomatic carotid stenosis, SCS=symptomatic carotid stenosis.

CEA. A slight trend for higher CBV in the contralateral hemisphere at the early postoperative stage is reflected in the interhemispheric ratio. In the WsR, no difference was seen between the anterior and posterior territories.

In comparing SCS patients with ACS patients, the SCS patients displayed longer ipsilateral MTT before CEA, most pronounced in the WM and WsR, which improved in subsequent measurements, whereas the ACS patients' hemodynamic improvement was only marginal or transient (Table 10a-c). SCS patients tended to have a slightly lower preoperative CBF. The CBV remained homogeneous between the groups. However, none of the perfusion parameters showed significant differences between ACS and SCS groups after correction for multiple correlations.

| | Stenotic Side | | Contralateral Side | |
|---|---|---|---|---|
| | **ACS** | **SCS** | **ACS** | **SCS** |
| **Gray Matter** | | | | |
| Preoperative | 4.3 (3.6-5.0) | 4.8 (4.3-5.3) | 4.1 (3.5-4.7) | 4.2 (3.8-4.7) |
| Postoperative | 3.9 (3.4-4.4) | 4.4 (4.0-4.8) | 3.8 (3.3-4.2) | 4.4 (4.0-4.8) |
| Chronic | 4.3 (3.8-4.8) | 4.0 (3.6-4.4) | 4.3 (3.7-4.8) | 3.9 (3.6-4.2) |
| **White Matter** | | | | |
| Preoperative | 5.6 (4.9-6.2) | 6.5 (5.7-7.2) | 5.3 (4.6-5.9) | 5.1 (4.6-5.5) |
| Postoperative | 4.5 (4.0-5.0) | 5.5 (4.9-6.1) | 4.4 (3.9-4.8) | 5.0 (4.6-5.5) |
| Chronic | 5.2 (4.7-5.8) | 4.8 (4.3-5.3) | 5.2 (4.7-5.8) | 4.6 (4.2-4.9) |
| **Watershed** | | | | |
| Preoperative | 5.4 (4.8-6.1) | 6.7 (5.9-7.4) | 5.1 (4.5-5.6) | 5.2 (4.7-5.7) |
| Postoperative | 4.5 (4.1-4.9) | 5.6 (5.0-6.2) | 4.4 (4.0-4.8) | 5.0 (4.6-5.4) |
| Chronic | 5.0 (4.5-5.5) | 5.0 (4.5-5.5) | 5.2 (4.7-5.7) | 4.6 (4.2-4.9) |

**Table 10c.** MTT (seconds) of CS patients (95% confidence interval) for ACS and SCS patient groups separately at three imaging stages. ACS=asymptomatic carotid stenosis, SCS=symptomatic carotid stenosis.

Fourteen patients had a visible perfusion deficit on the MTT map in the ipsilateral carotid territory (Figure 8). Twelve of these patients were symptomatic and only two asymptomatic ($p<0.01$). The ipsilateral MTT in the population with visualized hypoperfusion was in the WM 7.5 (6.7-8.3) seconds, in the WsR 7.2 (6.2-8.2) seconds, and in the GM 5.5 (4.9-6.2) seconds. The respective values for the population without a deficit were 5.4 (4.9-6.9, $p<0.001$) seconds, 5.5 (5.0-6.1, $p<0.01$) seconds, and 4.1 (3.7-4.6, $p<0.01$) seconds. In the visually hypoperfused subjects, the interhemispheric MTT ratio was 1.46 (1.32-1.60) for the WM, 1.39 (1.21-1.56) for the WsR, and 1.28 (1.13-1.42) for the GM. In subjects without a visible perfusion deficit, the respective values were 1.06 (1.01-1.11), 1.09 (1.04-1.15), and 1.02 (0.98-1.06) ($p<0.001$ for all comparisons). The patients with a visible deficit represented a higher grade of stenosis than those without,

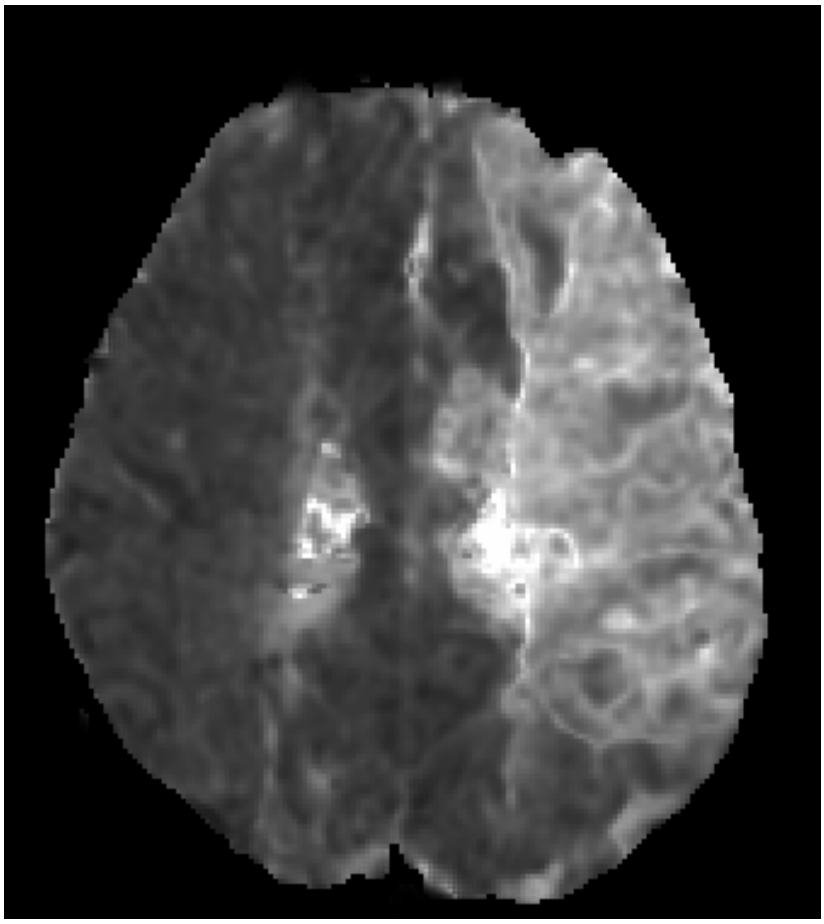

**Figure 8.** Preoperative MTT map of a 73-year-old male with a visible perfusion deficit.

85 (81-90) % versus 76 (73-79) % ($p<0.01$). The lowest degree of stenosis with a visually detected perfusion deficit was 71% (two subjects). In the postoperative maps, no hypoperfusion was seen.

# DISCUSSION

DWI and DSC MRI at 1.5 T were used to study several brain regions of a healthy population, ischemic stroke patients, CS patients before and after CEA, and subjects with LA. Age- and gender-dependency, the effect of ischemia, CS, CEA, and LA on $ADC_{av}$ values and perfusion parameters were tested. The studies yielded some expected results as well as several novel findings. The findings in each subpopulation are discussed first, then criticism and limitations of the study, and finally, a summary and concluding remarks are presented.

## HEALTHY BRAIN

While DWI and DSC MRI are widely used for diagnostic purposes, normal values for brain diffusion and perfusion parameters in a representative healthy population have not been available. Using DWI and DSC MRI, 80 healthy people aged 22 to 85 years were studied to establish quantitative $ADC_{av}$ values and perfusion parameters for several regions of the brain. The study population was homogeneous. As no reports of normal $ADC_{av}$ values and perfusion parameters for the brain in ethnically diverse populations could be found in the literature, our results cannot directly be extrapolated to people of different races. However, as macro- and microstructural properties of the human brain are identical in people of various races, the results are likely valid across ethnic populations.

The $ADC_{av}$ values and perfusion parameters of the cortical GM were higher than those of the WM, being in good agreement with the results of previous studies (Chien et al, 1990; Gideon et al, 1994; Koshimoto et al, 1999; Vonken et al, 1999; Tanner et al, 2000). The difference may partly be due to structural, functional, and circulation differences between the GM and the WM (Netter, 1991; Tatu et al, 1998), and partly to methodological issues. The GM contains more water and has a higher blood flow than the WM (de Groot and Chusid, 1991), both of which contribute to the $ADC_{av}$ values and perfusion parameters. Furthermore, a partial volume effect of the CSF and the major vessels of the meninges adjacent to the cortical GM may cause changes in these parameters (Latour and Warach, 2002). In the study of $ADC_{av}$ values (Study I), the very small variation within the cortical GM ROIs suggests that CSF contamination is unlikely. However, in the DSC MRI study (Study II), the range within the CBF of the GM was fairly large, indicating possible contamination of those ROIs with adjacent major vessels

of the meninges. The $ADC_{av}$ values of the CSF were more than twice as high as those of the GM and almost three times as high as those of the WM, since diffusion is much less restricted in the CSF than in brain tissue. In the basal ganglia and the thalamus, the $ADC_{av}$ values and perfusion parameters were between the values of the cortical GM and the WM, probably because of their microstructural properties and circulation (de Groot and Chusid, 1991; Tatu et al, 1998).

The brain lobes showed small variability in perfusion parameters, supporting the findings of earlier reports (Catafau et al., 1996; Tanaka et al., 2000). Temporal lobes tended to have higher perfusion rates than the other three lobes. The $ADC_{av}$ values of the 45 healthy people in Study III also showed small lobular variability, the frontal lobes having the highest values. This finding was, however, not supported by the results for 80 healthy people in Study I. This discrepancy may partly be due to the marginally different ROI analyses used (see below) or the slightly different subject populations concerning the amount and severity of LA. Generally, the differences between the brain lobes both in the DWI studies and in the DSC MRI study were small, and the clinical significance of these differences, if any, remains to be clarified in future studies. It may, however, be hypothesized that the lobular variability is partly due to differences in the microscopic structure and functional organization of the brain, and partly to the different vascular organization of the lobes (de Groot and Chusid, 1991; Tatu et al, 1998). The hypothesis of different vascular organization of the lobes receives some support from the findings of the WsR (Study III), since the anterior WsR showed higher $ADC_{av}$ values than the posterior one.

DWI and DSC MRI did not demonstrate any differences between brain hemispheres regardless of whether the analyses were conducted between the right and left hemispheres or between dominant and nondominant sides. Only the $ADC_{av}$ values of the left cerebellar GM were higher than those of the right one, but the finding was almost negligible and could have been the result of contamination of the cerebellar GM ROIs with the WM or CSF, because the cerebellar GM is thin and has extensive folia.

The absolute $ADC_{av}$ values and perfusion parameters found in the studies of the healthy population were in good correlation with those in the literature (Gideon et al, 1994; Østergaard et al, 1996a; Schreiber et al, 1998; Koshimoto et al, 1999; Engelter et al, 2000b; Tanner et al, 2000). However, despite the main results of the DSC MRI study being in agreement with earlier research, some differences were found in the CBF of the cortical GM (94±23 mL/100 g/min) and in the CBV of the WM (1.3±0.4 mL/100 g). Although within the upper range of the CBF reported in the literature (Naritomi et al, 1979; Herzog et al, 1996; Schreiber et al, 1998), the CBF of the cortical GM was still relatively high, especially when compared with the lower boundary (Leenders et al, 1990; Koshimoto et al, 1999). This finding may be due to major vessel contamination, which

inherently increases CBF. The ROIs of the cortical GM are situated near the vessels of the meninges, and thus, contamination is difficult to eliminate altogether. The CBV of the WM, by contrast, was slightly lower than values reported previously (Schreiber et al, 1998; Koshimoto et al, 1999). As data for the healthy population were collected with a SE-based sequence, the CBV may in fact represent the value for the microvasculature, which by definition is lower than the CBV obtained by GE-based sequences (Weisskoff et al, 1994; Boxerman et al, 1995). In addition, a clear difference in sample sizes between the DSC MRI study (n=80) and the studies of the literature (n=10-41) might account for this small difference in WM CBV. Since the above-mentioned deviations from the previous results were only marginal and the majority of the findings in Studies I and II were in excellent correlation with the literature, DSC MRI and especially DWI can be considered to be feasible methods in the study of cerebral hemodynamics and diffusional changes in healthy populations.

Generally, the $ADC_{av}$ values and perfusion parameters did not change with age. However, a significant age-dependent increase was observed in the $ADC_{av}$ values of the thalami and the CSF of the lateral ventricles, as well as in the MTT of the frontal and parietal GM. Moreover, although not significant, a tendency for an increase was seen in mean GM values of the MTT and CBV. Whether the increase in the thalami was due to structural or functional changes related to aging or was a mere statistical artifact remains to be shown. However, some tendency toward an age-related $ADC_{av}$ increase of the thalami (Engelter et al, 2000b) and the whole brain area (Rovaris et al, 2003) have also been found previously, but no firm conclusions could be drawn. The diffusional increase in the CSF of the lateral ventricles may be due to the aging brain becoming less compliant, with the age-related enlargement of the ventricles allowing for more pulsative movement of the CSF (Bakshi et al, 2000). This pulsative movement is likely to increase the turbulence of the CSF flow (Sherman et al., 1987), resulting in an increase in diffusion (Bakshi et al, 2000; Chen et al, 2001). The GM MTT increase found was in line with earlier reports (Fujishima and Omae, 1980). It may be hypothesized that the small increase in these values reflects a decrease in cerebral perfusion pressure with age. The results of all of the other perfusion parameters have been highly variable in the literature (Marchal et al, 1992; Gideon et al, 1994; Engelter et al, 2000b; Meltzer et al, 2000; Wirestam et al, 2000; Chen et al, 2001), and therefore, no conclusions can be drawn.

Although the search for gender-related differences in cerebral anatomy and physiology has been extensive, the findings of clinical and imaging methods have been highly variable (Jones et al., 1998; Gur et al, 1999). The findings of Studies I and II will not reduce the confusion. The $ADC_{av}$ values did not show any differences between genders. The marginal gender-related differences that were found in the MTT and CBV might be accounted for by differences in macro-to-microvascular hematocrit of males

and females. The generally higher blood volume in men than in women might be reflected in differences in MTT values. In addition, a possible effect due to the different sizes of men and women cannot be overlooked. However, the definitive reason for these small hemodynamic differences, if true, remains to be clarified in the future.

In conclusion, the findings of the $ADC_{av}$ values and perfusion parameters in a healthy population showed that aging and gender themselves, without known diseases, have only minor effects on cerebral water diffusion and blood circulation. These findings are important for future studies comparing disease states with normal aging.

## ISCHEMIC STROKE

The $ADC_{av}$ values of ten acute ischemic stroke patients without thrombolytic therapy from the hyperacute (less than six hours) to the chronic phase (three months) were studied as a comparison group for the subjects with LA (Study V). The results were in good correlation with the literature. In hyperacute to subacute stages (one week), the $ADC_{av}$ values were clearly lower (Warach et al, 1995; Lutsep et al, 1997; Ahlhelm et al, 2002) than those of the normal-appearing WM and leukoaraiotic regions. The ischemic lesions at a one-month stage (Lutsep et al, 1997; Schlaug et al, 1997) and the regions of LA could not be distinguished from each other solely by analysis of their $ADC_{av}$ values. The $ADC_{av}$ values of the chronic ischemic stroke group, by contrast, were clearly higher (Lutsep et al, 1997; Ahlhelm et al, 2002) than those of the regions of LA, and thus, easy to distinguish from them. The follow-up studies of the ischemic stroke $ADC_{av}$ values were consistent with these findings (Marks et al, 1996; Schlaug et al, 1997; Weber et al, 2000). It seems that DWI is useful in distinguishing ischemic stroke lesions of acute and chronic stages from regions of LA solely by means of $ADC_{av}$ values (Calli et al, 2003). As the $ADC_{av}$ values of one-month infarcts and the leukoaraiotic regions were similar, DWI appeared not to be useful in distinguishing LA from brain infarction at this time point. Here, conventional MR images are needed for the differential diagnosis. However, the use of conventional MR images is also recommended for more reliable differential diagnosis at other time points of ischemic stroke and LA.

The absolute $ADC_{av}$ values may identify the boundaries of the ischemic tissue precisely (Dardzinski et al., 1993), but their reliable use requires normal reference values for each brain region. A considerable amount of experimental work has been devoted to distinguishing normal and ischemic pixels from each other based on $ADC_{av}$ values (Dardzinski et al, 1993; Takano et al., 1996; Takano et al., 1997). The quantitative values for normal and pathologic structures are especially important when focal or diffuse abnormalities are suspected because minor changes may be difficult to detect by visual

inspection. In experimental studies, the comparison of the $ADC_{av}$ values of the same pixels before and after ischemia induction, or the difference in the $ADC_{av}$ values of the infarcted and the intact hemisphere have been used to detect early ischemia-induced $ADC_{av}$ changes (Mintorovitch et al., 1991; Davis et al., 1994; Roussel et al., 1994; Li et al., 1998). In humans, imaging before stroke insult is not feasible, and the use of the contralateral region for reference may have limitations due to possible earlier lesions. Therefore, $ADC_{av}$ values of the healthy population encompassing the entire brain are important as a normal value reference in the analysis of ischemic stroke patients as well as patients with other brain diseases.

DWI is highly reliable and accurate in the diagnosis of hyperacute stroke (Fiebach et al, 2002). However, the combination of DWI with PI and MRA should be obtained outside the three-hour time-window if thrombolytic therapy is considered (Röther et al, 2002; Schellinger et al, 2003). When a clear demarcation of the irreversibly damaged infarct core and the surrounding tissue-at-risk, i.e. the ischemic penumbra, is seen, thrombolytic therapy can be considered even after the three-hour time-window with acceptable safety. However, the finding of the visible perfusion deficit in a subgroup of CS patients (n=14) in Study IV should remind clinicians about possible chronic hypoperfusion underlying the diffusion-perfusion mismatch even in a patient with hyperacute ischemia. The benefit of thrombolytic therapy in such patients may be less than in patients without CS.

In conclusion, DWI combined with PI and MRA is highly reliable in the diagnosis of hyperacute stroke and in aiding the decision-making for thrombolytic therapy after the three-hour time-window has elapsed. The $ADC_{av}$ values of ischemic stroke have a typical evolution from the hyperacute to the chronic stage. The reference values for human stroke studies must be obtained from a strictly healthy human population, as was the case here.

## CAROTID STENOSIS AND ENDARTERECTOMY

DWI and DSC MRI were used to study the effect of CS and CEA on $ADC_{av}$ values and perfusion parameters in ACS and SCS patient groups separately. Forty-six unilateral CS patients were selected from the 102 CS patients included in the Helsinki Carotid Endarterectomy Study.

In the SCS patient group, the preoperative $ADC_{av}$ values and MTT were clearly elevated, and the CBF decreased in the WM and WsR of the hemisphere ipsilateral to the CS. The clear hemispheric differences in the perfusion parameters were not detected in the ACS patient group, but the ipsilateral $ADC_{av}$ values were elevated in that patient

group as well. By contrast, the CBV did not differentiate the hemispheres in either of the subgroups. The most substantial change linked to the hemodynamic effect of the CS was found in the MTT, supporting previous findings (Maeda et al, 1999; Lythgoe et al, 2000). The hypoperfusion, sufficiently severe to be visually detected in over half of the SCS patients, was significantly associated with the symptomatic status of the stenosis. The threshold for the visual detection of the perfusion deficit could be approximated as an ipsilateral prolongation of the MTT of more than 15-20%. The high prevalence of the visible perfusion deficit in the SCS patient group is a reminder of the potentially confounding role of chronic hypoperfusion in patients with hyperacute ischemic stroke, as it may erroneously be attributed to the acute thrombosis and be regarded as tissue-at-risk (Schlaug et al, 1999; Neumann-Haefelin et al, 2000b). In such cases, MRA demonstrating a tight CS without intracranial arterial occlusions should arouse suspicion of a chronic hypoperfusive state.

CEA was followed by a rapid decrease of the ipsilateral $ADC_{av}$ values of the WM and WsR near the levels of the contralateral hemisphere. This interesting finding is discussed in detail in the next section (Leukoaraiosis, see below). The increased MTT and the decreased CBF in the ipsilateral hemisphere of SCS patients reached the levels of the contralateral hemisphere; the CBV remained at the preoperational level. In ACS patients, the only significant change was observed in the $ADC_{av}$ values of the WM and WsR, as described above. In the contralateral hemisphere, no postoperative changes were detected other than a slight MTT improvement. The chronic-stage (three months) perfusion parameters approached the baseline values, especially in ACS patients. This may explain the small long-term changes in cerebral hemodynamics, also detected previously (Kluytmans et al, 1998a; Wiart et al, 2000).

The findings of the perfusion parameters did not support any particular hemodynamic vulnerability of the WsR or an asymmetrical impact on the anterior and posterior border zones (Wiart et al, 2000). The variation in the CBV was notably low. The CBV is not thought to be sensitive to delay and dispersion of the bolus (Calamante et al, 2000), and only small differences between the ACS and SCS patient groups were seen. Furthermore, the CBV is not likely to be the most sensitive indicator of the hemodynamic reserve. Completely deviating from the findings of the DSC MRI study, the $ADC_{av}$ values of the WsR showed clear differences between the anterior and posterior WsR. The anterior WsR had higher $ADC_{av}$ values than the posterior WsR at every time point. The finding was in good correlation with a previous DSC MRI study (Wiart et al, 2000), and with the finding of the highest $ADC_{av}$ levels in the WM of the frontal lobes. The CS in anterior circulation may be hypothesized to have a propensity to accentuate the differences between the lobes and WsR, depending on the degree of functioning collaterals from anterior or posterior circulation. Since the findings of the

DSC MRI study did not support the hemodynamic difference between the anterior and posterior WsR, no firm conclusions about this hypothesis can be drawn.

The $ADC_{av}$ values and perfusion parameters of the cortical GM and the thalamus did not display interhemispheric or postoperative variation (Wiart et al, 2000). Apart from the microstructural differences between the GM and the WM, the better preservation of the $ADC_{av}$ levels and perfusion parameters in these structures can also be explained by differences in their blood flow. In addition to their arterial supply, the cortical GM receives leptomeningeal collateral supply, and the thalamus vertebrobasilar collateral supply (Tatu et al, 1996; 1998). The findings corroborate the greater hemodynamic impairment of the WM as compared with the GM (Kluytmans et al, 1998a).

The $ADC_{av}$ variation occurred regardless of whether the patients' stenoses were symptomatic or asymptomatic, whereas the subtle hemodynamic preoperative impairment seen in the perfusion parameters of the SCS patient group and its more pronounced response to CEA in comparison with the ACS patient group were elicited. Since the levels of the $ADC_{av}$ values of the ipsilateral hemispheres and their development after CEA were uniform in the ACS and SCS patient groups, also appearing homogeneous in terms of patient characteristics (age, risk factors, and degree of CS), the $ADC_{av}$ measurements did not distinguish the effect of CS in ACS and SCS patient groups. These measurements also did not shed light on why or by which mechanisms some patients with similar CS become symptomatic and some do not.

In the contralateral hemisphere, no changes except for a small decrease in the MTT occurred after CEA. Still, it is notable that also the contralateral $ADC_{av}$ values were higher than in healthy controls. This underscores the pivotal difference between the patients and controls and reflects the greater propensity for leukoaraiotic changes in the presence of various risk factors for vascular disease.

In conclusion, the results of the DSC MRI study (Study IV) corroborate that the preoperative hemodynamic adaptation seems to be poorer in SCS patients than in ACS patients. This may be revealed as an abnormal interhemispheric ratio of the MTT, often producing a visible perfusion deficit in higher-grade stenoses. The ACS patients represented a more stable hemodynamic constitution, and their long-term hemodynamic response to the CEA was negligible. The better hemodynamic adaptation may partly account for the lesser benefit from surgery in these patients, and could also, at least to some extent, explain why they are asymptomatic. Although not having a direct impact on the treatment of CS, the findings serve as a reminder not to overlook the hemodynamic concept in viewing the determinants for SCS, and they encourage future trials to take advantage of more functional and dynamic imaging methods for improved evaluation and risk assessment in carotid disease. The results of the DWI study (Study III), by contrast, showed that DWI alone could not distinguish ACS and SCS patients by the effects of CS

and CEA by means of the $ADC_{av}$ values, nor did it shed light on why or by which mechanisms some patients with similar CS become symptomatic and some do not. However, the findings of the interhemispheric differences in the $ADC_{av}$ values of the WM and WsR, and the diffusional changes after CEA raised the possibility of their involvement in the etiology and pathogenesis of LA (discussed in detail in the next section).

## LEUKOARAIOSIS

DW images and conventional MR images were used to identify subjects with LA. The 85 subjects were selected from the previously described populations of healthy subjects, the Helsinki Carotid Endarterectomy Study subjects, and acute ischemic stroke patients. A validated rating scale was used to classify the leukoaraiotic changes into several groups of different severity (Mäntylä et al, 1999a). Different imaging methods and MR sequences detect the lesions in various ways (Mäntylä et al, 1999a); on the $ADC_{av}$ maps, LA is seen as hyperintense lesions, which are bilateral, and as either patchy or diffuse changes in the cerebral WM (Okada et al, 1999).

Although the etiology and pathogenesis of LA are manifold and somewhat controversial, chronic ischemia and hypoperfusion of the brain are the most popular hypotheses in recent literature (Oppenheimer et al, 1995; Pantoni and Garcia, 1997; Yamauchi et al, 1999; Markus et al, 2000; Brown et al, 2002; O'Sullivan et al, 2002; Hassan et al, 2003). The findings of Studies III and V seem to support these hypotheses since leukoaraiotic changes were found in all imaged stroke and almost all CS patients. As the rate of perfusion is estimated to constitute a few percentage points of the $ADC_{av}$ values of the brain tissue (Le Bihan et al, 1986), the expected consequence of a perfusion deficit in the CS patients would be a minor ipsilateral $ADC_{av}$ decrease. Interestingly, however, significantly higher ipsilateral $ADC_{av}$ values were found, indicating a more complex pathophysiology in these patients. Thus, it seems that it is not the short-term direct effect of reduced perfusion but the sequelae and other physiological mechanisms which dominate in the pathogenesis of LA (Rutgers et al., 2003). In experimentally induced chronic hypoperfusion, the WM has appeared to be the most vulnerable part of the brain, undergoing rarefaction with axonal and myelin changes (Kurumatani et al, 1998). The small difference found between the hemispheres of the leukoaraiotic regions of ipsilateral CS patients gives some further support to the notion of a potentially irreversible leukoaraiogenesis, in accordance with a previous PET study (Yamauchi et al, 1999).

Primarily elevated but potentially reversible $ADC_{av}$ values have been found to be associated with brain disease states that involve vasogenic edema such as hypertensive encephalography or eclampsia (Schwartz et al., 1998; Engelter et al., 2000a). Edematous change indicates altered permeability, redistribution of intra- and extracellular water, and overall increased water content of a tissue. According to the neuropathological investigations, one of the consequences of LA is axonal loss (Pantoni and Garcia, 1997), which may lead to an increase in the water content of a tissue, thereby increasing $ADC_{av}$ values and decreasing fractional anisotropy of the regions of LA (Jones et al, 1999). One may hypothesize that the finding of a relationship between severity of LA and increasing $ADC_{av}$ values reflects the extent of axonal loss. The partly reversible, preoperatively elevated ipsilateral $ADC_{av}$ values in the WM and WsR of CS patients suggest the concomitant existence of both reversible and irreversible components in the pathogenesis of LA, which is triggered and maintained by severe CS. The net decrease observed supports the hypothesis of a corrective effect on cellular-level mechanisms, one of which could be chronic, ipsilaterally focused relative ischemia. DWI provides information on the severity and extent of LA and detects areas of WM that are likely to undergo leukoaraiotic change over time, even though still appearing normal on conventional MRI. The findings of normal-appearing WM in subjects with LA and normal-appearing WM in the ipsilateral hemisphere of CS patients seem to represent a 'preleukoaraiotic' state, which is partly reversible with proper treatment.

The classification of LA according to its severity and extent is a real challenge (Pantoni et al, 2002). Several rating scales with varying approaches have been designed. Some make a distinction between different regions, while others use an overall estimate of LA (Mäntylä et al, 1997; Scheltens et al, 1998; Pantoni et al, 2002). The scales often refer to definite pulse sequences or imaging methods (Mäntylä et al, 1999a). A previously validated rating scale developed at our hospital (Mäntylä et al, 1999a) was chosen for the studies presented here. LA was evaluated on conventional MR images, with periventricular and other WM regions being examined separately. The rating scale used has the advantage of taking into account the number, size, and shape of the leukoaraiotic lesions. Although the numerous rating scales have different approaches to evaluating the LA, comparison of the results of previous studies has been deemed to be reasonable (Pantoni et al, 2002).

In conclusion, the severity of LA was directly related to the level of $ADC_{av}$ values, both in the lesions themselves and also in the normal-appearing WM. The same characteristic diffusional change with the preoperative elevation of the $ADC_{av}$ values in the ipsilateral WM and WsR was also detected in CS patients. This change was partly reversed after CEA. On the basis of these findings, the normal-appearing WM could be hypothesized to be associated with the early leukoaraiogenic process, which can partly be

reversed with proper management, in this case CEA. We coined the term 'preleukoaraiosis' to define the WM regions that appear normal on conventional MR images but have increased $ADC_{av}$ values, and either undergo leukoaraiotic change over time or improve to normal or near normal following proper treatment, such as CEA in patients with severe CS. However, further long-term follow-up studies with repeated MRI are necessary to confirm this concept, to verify to what extent these affected WM regions truly undergo leukoaraiotic change, with or without intervention, and to elucidate the effect on and interplay with other determinants of WM degeneration.

## LIMITATIONS OF METHODS

### DIFFUSION-WEIGHTED IMAGING

DWI methodology has rapidly developed during the last few years, and quantitative measurements of $ADC_{av}$ values have become feasible. However, the variability of the measurement protocols, imaging characteristics, and sequence characteristics (b values, diffusion time, gradient strength, TE, TR, cardiac gating) may still affect the $ADC_{av}$ values considerably (Sherman et al, 1987; Yoshiura et al, 2001; Wilson et al, 2002) and should be taken into account when comparing results between centers and studies.

The ROI analysis of the $ADC_{av}$ maps has some limitations which should also be considered when comparing results between studies and centers. The ROIs should be sufficiently large to exclude the effect of small blood vessels on the $ADC_{av}$ values, yet small enough to eliminate the contamination risk of the given ROIs with nearby regions. The ROIs of cerebral lesions are reliable when the lesions, such as those of ischemic and severely leukoaraiotic regions, are easily detected on $ADC_{av}$ maps. The degree of uncertainty increases when the lesions are more diffuse and therefore hard to detect. Conventional MR images with equivalent slices should be collected to further increase reliability. The ROIs of the cortical GM contaminate easily with the CSF or the WM. In Studies I, III, and V, however, this contamination was nearly excluded, as the range of the $ADC_{av}$ values in the GM ROIs was fairly small, and the values were quite constant between studies. The ROIs of the WM are easier to analyze because the WM is wider and the contamination risk by other regions is less probable. However, the regions of LA, especially when they are abundantly present in a patchy fashion, are pitfalls for ROI analysis of the WM since they can increase $ADC_{av}$ values considerably. As mentioned before, the differences between Studies I and III in $ADC_{av}$ values of the WM of healthy subjects may partly be due to this methodological weakness, albeit the impact of a possible difference in LA between the groups cannot be wholly excluded. However, since

the control values in each study are analyzed separately, and in Study III blindedly to the values of the CS patients, the impact of this difference could be considered negligible, and the findings and comparisons reliable.

Generally, DWI and quantitative analysis of $ADC_{av}$ maps can be deemed reliable so long as the pitfalls in ROI analysis and the methodological limitations are taken into account in comparisons of results.

## DYNAMIC SUSCEPTIBILITY CONTRAST IMAGING

DSC MRI has not yet fulfilled the criteria for strict quantitation or accuracy, essentially because of the simplified assumptions made about the underlying microvascular structure (Kiselev, 2001; Calamante et al, 2002). This technique has some inherent limitations, which have been discussed in the Review of the Literature section. These limitations are briefly outlined here with conclusions followed by a discussion about the analyses of the perfusion maps and the ROIs.

The quantitative analysis for absolute values of perfusion data is based entirely on determining an AIF, which cannot, however, be accurately ascertained by DSC MRI (Perthen et al, 2002). The shape of the AIF can be determined with rather good accuracy, but its height remains arbitrary (Østergaard et al, 1996b), and the proportionality factor relating MR signal change to concentration of Gd-DTPA is not equal in brain tissue and in larger vessels. Therefore, the size of the AIF has to be normalized to the injected dose of Gd-DTPA to produce quantitative results. The premises of the calculation may lead to a systematic error, although the values can be expected to be reasonably proportional to the actual blood flow.

For the calculation of the absolute perfusion parameters, the microvascular hematocrit is approximated to be 2/3 of the systemic blood hematocrit (Østergaard et al, 1996b); however, it is a more complex function of vessel size and physiological conditions, and therefore is more likely be subject-dependent. As the hematocrit ratio is directly associated with the scale factor of relating tissue first-pass area to the CBV, any errors in the hematocrit ratio are directly seen in the quantitative value of the CBV, and in other parameters afterwards.

The orientation of MCA with respect to the main magnetic field has a major effect on the MR signal in PI. In imaging sessions, this is taken into account as accurately as possible, but the anatomy of the brain vessels is often different between subjects, thus having an impact on the perfusion parameters.

A normalization factor for producing the absolute CBF by DSC MRI has been introduced which compares the MR CBF with the PET CBF among a small number of

normal subjects (Østergaard et al, 1998a; Østergaard et al, 1998b). However, the assumption that the same fraction of cardiac output reaches the brain in all subjects may not hold true with aging. The variation in the fraction of cardiac output reaching the brain is a potential confounding factor, especially in patients with heart failure, though not as likely in healthy subjects (Study II) or CS patients with cardiac diseases as exclusion criteria (Study IV). Partial refinement could become possible with correction algorithms (Lin et al, 2001).

The results of Studies II and IV are characteristic for the sequences and parameters used. Deviations from the values may occur with different sequence and parameter combinations. The importance of imaging both controls and patients with the same sequence, the same imaging parameters, and the same MR equipment is even clearer than in studies with DWI.

Because calculations of the perfusion maps rely almost entirely on the accuracy of the researcher, they are open to subjective errors. Inter- and intraobserver reliability was not, however, studied here. Completely automated software for measuring absolute perfusion parameters might be helpful for reliable quantitative calculations.

The ROI analysis of the perfusion maps has difficulties since the ROIs are easily contaminated by other regions or major vessels, despite great care being taken. Conventional MR images are therefore critical in the analysis. Conventional MR images should be imaged with identical slices and be used as guides for ROI selection. In Studies II and IV, conventional MR images were used to identify the ROIs, but the drawing was done directly on CBF maps. The results of the ROIs from the WM, the WsR, and the thalamus can be considered to be reliable because they were easy to detect on the CBF maps. The ROIs of the cortical GM, by contrast, are difficult to detect and less reliable because of contamination risk with the major vessels of the meninges.

In conclusion, while DSC MRI has some limitations, the data are fairly reliable when all steps of the analysis are carried out carefully. The methodology needs additional work for quantification and for more reliable use clinically, but in relative measures and in visual inspection, it already has its place in clinical settings.

## ROLE OF DIFFUSION-WEIGHTED AND DYNAMIC SUSCEPTIBILITY CONTRAST IMAGING IN CLINICAL DECISION-MAKING

DWI is a feasible noninvasive method for acutely ill patients, as it takes only a few seconds to complete and has a complication risk of near zero as long as the normal exclusion criteria for MRI (Shellock et al, 1993) are taken into account. The DWI sequence is easy to add to other MRI modalities.

DWI is at its best in imaging the hyperacute stroke, for which conventional MR images and CT often give almost normal results. With the analysis of $ADC_{av}$ values, the regions of ischemic stroke at different phases, the leukoaraiotic regions, and the normal-appearing WM can be differentiated from each other. As it detects areas of the normal-appearing WM at risk for becoming leukoaraiotic, it can be considered to be a neuropathologic tool in vivo.

Despite its limitations, the DSC MRI technique also has advantages over such imaging methods as PET, SPECT, and functional CT. It offers a good spatial and temporal resolution, is easy and fairly fast to complete, does not expose subjects to ionizing radiation, covers a large spatial volume with good structural images, and is widely available. Unfortunately, DSC MRI is not entirely noninvasive, as it demands intravenous contrast medium, thereby having a small risk of allergic reactions.

On the raw images of DSC MRI, the hyperacute stroke lesion remains bright, while other healthy-appearing regions lose their brightness during the passage of the contrast agent bolus through the brain. Combining the DWI and DSC MRI, the diagnosis of hyperacute stroke becomes increasingly accurate. The most important phase of stroke imaging for optimal decision-making regarding management, particularly thrombolytic therapy, is during the early post-stroke hours (Schellinger et al, 2003).

Age- and gender-matched controls are important in interpreting the results for any disease. The results of these studies showed no clinically significant changes with aging or gender, which is an important novel observation, although it requires confirmation by other studies. The most reliable data are yielded when both patients and controls are imaged with the same MR equipment and the same imaging parameters. In DSC MRI, this is even more important.

In conclusion, DWI and DSC MRI have become widely used MRI sequences in several clinical settings. Their use is fairly easy and they provide valuable information not available from conventional MRI. However, the analysis of quantitative $ADC_{av}$ values or perfusion parameters requires expertise and accuracy.

# CONCLUSIONS

DWI and DSC MRI were used to study several brain regions of a large, representative healthy population with equal numbers of both genders and a wide age range. The other populations comprised ischemic stroke patients imaged from hyperacute to chronic stage of stroke, CS patients before and at three and 100 days after CEA, and subjects with LA. Age-, gender-, and hemisphere-dependency, and the effect of ischemia, CS, CEA, and LA on $ADC_{av}$ values and perfusion parameters (CBV, CBF, and MTT) were tested. Based on these results, the following conclusions were drawn:

1. The $ADC_{av}$ values, CBV, CBF, and MTT in selected regions of the healthy human brain did not differ with age, gender, or brain hemisphere. An age-related change was, however, detected in the $ADC_{av}$ values of the lateral ventricles and the thalamus, and on the MTT of the cortical GM, supporting findings of previous studies. Small differences between genders on the CBV and MTT were detected in some brain regions, but their clinical significance was viewed as negligible and received no firm support from the literature. Diffusion and perfusion parameters between brain hemispheres of the healthy population were very similar. The parameters used in Studies I and II establish a wide reference base for clinical settings and future studies, but the limitations of the methods should be considered.

2. The $ADC_{av}$ values, CBF, and MTT were different between the brain hemispheres of SCS patients before CEA. In ACS patients, only a difference between hemispheric $ADC_{av}$ values was detected. No hemispheric differences in either patient group were found after CEA. Although the perfusion patterns over time differed between ACS and SCS patient groups, no such differences were observed in the $ADC_{av}$ values.

3. The $ADC_{av}$ values of the leukoaraiotic regions and the severity of LA were significantly correlated with each other; the more severe the LA, the higher the $ADC_{av}$ values of the lesions. The $ADC_{av}$ values could be used to distinguish leukoaraiotic regions from normal-appearing WM and from ischemic strokes at various stages, except in the ischemic stroke at one month. The $ADC_{av}$ values of the normal-appearing WM were also pathological and correlated with the severity of LA. DWI can be considered to be a tool for neuropathological investigations in vivo, as it detects areas of WM which may progress to LA, despite appearing normal on conventional images. However, such a process can only be verified in prospective follow-up studies. Additionally, the changes in

the normal-appearing WM seemed to be partly reversible, as indicated by the changes in the $ADC_{av}$ values on the ipsilateral hemisphere of CS after CEA. The concept of 'preleukoaraiosis with a partly reversible component' was introduced to describe such changes.

In conclusion, DWI and DSC MRI have become widely used MRI sequences in several clinical settings since they are fairly easy to use and they provide supplementory information to the conventional MRI. However, the analysis of $ADC_{av}$ values or perfusion parameters requires expertise and accuracy, and additional work for strict quantification is required.

## ACKNOWLEDGMENTS

During the processes of learning the principles of scientific work, imaging of subjects, preparing the articles, and writing this thesis, I have received the help and support of many people. I particularly want to express my gratitude to my supervisor Turgut Tatlisumak for his strict but encouraging and friendly guidance during the course of this work. Without his contagious enthusiasm and participation in all phases of the project, this work would have never been completed. I am especially thankful to Turgut for his justness and support in the difficult times.

My warmest thanks is also due to Professor Markku Kaste, Chairman of the Department of Neurology, for supervising this work and for believing in me despite my lack of experience and knowledge of clinical neurology at the age of 21 years. His congenial attitude towards colleagues, other hospital staff, and patients has made the Department of Neurology a fruitful environment for both good clinical practice and high-quality research.

I thank Joachim Röther and Steve Warach, the reviewers of my thesis, for constructive criticism and comments. I owe my warmest gratitude to Carol Ann Pelli for editing the language of this manuscript.

I am indebted to coworkers Jussi Perkiö, Oili Salonen, Eija Saimanen, Perttu J. Lindsberg, Aki Kangasmäki, Richard AD Carano, and Leif Østergaard for their participation in the studies included here and for generously sharing their ideas and expertise.

Without the friendly, relaxed atmosphere among my friends and colleagues at the Department of Neurology, I would never have begun this project. I, therefore, owe a debt of gratitude to Riitta Kärkkäinen, Saija Eirola, Riitta Lönnqvist, Kirsi Malmberg-Céder, Marjaana Tiainen, Elena Haapaniemi, Tiina Sairanen, Jukka Lyytinen, Mikko Kallela, Kirsi Rantanen, Helena Huhmar, Olli Häppölä, Risto O. Roine, Mika Saarela, Leena Hänninen, and all the others in the department. The person with the greatest influence on my starting this project was Lauri Soinne, whose skills with neurological patients had a huge impact on me. I am grateful to Lauri for his patience with my numerous questions about clinical neurology and scientific work as well as with my never-ending confusion regarding statistical matters.

I am thankful to all of my friends, who have made my life outside scientific world most enjoyable and have given me strength to complete this work, namely Susanna, Hannu, Hanne, Heidi, Patrick, Miina, Olli, Markus, Taras, Katja, Heli, Topi, Jussi, Jenni, Taru, Matti, Marikki, Sami, Piia, Kati, Simo, Jani, Sanna, Janne, Joni, Leila, Anssi, Mari,

Kimmo, Sonja, Anna, Salla, Johanna, Kaisa, Maria, Emmi, Leena, Mari, Mikko, Vilja, Tatu, Niina, Ville, Vilhelmiina, Tomi, Eeva, and Vesa. I also thank my friends and colleagues in Inari, Lapland, for the wonderful time I had there in the year 2002.

My heartfelt gratitude is due to my mother Sirpa, father Paavo, and brother Jaakko for their continuous support over the years. I am most grateful to my best friend and dear sister Laura, and her Jussi and Aaro, for companionship and support. And finally, I thank my soulmate, my beloved husband Timo, who has believed in my capabilities even during the difficult phases of this work, and has been a perfect father to our dear son Eero.

Financial support from the University of Helsinki, the Helsinki University Central Hospital, the Maire Taponen Foundation, the Paulo Foundation, the Finnish Cultural Foundation, the Helsinki Biomedical Graduate School, AstraZeneca, the Finnish Medical Foundation, and the Foundation of Neurology is gratefully acknowledged.

Oulu, 2004

Johanna Helenius

# REFERENCES


1. Adachi M, Hosoya T, Haku T, Yamaguchi K, and Kawanami T (1999) Evaluation of the substantia nigra in patients with Parkinsonian syndrome accomplished using multishot diffusion-weighted MR imaging. *AJNR Am J Neuroradiol* 20**:** 1500-1506.
2. Adams HP Jr, Bendixen BH, Kappelle LJ, Biller J, Love BB, Gordon D, and Marsh EE 3rd (1993) Classification of subtype of acute ischemic stroke. Definition for use in a multicenter clinical trial. TOAST. Trial of Org 10172 in Acute Stroke Treatment. *Stroke* 24**:** 35-41.
3. Agartz I, Sääf J, Wahlund LO, and Wetterberg L (1991) T1 and T2 relaxation time estimates in the normal human brain. *Radiology* 181**:** 537-543.
4. Agartz I, Sääf J, Wahlund LO, and Wetterberg L (1992) Quantitative estimations of cerebrospinal fluid spaces and brain regions in healthy controls using computer-assisted tissue classification of magnetic resonance images: relation to age and sex. *Magn Reson Imaging* 10**:** 217-226.
5. Ahlhelm F, Schneider G, Backens M, Reith W, and Hagen T (2002) Time course of the apparent diffusion coefficient after cerebral infarction. *Eur Radiol* 12**:** 2322-2329.
6. Akiguchi I, Tomimoto H, Suenaga T, Wakita H, and Budka H (1997) Alterations in glia and axons in the brains of Binswanger's disease patients. *Stroke* 28**:** 1423-1429.
7. Albers GW (1999) Expanding the window for thrombolytic therapy in acute stroke. The potential role of acute MRI for patient selection. *Stroke* 30**:** 2230-2237.
8. Alsop DC, Detre JA, and Grossman M (2000) Assessment of cerebral blood flow in Alzheimer's disease by spin-labeled magnetic resonance imaging. *Ann Neurol* 47**:** 93-100.
9. Apruzzese A, Silvestrini M, Floris R, Vernieri F, Bozzao A, Hagberg G, Caltagirone C, Masala S, and Simonetti G (2001) Cerebral hemodynamics in asymptomatic patients with internal carotid artery occlusion: a dynamic susceptibility contrast MR and transcranial doppler study. *AJNR Am J Neuroradiol* 22**:** 1062-1067.
10. Arfanakis K, Haughton VM, Carew JD, Rogers BP, Dempsey RJ, and Meyerand ME (2002) Diffusion tensor MR imaging in diffuse axonal injury. *AJNR Am J Neuroradiol* 23**:** 794-802.
11. Astrup J, Siesjö BK, and Symon L (1981) Thresholds in cerebral ischemia - the ischemic penumbra. *Stroke* 12**:** 723-725.
12. Babikian V and Ropper AH (1987) Binswanger's disease: a review. *Stroke* 18**:** 2-12.
13. Baird AE, Benfield A, Schlaug G, Siewert B, Lövblad KO, Edelman RR, and Warach S (1997) Enlargement of human cerebral ischemic lesion volumes measured by diffusion-weighted magnetic resonance imaging. *Ann Neurol* 41**:** 581-589.
14. Baird AE and Warach S (1998) Magnetic resonance imaging of acute stroke. *J Cereb Blood Flow Metab* 18**:** 583-609.
15. Bakshi R, Caruthers SD, Janardhan V, and Wasay M (2000) Intraventricular CSF pulsation artifact on fast fluid-attenuated inversion-recovery MR images: analysis of 100 consecutive normal studies. *AJNR Am J Neuroradiol* 21**:** 503-508.
16. Bamford J (2001) Risk stratification and carotid surgery: new technology but old trials. *Brain* 124**:** 455-456.
17. Bammer R, Stollberger R, Augustin M, Simbrunner J, Offenbacher H, Kooijman H, Ropele S, Kapeller P, Wach P, Ebner F, and Fazekas F (1999) Diffusion-weighted imaging with navigated interleaved echo-planar imaging and a conventional gradient system. *Radiology* 211**:** 799-806.
18. Barber PA, Darby DG, Desmond PM, Yang Q, Gerraty RP, Jolley D, Donnan GA, Tress BM, and Davis SM (1998) Prediction of stroke outcome with echoplanar perfusion- and diffusion-weighted MRI. *Neurology* 51**:** 418-426.
19. Barber R, Scheltens P, Gholkar A, Ballard C, McKeith I, Ince P, Perry R, and O'Brien J (1999) White matter lesions on magnetic resonance imaging in dementia with Lewy bodies, Alzheimer's disease, vascular dementia, and normal aging. *J Neurol Neurosurg Psychiatry* 67**:** 66-72.
20. Barbier EL, Lamalle L, and Decorps M (2001) Methodology of brain perfusion imaging. *J Magn Reson Imaging* 13**:** 496-520.
21. Barnett HJ, Kaste M, Meldrum H, and Eliasziw M (1996) Aspirin dose in stroke prevention: beautiful hypotheses slain by ugly facts. *Stroke* 27**:** 588-592.
22. Barnett HJ, Meldrum HE, and Eliasziw M (2002) The appropriate use of carotid endarterectomy. *CMAJ* 166**:** 1169-1179.

23. Baron JC, Bousser MG, Rey A, Guillard A, Comar D, and Castaigne P (1981) Reversal of focal "misery-perfusion syndrome" by extra-intracranial arterial bypass in hemodynamic cerebral ischemia. A case study with 15O positron emission tomography. *Stroke* 12**:** 454-459.
24. Barth A, Remonda L, Lövblad KO, Schroth G, and RW Seiler (2000) Silent cerebral ischemia detected by diffusion-weighted MRI after carotid endarterectomy. *Stroke* 31**:** 1824-1828.
25. Beaulieu C, de Crespigny A, Tong DC, Moseley ME, Albers GW, and Marks MP (1999) Longitudinal magnetic resonance imaging study of perfusion and diffusion in stroke: evolution of lesion volume and correlation with clinical outcome. *Ann Neurol* 46**:** 568-578.
26. Belliveau JW, Rosen BR, Kantor HL, Rzedzian RR, Kennedy DN, McKinstry RC, Vevea JM, Cohen MS, Pykett IL, and Brady TJ (1990) Functional cerebral imaging by susceptibility-contrast NMR. *Magn Reson Med* 14**:** 538-546.
27. Biller J and Love BB. (2000). Vascular diseases of the nervous system. A. Ischemic cerebrovascular disease. *In* "Neurology in clinical practice. The neurological disorders" (Bradley WG, Daroff RB, Fenichel GM, and Marsden CD, eds.), Vol. 2, pp. 1125-1166. Butterworth-Heinemann, Boston.
28. Bogousslavsky J, Kaste M, Skyhoj Olsen T, Hacke W, and Orgogozo JM (2000) Risk factors and stroke prevention. *Cerebrovasc dis* 10, suppl 3**:** 12-21.
29. Bonita R (1992) Epidemiology of stroke. *Lancet* 339**:** 342-344.
30. Boxerman JL, Hamberg LM, Rosen BR, and Weisskoff RM (1995) MR contrast due to intravascular magnetic susceptibility perturbations. *Magn Reson Med* 34**:** 555-566.
31. Breger RK, Yetkin FZ, Fischer ME, Papke RA, Haughton VM, and Rimm AA (1991) T1 and T2 in the cerebrum: correlation with age, gender, and demographic factors. *Radiology* 181**:** 545-547.
32. Breteler MM, van Amerongen NM, van Swieten JC, Claus JJ, Grobbee DE, van Gijn J, Hofman A, and van Harskamp F (1994) Cognitive correlates of ventricular enlargement and cerebral white matter lesions on magnetic resonance imaging. The Rotterdam Study. *Stroke* 25**:** 1109-1115.
33. Briley DP, Haroon S, Sergent SM, and Thomas S (2000) Does leukoaraiosis predict morbidity and mortality? *Neurology* 54**:** 90-94.
34. Britt PM, Heiserman JE, Snider RM, Shill HA, Bird CR, and Wallace RC (2000) Incidence of postangiographic abnormalities revealed by diffusion-weighted MR imaging. *AJNR Am J Neuroradiol* 21**:** 55-59.
35. Brockstedt S, Thomsen C, Wirestam R, Holtas S, and Stahlberg F (1998) Quantitative diffusion coefficient maps using fast spin-echo MRI. *Magn Reson Imaging* 16**:** 877-886.
36. Brown WR, Moody DM, Challa VR, Thore CR, and Anstrom JA (2002) Venous collagenosis and arteriolar tortuosity in leukoaraiosis. *J Neurol Sci* 203-204**:** 159-163.
37. Brown WR, Moody DM, Thore CR, and Challa VR (2000) Apoptosis in leukoaraiosis. *AJNR Am J Neuroradiol* 21**:** 79-82.
38. Burdette JH, Elster AD, and Ricci PE (1998) Calculation of apparent diffusion coefficients (ADCs) in brain using two-point and six-point methods. *J Comput Assist Tomogr* 22**:** 792-794.
39. Burdette JH, Elster AD, and Ricci PE (1999) Acute cerebral infarction: quantification of spin-density and T2 shine-through phenomena on diffusion-weighted MR images. *Radiology* 212**:** 333-339.
40. Calamante F, Gadian DG, and Connelly A (2000) Delay and dispersion effects in dynamic susceptibility contrast MRI: simulations using singular value decomposition. *Magn Reson Med* 44**:** 466-473.
41. Calamante F, Gadian DG, and Connelly A (2002) Quantification of perfusion using bolus tracking magnetic resonance imaging in stroke: assumptions, limitations, and potential implications for clinical use. *Stroke* 33**:** 1146-1151.
42. Calamante F, Thomas DL, Pell GS, Wiersma J, and Turner R (1999) Measuring cerebral blood flow using magnetic resonance imaging techniques. *J Cereb Blood Flow Metab* 19**:** 701-735.
43. Calli C, Kitis O, and Yunten N (2003) DWI findings of periventricular ischemic changes in patients with leukoaraiosis. *Comput Med Imaging Graph* 27**:** 381-386.
44. Caramia F, Pantano P, Di Legge SD, Piattella MC, Lenzi D, Paolillo A, Nucciarelli W, Lenzi GL, Bozzao L, and Pozzilli C (2002) A longitudinal study of MR diffusion changes in normal appearing white matter of patients with early multiple sclerosis. *Magn Reson Imaging* 20**:** 383-388.
45. Catafau AM, Lomena FJ, Pavia J, Parellada E, Bernardo M, Setoain J, and Tolosa E (1996) Regional cerebral blood flow pattern in normal young and aged volunteers: a 99mTc-HMPAO SPET study. *Eur J Nucl Med* 23**:** 1329-1337.
46. Cercignani M, Bozzali M, Iannucci G, Comi G, and Filippi M (2001) Magnetisation transfer ratio and mean diffusivity of normal appearing white and grey matter from patients with multiple sclerosis. *J Neurol Neurosurg Psychiatry* 70**:** 311-317.

47. Cercignani M, Iannucci G, Rocca MA, Comi G, Horsfield MA, and Filippi M (2000) Pathologic damage in MS assessed by diffusion-weighted and magnetization transfer MRI. *Neurology* 54**:** 1139-1144.
48. Cha S, Knopp EA, Johnson G, Wetzel SG, Litt AW, and Zagzag D (2002) Intracranial mass lesions: Dynamic contrast-enhanced susceptibility-weighted echo-planar perfusion MR imaging. *Radiology* 223**:** 11-29.
49. Chambers BR, You RX, and Donnan GA (2002) Carotid endarterectomy for asymptomatic carotid stenosis. *Cochrane Database of Systematic Reviews* Issue 3.
50. Chang L, Ernst T, Poland R, and Jenden D (1996) In vivo proton magnetic resonance spectroscopy of the normal aging human brain. *Life Sci* 58**:** 2049-2056.
51. Chaves CJ, Staroselskaya I, Linfante I, Llinas R, Capla LR, and Warach S (2003) Patterns of perfusion-weighted imaging in patients with carotid artery occlusive disease. *Arch Neurol* 60**:** 237-242.
52. Chen ZG, Li TQ, and Hindmarsh T (2001) Diffusion tensor trace mapping in normal adult brain using single-shot EPI technique. A methodological study of the aging brain. *Acta Radiol* 42**:** 447-458.
53. Chien D, Buxton RB, Kwong KK, Brady TJ, and Rosen BR (1990) MR diffusion imaging of human brain. *J Comp Assist Tomogr* 14**:** 514-520.
54. Chu K, Kang DW, Yoon BW, and Roh JK (2001) Diffusion-weighted magnetic resonance in cerebral venous thrombosis. *Arch Neurol* 58**:** 1569-1576.
55. Clark WM, Wissman S, Albers GW, Jhamandas JH, Madden KP, and Hamilton S (1999) Recombinant tissue-type plasminogen activator (Alteplase) for ischemic stroke 3 to 5 hours after symptom onset. The ATLANTIS Study: a randomized controlled trial. Alteplase Thrombolysis for Acute Noninterventional Therapy in Ischemic Stroke. *JAMA* 282**:** 2019-2026.
56. Conturo TE, Lori NF, Cull TS, Akbudak E, Snyder AZ, Shimony JS, McKinstry RC, Burton H, and Raichle ME (1999) Tracking neuronal fiber pathways in the living human brain. *PNAS* 96**:** 10422-10427.
57. Cutrer FM, Sorensen AG, Weisskoff RM, Østergaard L, Sanchez del Rio M, Lee EJ, Rosen BR, and Moskowitz MA (1998) Perfusion-weighted imaging defects during spontaneous migrainous aura. *Ann Neurol* 43**:** 25-31.
58. Darby DG, Barber PA, Gerraty RP, Desmond PM, Yang Q, Parsons M, Li T, Tress BM, and Davis SM (1999) Pathophysiological topography of acute ischemia by combined diffusion-weighted and perfusion MRI. *Stroke* 30**:** 2043-2052.
59. Dardzinski BJ, Sotak CH, Fisher M, Hasegawa Y, Li L, and Minematsu K (1993) Apparent diffusion coefficient mapping of experimental focal cerebral ischemia using diffusion-weighted echo-planar imaging. *Magn Reson Med* 1994**:** 318-325.
60. Davis D, Ulatowski J, Eleff S, Izuta M, Mori S, Shungu D, and van Zijl PC (1994) Rapid monitoring of changes in water diffusion coefficient during reversible ischemia in cat and rat brain. *Magn Reson Med* 31**:** 454-460.
61. de Groot J and Chusid JG. (1991). Correlative Neuroanatomy. *In*, pp. 319. Appleton & Lange, Connecticut.
62. Demaerel P, Heiner L, Robberecht W, Sciot R, and Wilms G (1999) Diffusion-weighted MRI in sporadic Creutzfeldt-Jakob disease. *Neurology* 52**:** 205-208.
63. Demaerel P, Sciot R, Robberecht W, Dom R, Vandermeulen D, Maes F, and Wilms G (2003) Accuracy of diffusion-weighted MR imaging in the diagnosis of sporadic Creutzfeldt-Jakob disease. *J Neurol* 250**:** 222-225.
64. Derdeyn CP, Grubb RL Jr, and Powers WJ (1999) Cerebral hemodynamic impairment: methods of measurement and association with stroke risk. *Neurology* 53**:** 251-259.
65. Derdeyn CP, Videen TO, Yundt KD, Fritsch SM, Carpenter DA, Grubb RL, and Powers WJ (2002) Variability of cerebral blood volume and oxygen extraction: stages of cerebral haemodynamic impairment revisited. *Brain* 125**:** 595-607.
66. Derdeyn CP, Yundt KD, Videen TO, Carpenter DA, Grubb RL Jr, and WJ Powers (1998) Increased oxygen extraction fraction is associated with prior ischemic events in patients with carotid occlusion. *Stroke* 29**:** 754-758.
67. Dirnagl U, Iadecola C, and Moskowitz MA (1999) Pathobiology of ischaemic stroke: an integrated view. *Trends Neurosci* 22**:** 391-397.
68. Doerfler A, Eckstein HH, Eichbaum M, Heiland S, Benner T, Allenberg JR, and Forsting M (2001) Perfusion-weighted magnetic resonance imaging in patients with carotid artery disease before and after carotid endarterectomy. *J Vasc Surg* 34**:** 587-593.

69. Droogan AG, Clark CA, Werring DJ, Barker GJ, McDonald WI, and Miller DH (1999) Comparison of multiple sclerosis clinical subgroups using navigated spin echo diffusion-weighted imaging. *Magn Reson Imaging* 17**:** 653-661.
70. Edelman RR, Wielopolski P, and Schmitt F (1994) Echo-planar MR imaging. *Radiology* 192**:** 600-612.
71. Engelter ST, Provenzale JM, and Petrella JR (2000a) Assessment of vasogenic edema in eclapsia using diffusion imaging. *Neuroradiology* 42**:** 818-820.
72. Engelter ST, Provenzale JM, Petrella JR, DeLong DM, and MacFall JR (2000b) The effect of aging on the apparent diffusion coefficient of normal-appearing white matter. *AJR Am J Radiol* 175**:** 425-430.
73. Eriksson SH, Symms MR, Rugg-Gunn FJ, Boulby PA, Wheeler-Kingshott CA, Barker GJ, Duncan JS, and Parker GJ (2002) Exploring white matter tracts in band heterotopia using diffusion tractography. *Ann Neurol* 52**:** 327-334.
74. European Carotid Surgery Trialists' Collaborative Group (1998) Randomised trial of endarterectomy for recently symptomatic carotid stenosis: final results of the MRC European Carotid Surgery Trial (ECST). *Lancet* 351**:** 1379-1387.
75. Falconer JC and Narayana PA (1997) Cerebrospinal fluid-suppressed high-resolution diffusion imaging of human brain. *Magn Reson Med* 37**:** 119-123.
76. Feiwell RJ, Besmertis L, Sarkar R, Saloner DA, and Rapp JH (2001) Detection of clinically silent infarcts after carotid endarterectomy by use of diffusion-weighted imaging. *AJNR Am J Neuroradiol* 22**:** 646-649.
77. Fiebach JB, Schellinger PD, Jansen O, Meyer M, Wilde P, Bender J, Schramm P, Juttler E, Oehler J, Hartmann M, Hahnel S, Knauth M, Hacke W, and Sartor K (2002) CT and diffusion-weighted MR imaging in randomized order: diffusion-weighted imaging results in higher accuracy and lower interrater variability in the diagnosis of hyperacute ischemic stroke. *Stroke* 33**:** 2206-2210.
78. Fiehler J, Fiebach JB, Gass A, Hoehn M, Kucinski T, Neumann-Haefelin T, Schellinger PD, Siebler M, Villringer A, and J Röther (2002a) Diffusion-weighted imaging in acute stroke--a tool of uncertain value? *Cerebrovasc Dis* 14**:** 187-196.
79. Fiehler J, Foth M, Kucinski T, Knab R, von Bezold M, Weiller C, Zeumer H, and Röther J (2002b) Severe ADC decreases do not predict irreversible tissue damage in humans. *Stroke* 33**:** 79-86.
80. Fiehler J, Knab R, Reichenbach JR, Fitzek C, Weiller C, and Röther J (2001) Apparent diffusion coefficient decreases and magnetic resonance imaging perfusion parameters are associated in ischemic tissue of acute stroke patients. *J Cereb Blood Flow Metab* 21**:** 577-584.
81. Fiehler J, von Bezold M, Kucinski T, Knab R, Eckert B, Wittkügel O, Zeumer H, and Röther J (2002c) Cerebral blood flow predicts lesion growth in acute stroke patients. *Stroke* 33**:** 2421-2425.
82. Fisel CR, Ackerman JL, Buxton RB, Garrido L, Belliveau JW, Rosen BR, and Brady TJ (1991) MR contrast due to microscopically heterogeneous magnetic susceptibility: numerical simulations and applications to cerebral physiology. *Magn Reson Med* 17**:** 336-347.
83. Fisher M and Albers GW (1999) Application of diffusion-perfusion magnetic resonance imaging in acute ischemic stroke. *Neurology* 52**:** 1750-1756.
84. Fitzek C, Weissmann M, Speckter H, Fitzek S, Hopf HC, Schulte E, and Stoeter P (2001) Anatomy of brain-stem white-matter tracts shown by diffusion-weighted imaging. *Neuroradiology* 43**:** 953-960.
85. Fogelholm R, Murros K, Rissanen A, and Ilmavirta M (1997) Decreasing incidence of stroke in central Finland, 1985-1993. *Acta Neurol Scand* 95**:** 38-43.
86. Fujishima M and Omae T (1980) Brain blood flow and mean transit time as related to aging. *Gerontology* 26**:** 104-107.
87. Geijer B, Lindgren A, Brockstedt S, Ståhlberg F, and Holtas S (2001) Persistent high signal on diffusion-weighted MRI in the late stages of small cortical and lacunar ischaemic lesions. *Neuroradiology* 43**:** 115-122.
88. Gideon P, Thomsen C, and Henriksen O (1994) Increased self-diffusion of brain water in normal aging. *J Magn Reson imaging* 4**:** 185-188.
89. Gillard JH, Hardingham CR, Kirkpatrick PJ, Antoun NM, Freer CEL, and Griffiths PD (1998) Evaluation of carotid endarterectomy with sequential MR perfusion imaging: a preliminary report. *AJNR Am J Neuroradiol* 19**:** 1747-1752.
90. Gonzalez RG, Schaefer PW, Buonanno FS, Schwamm LH, Budzik RF, Rordorf G, Wang B, Sorensen AG, and Koroshetz WJ (1999) Diffusion-weighted MR imaging: diagnostic accuracy in patients imaged within 6 hours of stroke symptom onset. *Radiology* 210**:** 155-162.

91. Gordon DL, Bendixen BH, Adams HP Jr, Clarke W, Kappelle LJ, and Woolson RF (1993) Interphysician agreement in the diagnosis of subtypes of acute ischemic stroke: impilications for clinical trials. The TOAST investigators. *Neurology* 43**:** 1021-1027.
92. Grant PE, He J, Halpern EF, Wu O, Schaefer PW, Schwamm LH, Budzik RF, Sorensen AG, Koroshetz WJ, and Gonzalez RG (2001) Frequency and clinical context of decreased apparent diffusion coefficient reversal in the human brain. *Radiology* 221**:** 43-50.
93. Griffiths PD, Wilkinson ID, Wels T, and Hoggard N (2001) Brain MR perfusion imaging in humans. *Acta Radiol* 42**:** 555-559.
94. Guo AC, Jewells VL, and Provenzale JM (2001) Analysis of normal-appearing white matter in multiple sclerosis: comparison of diffusion tensor MR imaging and magnetization transfer imaging. *AJNR Am J Neuroradiol* 22**:** 1893-1900.
95. Guo AC, MacFall JR, and Provenzale JM (2002) Multiple sclerosis: diffusion tensor MR imaging for evaluation of normal-appearing white matter. *Radiology* 222**:** 729-36.
96. Gur RC, Turetsky BI, Matsui M, Yan M, Bilker W, Hughett P, and Gur RE (1999) Sex differences in brain gray and white matter in healthy young adults: correlations with cognitive performance. *J Neurosci* 19**:** 4065-4072.
97. Guttmann CRG, Jolesz FA, Kikinis R, Killiany RJ, Moss MB, Sandor T, and Albert MS (1998) White matter changes with normal aging. *Neurology* 50**:** 972-978.
98. Haacke EM, Brown RW, Thompson MR, and Venkatesan R (eds.) (1999). Magnetic resonance imaging - physical principles and sequence design. "Magnetic resonance imaging - physical principles and sequence design." Wiley-Liss, New York.
99. Hachinski VC, Potter P, and Merskey H (1987) Leukoaraiosis. *Arch Neurol* 44**:** 21-23.
100. Hacke W, Kaste M, Fieschi C, Toni D, Lesaffre E, von Kummer R, Boysen G, Bluhmki E, Hoxter G, Mahagne MH, and al et (1995) Intravenous thrombolysis with recombinant tissue plasminogen activator for acute hemispheric stroke. The European Cooperative Acute Stroke Study (ECASS). *JAMA* 274**:** 1017-1025.
101. Hacke W, Kaste M, Skyhoj Olsen T, Bogousslavsky J, and Orgogozo JM (2000) Acute treatment of ischemic stroke. *Cerebrovasc dis* 10, suppl 3**:** 22-33.
102. Hamill RW and Pilgrim DM. (2000). Geriatric neurology. *In* "Neurology in clinical practice. The neurological disorders" (Bradley WG, Daroff RB, Fenichel GM, and Marsden CD, eds.), Vol. 2, pp. 2269-2296. Butterworth-Heinemann, Boston.
103. Hanuy H, Asano T, Sakurai H, Imon Y, Iwamoto T, Takasaki M, Shindo H, and Abe K (1999) Diffusion-weighted and magnetization transfer imagin of the corpus callosum in Alzheimer's disease. *J Neurol Sci* 167**:** 37-44.
104. Hanuy H, Sakurai H, Iwamoto T, Takasaki M, Shindo H, and Abe K (1998) Diffusion-weighted MR imaging of the hippocampus and temporal white matter in Alzheimer's disease. *J Neurol Sci* 156**:** 195-200.
105. Harada K, Fujita N, Sakurai K, Akai Y, Fujii K, and Kozuka T (1991) Diffusion imaging of the human brain: a new pulse sequence application for a 1.5-T standard MR system. *AJNR Am J Neuroradiol* 12**:** 1143-1148.
106. Hartl WH, Janssen I, and Furst H (1994) Effect of carotid endarterectomy on patterns of cerebrovascular reactivity in patients with unilateral carotid artery stenosis. *Stroke* 25**:** 1952-1957.
107. Haselgrove JC and Moore JR (1996) Correction for distortion of echo-planar images used to calculate the apparent diffusion coefficient. *MRM* 36**:** 960-964.
108. Haselhorst R, Kappos L, Bilecen D, Scheffler K, Möri D, Radü EW, and Seelig J (2000) Dynamic susceptibility contrast MR imaging of plaque development in multiple sclerosis: application of an extended blood-brain barrier leakage correction. *J Magn Reson Imaging* 11**:** 495-505.
109. Hassan A, Hunt BJ, O'Sullivan M, Parmar K, Bamford JM, Briley D, Brown MM, Thomas DL, and Markus HS (2003) Markers of endothelial dysfunction in lacunar infarction and ischemic leukoaraiosis. *Brain* 126**:** 424-432.
110. Helpern JA and Huang N (1995) Diffusion-weighted imaging in epilepsy. *Magn Reson Imaging* 13**:** 1227-1231.
111. Herzog H, Seitz RJ, Tellmann L, Rota Kops E, Julicher F, Schlaug G, Kleinschmidt A, and Muller-Gartner HW (1996) Quantitation of regional cerebral blood flow with 15O-butanol and positron emission tomography in humans. *J Cereb Blood Flow Metab* 16**:** 645-649.
112. Hoehn M, Nicolay K, Franke C, and van der Sanden B (2001) Application of magnetic resonance to animal models of cerebral ischemia. *J Magn Reson Imaging* 14**:** 491-509.
113. Horowitz AL (1995) Physics for radiologists - a visual approach. "Physics for radiologists - a visual approach." Springler-Verlag, New York.

114. Hossmann KA (1994) Glutamate-mediated injury in focal cerebral ischemia: the excitotoxin hypothesis revised. *Brain Pathol* **4:** 23-36.
115. Hossmann KA and Hoehn-Berlage M (1995) Diffusion and perfusion MR imaging of cerebral ischemia. *Cerebr Brain Metab Rev* 7**:** 187-217.
116. Hugg JW, Butterworth EJ, and Kuzniecky RI (1999) Diffusion mapping applied to mesial temporal lobe epilepsy. *Neurology* 53**:** 173-176.
117. Hunsche S, Sauner D, Schreiber WG, Oelkers P, and Stoeter P (2002) FAIR and dynamic susceptibility contrast-enhanced perfusion imaging in healthy subjects and stroke patients. *J Magn Reson Imaging* 16**:** 137-146.
118. Inzitari D (2003) Leukoaraiosis: an independent risk factor for stroke? *Stroke* 34**:** 2067-2071.
119. Inzitari D, Cadelo M, Marranci ML, Pracucci G, and Pantoni L (1997) Vascular deaths in elderly neurological patients with leukoaraiosis. *J Neurol Neurosurg Psychiatry* 62**:** 177-181.
120. Jaeger HJ, Mathias KD, Hauth E, Drescher R, Gissler HM, Hennigs S, and Christmann A (2002) Cerebral ischemia detected with diffusion-weighted MR imaging after stent implantation in the carotid artery. *AJNR Am J Neuroradiol* 23**:** 200-207.
121. Jezzard P, Barnett AS, and Pierpaoli C (1998) Characterization of and correction for eddy current artifact in echo planar diffusion imaging. *MRM* 39**:** 801-812.
122. Jones DK, Lythgoe D, Horsfield MA, Simmons A, Williams SC, and Markus HS (1999) Characterization of white matter damage in ischemic leukoaraiosis with diffusion tensor MRI. *Stroke* 30**:** 393-397.
123. Jones K, Johnson KA, Becker JA, Spiers PA, Albert MS, and Holman BL (1998) Use of singular value decomposition to characterize age and gender differences in SPECT cerebral perfusion. *J Nucl Med* 39**:** 965-973.
124. Jørgensen HS, Nakayama H, Raaschou HO, Gam J, and Olsen TS (1994) Silent infarction in acute stroke patients. Prevalence, localization, risk factors, and clinical significance: the Copenhagen Stroke Study. *Stroke* 25**:** 97-104.
125. Kahn MB, Patterson HK, Seltzer J, Fitzpatrick M, Smullens S, Bell R, DiMuzio P, and Carabasi RA (1999) Early carotid endarterectomy in selected stroke patients. *Ann Vasc Surg* 13**:** 463-467.
126. Kajimoto K, Moriwaki H, Yamada N, Hayashida K, Kobayashi J, Miyashita K, and Naritomi H (2003) Cerebral hemodynamic evaluation using perfusion-weighted magnetic resonance imaging: comparison with positron emission tomography values in chronic occlusive carotid disease. *Stroke* 34**:** 1662-1666.
127. Kang DW, Chu K, Ko SB, Kwon SJ, Yoon BW, and Roh JK (2002) Lesion patterns and mechanism of ischemia in internal carotid artery disease: a diffusion-weighted imaging study. *Arch Neurol* 59**:** 1577-1582.
128. Karonen JO, Liu Y, Vanninen RL, Østergaard L, Partanen PL, Vainio PA, Vanninen EJ, Nuutinen J, Roivainen R, Soimakallio S, Kuikka JT, and Aronen HJ (2000) Combined perfusion- and diffusion-weighted MR imaging in acute ischemic stroke during the 1st week: a longitudinal study. *Radiology* 217**:** 886-894.
129. Karonen JO, Vanninen RL, Liu Y, Østergaard L, Kuikka JT, Nuutinen J, Vanninen EJ, Partanen PL, Vainio PA, Korhonen K, Perkiö J, Roivainen R, Sivenius J, and Aronen HJ (1999) Combined diffusion and perfusion MRI with correlation to single-photon emission CT in acute ischemic stroke. Ischemic penumbra predicts infarct growth. *Stroke* 30**:** 1583-1590.
130. Kaste M (2003) Approval of alteplase in Europe: will it change stroke management? *Lancet Neurol* 2**:** 207-208.
131. Kaste M, Skyhoj Olsen T, Orgogozo JM, Bogousslavsky J, and Hacke W (2000) Organization of stroke care: education, stroke units and rehabilitation. *Cererbrovasc dis* 10, suppl 3**:** 1-11.
132. Kastrup A, Schulz JB, Mader I, Dichgans J, and Kuker W (2002) Diffusion-weighted MRI in patients with symptomatic internal carotid artery disease. *J Neurol* 249**:** 1168-1174.
133. Kiselev VG (2001) On the theoretical basis of perfusion measurements by dynamic susceptibility contrast MRI. *Magn Reson Med* 46**:** 1113-1122.
134. Klijn CJ, Kappelle LJ, Tulleken CA, and van Gijn J (1997) Symptomatic carotid artery occlusion. A reappraisal of hemodynamic factors. *Stroke* 28**:** 2084-2093.
135. Kluytmans M, van der Grond J, Eikelboom BC, and Viergever MA (1998a) Long-term hemodynamic effects of carotid endarterectomy. *Stroke* 29**:** 1567-1572.
136. Kluytmans M, van der Grond J, Folkers PJ, Mali WP, and Viergever MA (1998b) Differentiation of gray matter and white matter perfusion in patients with unilateral internal carotid artery occlusion. *J Magn Reson Imaging* 8**:** 767-774.

137. Knopp EA, Cha S, Johnson G, Mazumdar A, Golfinos JG, Zagzag D, Miller DC, Kelly PJ, and Kricheff II (1999) Glial neoplasms: dynamic contrast-enhanced T2*-weighted MR imaging. *Radiology* 211**:** 791-798.
138. Kono K, Inoue Y, Nakayama K, Shakudo M, Morino M, Ohata K, Wakasa K, and Yamada R (2001) The role of diffusion-weighted imaging in patients with brain tumors. *AJNR Am J Neuroradiol* 22**:** 1081-1088.
139. Koshimoto Y, Yamada H, Kimura H, Maeda M, Tsuchida C, Kawamura Y, and Ishii Y (1999) Quantitative analysis of cerebral microvascular hemodynamics with T2-weighted dynamic MR imaging. *J Magn Reson Imaging* 9**:** 462-467.
140. Krausz Y, Bonne O, Gorfine M, Karger H, Lerer B, and Chisin R (1998) Age-related changes in brain perfusion of normal subjects detected by 99mTc-HMPAO SPECT. *Neuroradiology* 40**:** 428-434.
141. Kurumatani T, Kudo T, Ikura Y, and Takeda M (1998) White matter changes in the gerbil brain under chronic cerebral hypoperfusion. *Stroke* 29**:** 1058-1062.
142. Lassen NA (1985) Normal average value of cerebral blood flow in younger adults is 50 ml/100 g/min. *J Cereb Blood Flow Metab* 5**:** 347-349.
143. Latour LL and Warach S (2002) Cerebral spinal fluid contamination of the measurement of the apparent diffusion coefficient of water in acute stroke. *MRM* 48**:** 478-486.
144. Le Bihan D (1990) Magnetic resonance imaging of perfusion. *Magn Reson Med* 14**:** 283-292.
145. Le Bihan D, Breton E, Lallemand D, Grenier P, Canabis E, and Laval-Jeantet M (1986) MR imaging of intravoxel incoherent motions: application to diffusion and perfusion in neurological disorders. *Radiology* 161**:** 401-407.
146. Le Bihan D, Mangin JF, Poupon C, Clark CA, Pappata S, Molko N, and Chabriat H (2001) Diffusion tensor imaging: concepts and applications. *J Magn Reson Imaging* 13**:** 534-546.
147. Le Bihan D, Turner R, Douek P, and Patronas N (1992) Diffusion MR imaging: clinical applications. *AJR Am J Radiol* 159**:** 591-599.
148. Leenders KL, Perani D, Lammertsma AA, Heather JD, Buckingham P, Healy MJ, Gibbs JM, Wise RJ, Hatazawa J, Herold S, Beaney RP, Brooks DJ, Spinks T, Rhodes C, Frackowiak RSJ, and Jones T (1990) Cerebral blood flow, blood volume and oxygen utilization. Normal values and effect of age. *Brain* 113**:** 27-47.
149. Li F, Han SS, Tatlisumak T, Carano RAD, Irie K, Sotak CH, and Fisher M (1998) A new method to improve in-bore middle cerebral artery occlusion in rats. Demonstration with diffusion- and perfusion-weighted imaging. *Stroke* 29**:** 1715-1720.
150. Li F, Han SS, Tatlisumak T, Liu KF, Garcia JH, Sotak CH, and Fisher M (1999) Reversal of acute apparent diffusion coefficient abnormalities and delayed neuronal death following transient focal cerebral ischemia in rats. *Ann Neurol* 46**:** 333-342.
151. Li TQ, Guang Chen Z, Østergaard L, Hindmarsh T, and Moseley ME (2000) Quantification of cerebral blood flow by bolus tracking and artery spin tagging methods. *Magn Reson Imaging* 18**:** 503-512.
152. Lin W, Celik A, Derdeyn C, An H, Lee Y, Videen T, Østergaard L, and Powers WJ (2001) Quantitative measurements of cerebral blood flow in patients with unilateral carotid artery occlusion: a PET and MR study. *J Magn Reson Imaging* 14**:** 659-667.
153. Lindgren A, Staaf G, Geijer B, Brockstedt S, Stahlberg F, Holtas S, and Norrving B (2000) Clinical lacunar syndromes as predictors of lacunar infarcts. A comparison of acute clinical lacunar syndromes and findings on diffusion-weighted MRI. *Acta Neurol Scand* 101**:** 128-134.
154. Longstreth WT Jr, Diehr P, Manolio TA, Beauchamp NJ, Jungreis CA, and Lefkowitz D (2001) Cluster analysis and patterns of findings on cranial magnetic resonance imaging of the elderly: the Cardiovascular Health Study. *Arch Neurol* 58**:** 635-640.
155. Lutsep HL, Albers GW, DeCrespigny A, Kamat GN, Marks MP, and Moseley ME (1997) Clinical utility of diffusion-weighted magnetic resonance imaging in the assessment of ischemic stroke. *Ann Neurol* 41**:** 574-580.
156. Lythgoe DJ, Østergaard L, William SC, Cluckie A, Buxton-Thomas M, Simmons A, and Markus HS (2000) Quantitative perfusion imaging in carotid artery stenosis using dynamic susceptibility contrast-enhanced magnetic resonance imaging. *Magn Reson Imaging* 18**:** 1-11.
157. Maeda M, Yuh WT, Ueda T, Maley JE, Crosby DL, Zhu MW, and Magnotta VA (1999) Severe occlusive carotid artery disease: hemodynamic assessment by MR perfusion imaging in symptomatic patients. *AJNR Am J Neuroradiol* 20**:** 43-51.
158. Mamata H, Mamata Y, Westin CF, Shenton ME, Kikinis R, Jolesz FA, and Maier SE (2002) High-resolution line scan diffusion tensor MR imaging of white matter fiber tract anatomy. *AJNR Am J Neuroradiol* 23**:** 67-75.

159. Marchal G, Rioux P, Petit-Taboue MC, Sette G, Travere JM, Le Poec C, Courtheoux P, Derlon JM, and Baron JC (1992) Regional cerebral oxygen consumption, blood flow, and blood volume in healthy human aging. *Arch Neurol* 49**:** 1013-1020.
160. Marks MP, de Crespigny A, Lentz D, Enzmann DR, Albers GW, and Moseley ME (1996) Acute and chronic stroke: navigated spin-echo diffusion-weighted MR imaging. *Radiology* 199**:** 403-408.
161. Marks MP, Tong DC, Beaulieu C, Albers GW, de Crespigny A, and Moseley ME (1999) Evaluation of early reperfusion and i.v. tPA therapy using diffusion- and perfusion-weighted MRI. *Neurology* 52**:** 1792-1798.
162. Markus H and Cullinane M (2001) Severely impaired cerebrovascular reactivity predicts stroke and TIA risk in patients with carotid artery stenosis and occlusion. *Brain* 124**:** 457-467.
163. Markus HS, Lythgoe DJ, Østergaard L, O'Sullivan M, and Williams SC (2000) Reduced cerebral blood flow in white matter in ischaemic leukoaraiosis demonstrated using quantitative exogenous contrast based perfusion MRI. *J Neurol Neurosurg Psychiatry* 69**:** 48-53.
164. Martin AJ, Friston KJ, Colebatch JG, and Frackowiak RS (1991) Decreases in regional cerebral blood flow with normal aging. *J Cereb Blood Flow Metab* 11**:** 684-689.
165. Mascalchi M, Moretti M, Della Nave R, Lolli F, Tessa C, Carlucci G, Bartolini L, Pracucci G, Pantoni L, Filippi M, and Inzitari D (2002a) Longitudinal evaluation of leukoaraiosis with whole brain ADC histograms. *Neurology* 59**:** 938-940.
166. Mascalchi M, Tessa C, Moretti M, Della Nave R, Boddi V, Martini S, Inzitari D, and Villari N (2002b) Whole brain apparent diffusion coefficient histogram: a new tool for evaluation of leukoaraiosis. *J Magn Reson Imaging* 15**:** 144-148.
167. Matsubayashi K, Okumiya K, Wada T, Osaki Y, Fujisawa M, Doi Y, and Ozawa T (1997) Postural dysregulation in systolic blood pressure is associated with worsened scoring on neurobehavioral function tests and leukoaraiosis in the older elderly living in a community. *Stroke* 28**:** 2169-2173.
168. McHenry LC Jr, Merory J, Bass E, Stump DA, Williams R, Witcofski R, Howard G, and Toole JF (1978) Xenon-133 inhalation method for regional cerebral blood flow measurements: normal values and test-retest results. *Stroke* 9**:** 396-399.
169. Meier P and Zierler KL (1954) On the theory of the indicator-dilution method for measurement of blood flow and volume. *J Appl Physiol* 6**:** 731-744.
170. Meltzer CC, Cantwell MN, Greer PJ, Ben-Eliezer D, Smith G, Frank G, Kaye WH, Houck PR, and Price JC (2000) Does cerebral blood flow decline in healthy aging? A PET study with partial-volume correction. *J Nucl Med* 41**:** 1842-1848.
171. Mintorovitch J, Moseley ME, Chileuitt L, Shimizu H, Cohen Y, and Weinstein PR (1991) Comparison of diffusion- and T2-weighted MRI for the early detection of cerebral ischemia and reperfusion in rats. *Magn Reson Med* 18**:** 39-50.
172. Moody DM, Brown WR, Challa VR, and Anderson RL (1995) Periventricular venous collagenosis: association with leukoaraiosis. *Radiology* 194**:** 469-476.
173. Moseley ME, Kucharczyk J, Mintorovitch J, Cohen Y, Kurhanewicz J, Derugin N, Asgari H, and Norman D (1990) Diffusion-weighted MR imaging of acute stroke: correlation with T2-weighted and magnetic susceptibility-enhanced MR imaging in cats. *AJNR Am J Neuroradiol* 11**:** 423-429.
174. Mrak RE, Griffin ST, and Graham DI (1997) Aging-associated changes in human brain. *J Neuropathol Exp Neurol* 56**:** 1269-1275.
175. Mullins ME, Lev MH, Schellingerhout D, Koroshetz WJ, and Gonzalez RG (2002) Influence of availability of clinical history on detection of early stroke using unenhanced CT and diffusion-weighted MR imaging. *AJR Am J Roentgenol* 179**:** 223-228.
176. Murdoch G (2000) Staining for apoptosis: now neuropathologists can "see" leukoaraiosis. *AJNR Am J Neuroradiol* 21**:** 42-43.
177. Müller M, Reiche W, Langenscheidt P, Hassfeld J, and Hagen T (2000) Ischemia after carotid endarterectomy: comparison between transcranial Doppler sonography and diffusion-weighted MR imaging. *AJNR Am J Neuroradiol* 21**:** 47-54.
178. Mäntylä R, Aronen HJ, Salonen O, Korpelainen M, Peltonen T, Standertskjöld-Nordenstam C, and Erkinjuntti T (1999a) The prevalence and distribution of white-matter changes on different MRI pulse sequences in a post-stroke cohort. *Neuroradiology* 41**:** 657-665.
179. Mäntylä R, Aronen HJ, Salonen O, Pohjasvaara T, Korpelainen M, Peltonen T, Standertskjöld-Nordenstam CG, Kaste M, and Erkinjuntti T (1999b) Magnetic resonance imaging white matter hyperintensities and mechanism of ischemic stroke. *Stroke* 30**:** 2053-2058.
180. Mäntylä R, Erkinjuntti T, Salonen O, Aronen HJ, Peltonen T, Pohjasvaara T, and Standertskjöld-Nordenstam CG (1997) Variable agreement between visual rating scales for white matter

hyperintensities on MRI. Comparison of 13 rating scales in a poststroke cohort. *Stroke* 28**:** 1614-1623.
181. Na DL, Suh CK, Choi SH, Moon HS, Seo DW, Kim SE, Na DG, and Adair JC (1999) Diffusion-weighted magnetic resonance imaging in probable Creutzfeldt-Jakob disease: a clinical-anatomic correlation. *Arch Neurol* 56**:** 951-957.
182. Naritomi H, Meyer JS, Sakai F, Yamaguchi F, and Shaw T (1979) Effects of advancing age on regional cerebral blood flow. Studies in normal subjects and subjects with risk factors for atherothrombotic stroke. *Arch Neurol* 36**:** 410-416.
183. Neil JJ, Shiran SI, McKinstry RC, Schefft GL, Snyder AZ, Almli CR, Akbudak E, Aronovitz JA, Miller JP, Lee BCP, and Conturo TE (1998) Normal brain in human newborn: apparent coefficient and diffusion anisotropy measured by using diffusion tensor MR imaging. *Radiology* 209**:** 57-66.
184. Netter FH (1991) Atlas of human anatomy. "Atlas of human anatomy." Ciba-Geigy, Basle.
185. Neumann-Haefelin T, Moseley ME, and Albers GW (2000a) New magnetic resonance imaging methods for cerebrovascular disease: emerging clinical applications. *Ann Neurol* 47**:** 559-570.
186. Neumann-Haefelin T, Wittsack HJ, Fink GR, Wenserski F, Li TQ, Seitz RJ, Siebler M, Modder U, and Freund HJ (2000b) Diffusion- and perfusion-weighted MRI: influence of severe carotid artery stenosis on the DWI/PWI mismatch in acute stroke. *Stroke* 31**:** 1311-1317.
187. Neumann-Haefelin T, Wittsack HJ, Wenserski F, Siebler M, Seitz RJ, Modder U, and Freund HJ (1999) Diffusion- and perfusion-weighted MRI. The DWI/PWI mismatch region in acute stroke. *Stroke* 30**:** 1591-1597.
188. Nighoghossian N, Berthezene Y, Meyer R, Cinotti L, Adeleine P, Philippon B, Froment JC, and Trouillas P (1997) Assessment of cerebrovascular reactivity by dynamic susceptibility contrast-enhanced MR imaging. *J Neurol Sci* 149**:** 171-176.
189. Nighoghossian N, Berthezene Y, Philippon B, Adeleine P, Froment JC, and Trouillas P (1996) Hemodynamic parameter assessment with dynamic susceptibility contrast magnetic resonance imaging in unilateral symptomatic internal carotid artery occlusion. *Stroke* 27**:** 474-479.
190. Nighoghossian N, Trouillas P, Philippon B, Itti R, and Adeleine P (1994) Cerebral blood flow reserve assessment in symptomatic versus asymptomatic high-grade internal carotid artery stenosis. *Stroke* 25**:** 1010-1013.
191. North American Symptomatic Carotid Endarterectomy Trial Collaborators (1991) Beneficial effect of carotid endarterectomy in symptomatic patients with high-grade carotid stenosis. *N Engl J Med* 325**:** 445-453.
192. Nusbaum AO, Tang CY, Buchsbaum MS, Wei TC, and Atlas SW (2001) Regional and global changes in cerebral diffusion with normal aging. *AJNR Am J Neuroradiol* 22**:** 136-142.
193. Nusbaum AO, Tang CY, Wei T, Buchsbaum MS, and Atlas SW (2000) Whole-brain diffusion MR histograms differ between MS subtypes. *Neurology* 54**:** 1421-1427.
194. Oishi M and Mochizuki Y (1998) Regional cerebral blood flow and cerebrospinal fluid glutamate in leukoaraiosis. *J Neurol* 245**:** 777-780.
195. Okada K, Wu LH, and Kobayashi S (1999) Diffusion-weighted MRI in severe leukoaraiosis. *Stroke* 30**:** 478-479 [letter].
196. Oliveira-Filho J, Ay H, Schaefer PW, Buonanno FS, Chang Y, Gonzalez RG, and Koroshetz WJ (2000) Diffusion-weighted magnetic resonance imaging identifies the "clinically relevant" small-penetrator infarcts. *Arch Neurol* 57**:** 1009-1014.
197. Oppenheimer SM, Bryan RN, Conturo TE, Soher BJ, Preziosi TJ, and Barker PB (1995) Proton magnetic resonance spectroscopy and gadolinium-DTPA perfusion imaging of asymptomatic MRI white matter lesions. *Magn Reson Med* 33**:** 61-68.
198. O'Sullivan M, Lythgoe DJ, Pereira AC, Summers PE, Jarosz JM, Williams SC, and Markus HS (2002) Patterns of cerebral blood flow reduction in patients with ischemic leukoaraiosis. *Neurology* 59**:** 321-326.
199. O'Sullivan M, Summers PE, Jones DK, Jarosz JM, Williams SC, and Markus HS (2001) Normal-appearing white matter in ischemic leukoaraiosis: a diffusion tensor MRI study. *Neurology* 57**:** 2307-2310.
200. Pantano P, Baron JC, Lebrun-Grandie P, Duquesnoy N, Bousser MG, and Comar D (1984) Regional cerebral blood flow and oxygen consumption in human aging. *Stroke* 15**:** 635-641.
201. Pantoni L and Garcia JH (1995) The significance of cerebral white matter abnormalities 100 years after Binswanger's report. A review. *Stroke* 26**:** 1293-1301.
202. Pantoni L and Garcia JH (1997) Pathogenesis of leukoaraiosis: a review. *Stroke* 28**:** 652-659.

203. Pantoni L, Simoni M, Pracucci G, Schmidt R, Barkhof F, and Inzitari D (2002) Visual rating scales for age-related white matter changes (leukoaraiosis): can the heterogeneity be reduced? *Stroke* 33**:** 2827-2833.
204. Parsons MW, Barber PA, Chalk J, Darby DG, Rose S, Desmond PM, Gerraty RP, Tress BM, Wright PM, Donnan GA, and Davis SM (2002) Diffusion- and perfusion-weighted MRI response to thrombolysis in stroke. *Ann Neurol* 51**:** 28-37.
205. Pereira RS, Harris AD, Sevick RJ, and Frayne R (2002) Effect of b value on contrast during diffusion-weighted magnetic resonance imaging assessment of acute ischemic stroke. *J Magn Reson Imaging* 15**:** 591-596.
206. Perkiö J, Aronen HJ, Kangasmäki A, Liu Y, Karonen J, Savolainen S, and Østergaard L (2002) Evaluation of four post processing methods for determination of cerebral blood volume and mean transit time by dynamic susceptibility contrast imaging. *Magn Reson Med* 47**:** 973-981.
207. Perthen JE, Calamante F, Gadian DG, and Connelly A (2002) Is quantification of bolus tracking MRI reliable without deconvolution? *Magn Reson Med* 47**:** 61-67.
208. Petrella JR, DeCarli C, Dagli M, Grandin CB, Duyn JH, Frank JA, Hoffman EA, and Theodore WH (1998) Age-related vasodilatory response to acetazolamide challenge in healthy adults: a dynamic contrast-enhanced MR study. *AJNR Am J Neuroradiol* 19**:** 39-44.
209. Pierpaoli C, Jezzard P, Basser PJ, Barnett A, and Di Chiro G (1996) Diffusion tensor MR imaging of the human brain. *Radiology* 201**:** 637-648.
210. Powers WJ (1991) Cerebral hemodynamics in ischemic cerebrovascular disease. *Ann Neurol* 29**:** 231-240.
211. Powers WJ, Press GA, Grubb RL Jr, Gado M, and Raichle ME (1987) The effect of hemodynamically significant carotid artery disease on the hemodynamic status of the cerebral circulation. *Ann Intern Med* 106**:** 27-34.
212. Rao SM, Mittenberg W, Bernardin L, Haughton V, and Leo GJ (1989) Neuropsychological test findings in subjects with leukoaraiosis. *Arch Neurol* 46**:** 40-44.
213. Reith W, Heiland S, Erb G, Benner T, Forsting M, and Sartor K (1997) Dynamic contrast-enhanced T2*-weighted MRI in patients with cerebrovascular disease. *Neuroradiology* 39**:** 250-257.
214. Rordorf G, Koroshetz WJ, Copen WA, Cramer SC, Schaefer PW, Budzik RF Jr, Schwamm LH, Buonanno F, Sorensen AG, and Gonzalez G (1998) Regional ischemia and ischemic injury in patients with acute middle cerebral artery stroke as defined by early diffusion-weighted and perfusion-weighted MRI. *Stroke* 29**:** 939-943.
215. Rosen BR, Belliveau JW, Aronen HJ, Kennedy D, Buchbinder BR, Fischman AJ, Gruber M, Glas J, Weisskoff RM, Cohen MS, Hochberg FH, and Brady TJ (1991) Susceptibility contrast imaging of cerebral blood volume: human experience. *Magn Reson Med* 22**:** 293-303.
216. Roussel SA, van Bruggen N, King MD, Houseman J, Williams SR, and Gadian DG (1994) Monitoring the initial expansion of focal ischemic changes by diffusion-weighted MRI using a remote controlled method of occlusion. *NMR Biomed* 7**:** 21-28.
217. Rovaris M, Bozzali M, Iannucci G, Ghezzi A, Caputo D, Montanari E, Bertolotto A, Bergamaschi R, Capra R, Mancardi GL, Martinelli V, Comi G, and Filippi M (2002) Assessment of normal-appearing white and gray matter in patients with primary progressive multiple sclerosis: a diffusion-tensor magnetic resonance imaging study. *Arch Neurol* 59**:** 1406-1412.
218. Rovaris M, Iannucci G, Cercignani M, Sormani MP, De Stefano N, Gerevini S, Comi G, and Filippi M (2003) Age-related changes in conventional, magnetization transfer, and diffusion-tensor MR imaging findings: study with whole-brain tissue histogram analysis. *Radiology* 227**:** 731-738.
219. Rutgers DR, Klijn CJ, Kappelle LJ, Eikelboom BC, van Huffelen AC, and van der Grond J (2001) Sustained bilateral hemodynamic benefit of contralateral carotid endarterectomy in patients with symptomatic internal carotid artery occlusion. *Stroke* 32**:** 728-734.
220. Rutgers DR, van Osch MJ, Kappelle LJ, Mali WP, and van der Grond J (2003) Cerebral hemodynamics and metabolism in patients with symptomatic occlusion of the internal carotid artery. *Stroke* 34**:** 648-652.
221. Röther J, de Crespigny AJ, D'Arceuil H, and Moseley ME (1996) MR detection of cortical spreading depression immediately after focal ischemia in the rat. *J Cereb Blood Flow Metab* 16**:** 214-220.
222. Röther J, Schellinger PD, Gass A, Siebler M, Villringer A, Fiebach JB, Fiehler J, Jansen O, Kucinski T, Schöder V, Szabo K, Jünge-Hulsing GJ, Hennerici M, Zeumer H, Sartor K, Weiller C, Hacke W, and Kompetenznetzwerk Schlaganfall Study Group (2002) Effect of intravenous thrombolysis on MRI parameters and functional outcome in acute stroke <6 hours. *Stroke* 33**:** 2438-2445.

223. Sakakibara R, Hattori T, Uchiyama T, and Yamanishi T (1999) Urinary function in elderly people with and without leukoaraiosis: relation to cognitive and gait function. *J Neurol Neurosurg Psychiatry* 67**:** 658-660.
224. Sakuma H, Nomura Y, Takeda K, Tagami T, Nakagawa T, Tamagawa Y, Ishii Y, and Tsukamoto T (1991) Adult and neonatal human brain: diffusional anisotropy and myelination with diffusion-weighted MR imaging. *Radiology* 180**:** 229-233.
225. Salonen O, Autti T, Raininko R, Ylikoski A, and Erkinjuntti T (1997) MRI of the brain in neurologically healthy middle-aged and elderly individuals. *Neuroradiol* 39**:** 537-545.
226. Sanchez del Rio M, Bakker D, Wu O, Agosti R, Mitsikostas DD, Østergaard L, Wells WA, Rosen BR, Sorensen G, Moskowitz MA, and Cutrer FM (1999) Perfusion weighted imaging during migraine: spontaneous visual aura and headache. *Cephalalgia* 19**:** 701-707.
227. Sandson TA, O'Connor M, Sperling RA, Edelman RR, and Warach S (1996) Noninvasive perfusion MRI in Alzheimer's disease: a preliminary report. *Neurology* 47**:** 1339-1342.
228. Saur D, Kucinski T, Grzyska U, Eckert B, Eggers C, Niesen W, Schöder V, Zeumer H, Weiller C, and Röther J (2003) Sensitivity and interrater agreement of CT and diffusion-weighted MR imaging in hyperacute stroke. *AJNR Am J Neuroradiol* 24**:** 878-885.
229. Schaefer PW, Grant PE, and Gonzalez RG (2000) Diffusion-weighted MR imaging of the brain. *Radiology* 217**:** 331-345.
230. Schellinger PD, Fiebach JB, and Hacke W (2003) Imaging-based decision making in thrombolytic therapy for ischemic stroke: present status. *Stroke* 34**:** 575-583.
231. Schellinger PD, Fiebach JB, Jansen O, Ringleb PA, Mohr A, Steiner T, Heiland S, Schwab S, Pohlers O, Ryssel H, Orakcioglu B, Sartor K, and Hacke W (2001) Stroke magnetic resonance imaging within 6 hours after onset of hyperacute cerebral ischemia. *Ann Neurol* 49**:** 460-469.
232. Scheltens P, Erkinjuntti T, Leys D, Wahlund LO, Inzitari D, del Ser T, Pasquier F, Barkhof F, Mäntylä R, Bowler J, Wallin A, Ghika J, Fazekas F, and Pantoni L (1998) White matter changes on CT and MRI: an overview of visual rating scales. European Task Force on Age-Related White Matter Changes. *Eur Neurol* 39**:** 80-89.
233. Schlaug G, Benfield A, Baird AE, Siewert B, Lovblad KO, Parker RA, Edelman RR, and Warach S (1999) The ischemic penumbra: operationally defined by diffusion and perfusion MRI. *Neurology* 53**:** 1528-1537.
234. Schlaug G, Siewert B, Benfield A, Edelman RR, and Warach S (1997) Time course of the apparent diffusion coefficient (ADC) abnormality in human stroke. *Neurology* 49**:** 113-119.
235. Schreiber WG, Guckel F, Stritzke P, Schmiedek P, Schwartz A, and Brix G (1998) Cerebral blood flow and cerebrovascular reserve capacity: estimation by dynamic magnetic resonance imaging. *J Cereb Blood Flow Metab* 18**:** 1143-1156.
236. Schwartz RB, Mulkern RV, Gudbjartsson H, and Jolesz FA (1998) Diffusion-weighted MR imaging in hypertensive encephalography: clues to pathogenesis. *AJNR Am J Neuroradiol* 19**:** 859-862.
237. Shellock FG, Morisoli S, and Kanal E (1993) MR procedures and biomedical implants, materials, and devices: 1993 update. *Radiology* 189**:** 587-599.
238. Sherman JL, Citrin CM, Gangarosa RE, and Bowen BJ (1987) The MR appearance of CSF flow in patients with ventriculomegaly. *AJR Am J Roentgenol* 148**:** 193-199.
239. Shimony JS, McKinstry RC, Akbudak E, Aronovitz JA, Snyder AZ, Lori NF, Cull TS, and Conturo TE (1999) Quantitative diffusion-tensor anistropy brain MR imaging: normative human data and anatomic analysis. *Radiology* 212**:** 770-784.
240. Shintani S, Shiigai T, and Arinami T (1998) Silent lacunar infarction on magnetic resonance imaging (MRI): risk factors. *J Neurol Sci* 160**:** 82-86.
241. Shuaib A, Lee D, Pelz D, Fox A, and Hachinski VC (1992) The impact of magnetic resonance imaging on the management of acute ischemic stroke. *Neurology* 42**:** 816-818.
242. Siewert B, Schlaug G, Edelman RR, and Warach S (1997) Comparison of EPISTAR and T2*-weighted gadolinium-enhanced perfusion imaging in patients with acute cerebral ischemia. *Neurology* 48**:** 673-679.
243. Silver N, Barker G, MacManus D, Tofts P, and Miller D (1997) Magnetisation transfer ratio of normal brain white matter: a normative database spanning four decades of life. *J Neurol Neurosurg Psychiatry* 62**:** 223-228.
244. Silvestrini M, Troisi E, Matteis M, Cupini LM, and Caltagirone C (1996) Transcranial Doppler assessment of cerebrovascular reactivity in symptomatic and asymptomatic severe carotid stenosis. *Stroke* 27**:** 1970-1973.

245. Simonsen CZ, Østergaard L, Smith DF, Vestergaard-Poulsen P, and Gyldensted C (2000) Comparison of gradient- and spin-echo imaging: CBF, CBV, and MTT measurements by bolus tracking. *J Magn Reson Imaging* 12**:** 411-416.
246. Singer MB, Chong J, Lu D, Schonewille WJ, Tuhrim S, and Atlas SW (1998) Diffusion-weighted MRI in acute subcortical infarction. *Stroke* 29**:** 133-136.
247. Smith AM, Grandin CB, Duprez T, Mataigne F, and Cosnard G (2000) Whole brain quantitative CBF and CBV measurements using MRI bolus tracking: comparison of methodologies. *Magn Reson Med* 43**:** 559-564.
248. Sorensen AG (2001) What is the meaning of quantitative CBF? *AJNR Am J Neuroradiol* 22**:** 235-236.
249. Sorensen AG, Copen WA, Østergaard L, Buonanno FS, Gonzalez RG, Rordorf G, Rosen BR, Schwamm LH, Weisskoff RM, and Koroshetz WJ (1999a) Hyperacute stroke: simultaneous measurement of relative cerebral blood volume, relative cerebral blood flow, and mean tissue transit time. *Radiology* 210**:** 519-527.
250. Sorensen AG, Wu O, Copen WA, Davis TL, Gonzalez RG, Koroshetz WJ, Reese TG, Rosen BR, Wedeen VJ, and Weisskoff RM (1999b) Human acute cerebral ischemia: detection of changes in water diffusion anisotropy by using MR imaging. *Radiology* 212**:** 785-792.
251. Speck O, Chang L, DeSilva NM, and Ernst T (2000) Perfusion MRI of the human brain with dynamic susceptibility contrast: gradient-echo versus spin-echo techniques. *J Magn Reson Imaging* 12**:** 381-387.
252. Stark DD and Bradley WG (eds.) (1992). Magnetic resonance imaging. "Magnetic resonance imaging.", St Louis.
253. Steifler JY, Eliasziw M, Benavente OR, Alamowitch S, Fox AJ, Hachinski VC, Barnett HJ, and North American Symptomatic Carotid Endarterectomy Trial Collaborators (2002) Prognostic importance of leukoaraiosis in patients with symptomatic internal carotid artery stenosis. *Stroke* 33**:** 1651-1655.
254. Stejskal E and Tanner J (1965) Spin diffusion measurements: spin echos in the presence of time-dependent field gradient. *J Chem Phys* 42**:** 288-292.
255. Stewart GN (1984) Researches on the circulation time in organs and on the influences which affect it. Parts I-III. *J Physiol (London)* 15**:** 1-89.
256. Sunshine JL, Tarr RW, Lanzieri CF, Landis DM, Selman WR, and Lewin JS (1999) Hyperacute stroke: ultrafast MR imaging to triage patients prior to therapy. *Radiology* 212**:** 325-332.
257. Szabo K, Kern R, Gass A, Hirsch J, and Hennerici M (2001) Acute stroke patterns in patients with internal carotid artery disease: a diffusion-weighted magnetic resonance imaging study. *Stroke* 32**:** 1323-1329.
258. Szeszko PR, Vogel J, Ashtari M, Malhotra AK, Bates J, Kane JM, Bilder RM, Frevert T, and Lim K (2003) Sex differences in frontal lobe white matter microstructure: a DTI study. *Neuroreport* 14**:** 2469-2473.
259. Takahashi K, Kobayashi S, Matui R, Yamaguchi S, and Yamashita K (2002) The differences of clinical parameters between small multiple ischemic lesions and single lesion detected by diffusion-weighted MRI. *Acta Neurol Scand* 106**:** 24-29.
260. Takano K, Latour LL, Formato JE, Carano RAD, Helmer KG, Hasegawa Y, Sotak CH, and Fisher M (1996) The role of spreading depression in focal ischemia evaluated by diffusion mapping. *Ann Neurol* 39**:** 308-318.
261. Takano K, Tatlisumak T, Formato JE, Carano RAD, Bergmann AG, Pullan LM, Bare TM, Sotak CH, and Fisher M (1997) A glycine site antagonist attenuates infarct size in experimental focal ischemia: postmortem and diffusion mapping studies. *Stroke* 28**:** 1255-1263.
262. Tanaka F, Vines D, Tsuchida T, Freedman M, and Ichise M (2000) Normal patterns on 99mTc-ECD brain SPECT scans in adults. *J Nucl Med* 41**:** 1456-1464.
263. Tanner SF, Ramenghi LA, Ridgway JP, Berry E, Saysell MA, Martinez D, Arthur RJ, Smith MA, and Levene MI (2000) Quantitative comparison of intrabrain diffusion in adults and preterm and term neonates and infants. *AJR Am J Roentgenol* 174**:** 1643-1649.
264. Tarvonen-Schröder S, Röyttä M, Räihä I, Kurki T, Rajala T, and Sourander L (1996) Clinical features of leuko-araiosis. *J Neurol Neurosurg Psychiatry* 60**:** 431-436.
265. Tatu L, Moulin T, Bogousslavsky J, and Duvernoy H (1996) Arterial territories of human brain: brainstem and cerebellum. *Neurology* 47**:** 1125-1135.
266. Tatu L, Moulin T, Bogousslavsky J, and Duvernoy H (1998) Arterial territories of the human brain: cerebral hemispheres. *Neurology* 50**:** 1699-1708.
267. The National Institute of Neurological Disorders and Stroke rt-PA Stroke Study Group (1995) Tissue plasminogen activator for acute ischemic stroke. *N Engl J Med* 333**:** 1581-1587.

268. Toft PB, Leth H, Peitersen B, Lou HC, and Thomsen C (1996) The apparent diffusion coefficient of water in gray and white matter of the infant brain. *J Comp Assist Tomogr* 20**:** 1006-1011.
269. Tong DC, Yenari MA, Albers GW, O'Brien M, Marks MP, and Moseley ME (1998) Correlation of perfusion- and diffusion-weighted MRI with NIHSS score in acute (<6.5 hour) ischemic stroke. *Neurology* 50**:** 864-870.
270. Ueda T, Yuh WT, Maley JE, Quets JP, Hahn PY, and Magnotta VA (1999a) Outcome of acute ischemic lesions evaluated by diffusion and perfusion MR imaging. *AJNR Am J Neuroradiol* 20**:** 983-989.
271. Ueda T, Yuh WT, and Taoka T (1999b) Clinical application of perfusion and diffusion MR imaging in acute ischemic stroke. *J Magn Reson Imaging* 10**:** 305-309.
272. Ulug AM, Beauchamp N Jr, Bryan RN, and van Zijl PCM (1997) Absolute quantitation of diffusion constants in human stroke. *Stroke* 28**:** 483-490.
273. Waldemar G, Hasselbalch SG, Andersen AR, Delecluse F, Petersen P, Johnsen A, and Paulson OB (1991) 99mTc-d,l-HMPAO and SPECT of the brain in normal aging. *J Cereb Blood Flow Metab* 11**:** 508-502.
274. van Everdingen K, van der Grond J, Kappelle LJ, Ramos LM, and Mali WP (1998) Diffusion-weighted magnetic resonance imaging in acute stroke. *Stroke* 29**:** 1783-1790.
275. van Gijn J (1998) Leukoaraiosis and vascular dementia. *Neurology* 51(3 Suppl 3)**:** 3-8.
276. van Osch MJP, Rutgers DR, Vonken EPA, van Huffelen AC, Klijn CJM, Bakker CJG, and van der Grond J (2002) Quantitative cerebral perfusion MRI and CO2 reactivity measurements in patients with symptomatic internal carotid artery occlusion. *Neuroimage* 17**:** 469-478.
277. Wang J, Alsop DC, Li L, Listerud J, Gonzalez-At JB, Schnall MD, and Detre JA (2002) Comparison of quantitative perfusion imaging using arterial spin labeling at 1.5 and 4.0 Tesla. *Magn Reson Med* 48**:** 242-254.
278. Vanninen E, Kuikka JT, Aikia M, Kononen M, and Vanninen R (2003) Heterogeneity of cerebral blood flow in symptomatic patients undergoing carotid endarterectomy. *Nucl Med Commun* 24**:** 893-900.
279. Vanninen R, Koivisto K, Tulla H, Manninen H, and Partanen K (1995) Hemodynamic effects of carotid endarterectomy by magnetic resonance flow quantification. *Stroke* 26**:** 84-89.
280. Warach S (2001) Use of diffusion and perfusion magnetic resonance imaging as a tool in acute stroke clinical trials. *Curr Control Trials Med* 2**:** 38-44.
281. Warach S, Chien D, Li W, Ronthal M, and Edelman RR (1992) Fast magnetic resonance diffusion-weighted imaging of acute human stroke. *Neurology* 42**:** 1717-1723.
282. Warach S, Dashe J, and Edelman R (1996) Clinical outcome in ischemic stroke predicted by early diffusion-weighted and perfusion magnetic resonance imaging: a preliminary analysis. *J Cereb Blood Flow Metab* 16**:** 53-59.
283. Warach S, Gaa J, Siewert B, Wielopolski P, and Edelman RR (1995) Acute human stroke studied by whole brain echo planar diffusion-weighted magnetic resonance imaging. *Ann Neurol* 37**:** 231-241.
284. Wardlaw JM, Keir SL, Bastin ME, Armitage PA, and Rana AK (2002) Is diffusion imaging appearance an independent predictor of outcome after ischemic stroke? *Neurology* 59**:** 1381-1387.
285. Weber J, Mattle HP, Heid O, Remonda L, and Schroth G (2000) Diffusion-weighted imaging in ischaemic stroke: a follow-up study. *Neuroradiology* 42**:** 184-191.
286. Weisskoff RM, Chesler D, Boxerman JL, and Rosen BR (1993) Pitfalls in MR measurement of tissue blood flow with intravascular tracers: which mean transit time? *Magn Reson Med* 29**:** 553-558.
287. Weisskoff RM, Zuo CS, Boxerman JL, and Rosen BR (1994) Microscopic susceptibility variation and transverse relaxation: Theory and experiment. *Magn Reson Med* 31**:** 601-610.
288. Vernieri F, Pasqualetti P, Matteis M, Passarelli F, Troisi E, Rossini PM, Caltagirone C, and Silvestrini M (2001) Effect of collateral blood flow and cerebral vasomotor reactivity on the outcome of carotid artery occlusion. *Stroke* 32**:** 1552-1558.
289. Wiart M, Berthezene Y, Adeleine P, Feugier P, Trouillas P, Froment JC, and Nighoghossian N (2000) Vasodilatory response of border zones to acetazolamide before and after endarterectomy : an echo planar imaging-dynamic susceptibility contrast-enhanced MRI study in patients with high-grade unilateral internal carotid artery stenosis. *Stroke* 31**:** 1561-1565.
290. Villringer A, Rosen BR, Belliveau JW, Ackerman JL, Lauffer RB, Buxton RB, Chao YS, Wedeen VJ, and Brady TJ (1988) Dynamic imaging with lanthanide chelates in normal brain: contrast due to magnetic susceptibility effects. *Magn Reson Med* 6**:** 164-174.
291. Wilson M, Morgan PS, and Blumhardt LD (2002) Quantitative diffusion characteristics of the human brain depend on MRI sequence parameters. *Neuroradiology* 44**:** 586-591.

292. Wirestam R, Andersson L, Østergaard L, Bolling M, Aunola JP, Lindgren A, Geijer B, Holtas S, and Stahlberg F (2000) Assessment of regional cerebral blood flow by dynamic susceptibility contrast MRI using different deconvolution techniques. *Magn Reson Med* 43**:** 691-700.
293. Wiszniewska M, Devuyst G, Bogousslavsky J, Ghika J, and van Melle G (2000) What is the significance of leukoaraiosis in patients with acute ischemic stroke? *Arch Neurol* 57**:** 967-973.
294. Wittsack HJ, Ritzl A, Fink GR, Wenserski F, Siebler M, Seitz RJ, Modder U, and Freund HJ (2002) MR imaging in acute stroke: diffusion-weighted and perfusion imaging parameters for predicting infarct size. *Radiology* 222**:** 397-403.
295. Vonken EJ, van Osch MJ, Bakker CJ, and Viergever MA (1999) Measurement of cerebral perfusion with dual-echo multi-slice quantitative dynamic susceptibility contrast MRI. *J Magn Reson Imaging* 10**:** 109-117.
296. Vonken EP, van Osch MJ, Bakker CJ, and Viergever MA (2000) Simultaneous quantitative cerebral perfusion and Gd-DTPA extravasation measurement with dual-echo dynamic susceptibility contrast MRI. *Magn Reson Med* 43**:** 820-827.
297. Xing D, Papadakis NG, Huang CL, Lee VM, Carpenter TA, and Hall LD (1997) Optimized diffusion-weighting for measurements of apparent diffusion coefficient (ADC) in human brain. *Magn Reson Imaging* 15**:** 771-784.
298. Yamada K, Gonzalez RG, Østergaard L, Komili S, Weisskoff RM, Rosen BR, Koroshetz WJ, Nishimura T, and Sorensen AG (2002) Iron-induced susceptibility effect at the globus pallidus causes underestimation of flow and volume on dynamic susceptibility contrast-enhanced MR perfusion images. *AJNR Am J Neuroradiol* 23**:** 1022-1029.
299. Yamaguchi T, Kanno I, Uemura K, Shishido F, Inugami A, Ogawa T, Murakami M, and Suzuki K (1986) Reduction in regional cerebral metabolic rate of oxygen during human aging. *Stroke* 17**:** 1220-1228.
300. Yamauchi H, Fukuyama H, Nagahama Y, Nabatame H, Nakamura K, Yamamoto Y, Yonekura Y, Konishi J, and Kimura J (1996) Evidence of misery perfusion and risk for recurrent stroke in major cerebral arterial occlusive diseases from PET. *J Neurol Neurosurg Psychiatry* 61**:** 18-25.
301. Yamauchi H, Fukuyama H, Nagahama Y, Shiozaki T, Nishizawa S, Konishi J, Shio H, and Kimura J (1999) Brain arteriolosclerosis and hemodynamic disturbance may induce leukoaraiosis. *Neurology* 53**:** 1833-1838.
302. Yamauchi H, Fukuyama H, and Shio H (2000) Corpus callosum atrophy in patients with leukoaraiosis may indicate global cognitive impairment. *Stroke* 31**:** 1515-1520.
303. Ylikoski R, Ylikoski A, Erkinjuntti T, Sulkava R, Raininko R, and Tilvis R (1993) White matter changes in healthy elderly persons correlate with attention and speed of mental processing. *Arch Neurol* 50**:** 818-824.
304. Yoo SY, Chang KH, Song IC, Han MH, Kwon BJ, Lee SH, Yu IK, and Chun CK (2002) Apparent diffusion coefficient value of the hippocampus in patients with hippocampal sclerosis and in healthy volunteers. *AJNR Am J Neuroradiol* 23**:** 809-812.
305. Yoshiura T, Wu O, Zaheer A, Reese TG, and Sorensen AG (2001) Highly diffusion-sensitized MRI of brain: dissociation of gray and white matter. *Magn Reson Med* 45**:** 734-740.
306. Zhai G, Lin W, Wilber KP, Gerig G, and Gilmore JH (2003) Comparisons of regional white matter diffusion in healthy neonates and adults performed with a 3.0-T head-only MR imaging unit. *Radiology* 229**:** 673-681.
307. Østergaard L (1998) CBF/MTT/CBV Guide.
308. Østergaard L, Johannsen P, Höst-Poulsen P, Vestergaard-Poulsen P, Asboe H, Gee AD, Hansen SB, Cold GE, Gjedde A, and Gyldensted C (1998a) Cerebral blood flow measurements by magnetic resonance imaging bolus tracking: comparison with [15O]H2O positron emission tomography in humans. *J Cereb Blood Flow Metab* 18**:** 935-940.
309. Østergaard L, Smith DF, Vestergaard-Poulsen P, Hansen SB, Gee AD, Gjedde A, and Gyldensted C (1998b) Absolute cerebral blood flow and blood volume measured by magnetic resonance imaging bolus tracking: comparison with positron emission tomography values. *J Cereb Blood Flow Metab* 18**:** 425-432.
310. Østergaard L, Sorensen A, Kwong K, Weisskoff R, Gyldensted C, and Rosen B (1996a) High resolution measurement of cerebral blood flow using intravascular tracer bolus passages. Part II: experimental comparison and preliminary results. *MRM* 36**:** 726-736.
311. Østergaard L, Weisskoff R, Chesler D, Gyldensted C, and Rosen B (1996b) High resolution measurement of cerebral blood flow using intravascular tracer bolus passages. Part I: mathematical approach and statistical analysis. *MRM* 36**:** 715-725.